

**Site-Specific Incorporation of Unnatural Amino Acids  
into Receptors Expressed in Mammalian Cells**

Thesis by:

**Sarah Lynn Monahan**

In Partial Fulfillment of the Requirements  
for the Degree of Doctor of Philosophy  
in Chemistry

California Institute of Technology

Pasadena, CA 91125

2004

(Defended May 17, 2004)

©2004

Sarah Lynn Monahan

All Rights Reserved

*Dedicated to my grandparents,*

*Bill and Elinor Butterfield*

*Hugh and Agnes Monahan*

## Acknowledgements

I need to first thank Dennis Dougherty for being a model supervisor. He does science the way it should be done - with a great love for knowledge - and that has inspired me immensely. I also very much appreciate his human side. My time at Caltech has had some ups and downs, and his support has helped me see this degree through to completion. He has been especially patient when it came to my extracurricular activities. It has been wonderful to work for someone who understands that life doesn't stop just because you are a PhD student. I hold him in the highest regard as a scientist and as a human being.

I of course must thank my committee, Harry Gray, Peter Dervan, Erin Schuman and Henry Lester for helping me get through this whole process, and for keeping me on my toes. All of them have been excellent role models for me since I first arrived at Caltech.

Working in the Dougherty lab is a unique experience. Only the greatest people seem to join the lab, and the absence of lab politics has made my experience here at Caltech a great one. Some former group members that I would like to thank include Gabriel Brandt, Joshua Maurer, Niki Zacharias, Donald Elmore, Lintong Li and Justin Gallivan - as well as David Dahan who will soon be a former group member as well. All of these people helped shape my graduate school experience in a positive way; Gabe, Josh, Niki and Justin taught me everything I know about molecular biology, among other things. Niki and Gabe were also two of the best housemates anyone could want. My lab mates James Petersson, Steve Spronk, and Darren Beene - who all started at the same

time as me - have also been good friends over the years. My experience would have been diminished without them. James was especially there for me during the earlier years of grad school, and I'm grateful for that. And of course the newer group members (some not so new anymore!) including Kiowa Bower, Amanda Cashin, Amy Eastwood, Ariele Hanek, Lori Lee, Katie McMenimen, Tingwei Mu, Julian Revie, Erik Rodriguez, Mike Torrice, and Joanne Xiu have all maintained the Dougherty group atmosphere as it should be - fun. I have very much enjoyed the work and social atmosphere that has been created by all of these wonderful people.

The Lester lab has also had a major influence on my graduate school career. It has been wonderful to collaborate with "actual" biologists. Henry Lester has provided much needed guidance and insight over the years. Like Dennis, he also values life outside the lab, and I equally appreciate him for that quality. Raad Nashmi taught me everything I know about electrophysiology, and I will always be grateful for his help. I also want to thank Fraser Moss and Rigo Pantoja for their helpful discussions. Finally, I have to thank Purnima Deshpande, Cesar Labarca and Sheri McKinney for all of their support.

I have made some wonderful friends outside of the lab, who also need to be mentioned. First, Jennifer Ambroggio was luckily one of the first people that I met in Pasadena. She has been a true friend, and I can't imagine what life in Pasadena would have been like not knowing her. Shelley Starck has also been such a supportive friend to me in the past, when I needed it the most. Her strength and ambition are an inspiration to me. Wendy Steiner has also been a great friend, who has helped me keep a good perspective on life. Finally, I have to thank Candace Rypisi and Jennifer Cichocki of the

Caltech Women's Center. They do so much for all women at Caltech, and the campus would not be the same without them! All of these women have done more for me than they are probably aware.

I also want to thank two non-science mentors that I have had for a couple of years. Bill Youngblood took me under his wing as his photography assistant, and has given me encouragement and the confidence to pursue a career in photography. He did this knowing I was "only" a scientist, and had minimal experience as a professional photographer. He is a fabulous photographer, and I've been so lucky to work with him. I also want to thank my Masters Swim coach, Kenny Grace. I always looked forward to swimming, even when I was exhausted, if I knew he would be there. He has helped counteract all of my chocolate consumption.

Of course, my family has always been my lifeline, and I will never be able to thank them enough. Without a doubt, I have the most wonderful parents in the world. I am grateful that they would never let me quit something that I had started - including my undergraduate career - even when I was at the end of my rope. I will also be forever grateful that they are now (ironically) supporting my career in photography, even after spending twelve years to get three degrees in Chemistry. Finally, I also have to thank my brother Adam, and my sister Erin. They add so much to my life - I don't know where I would be without them.

Last, but of course not least, I have to thank my husband Jeremy May. He has been an enormous support to me over the last couple of years. Not only has he supported me emotionally, but he has also been my proofreader, photography assistant, personal chef, and best friend. I will never be able to thank him enough for all that he does.

## Abstract

Unnatural amino acid incorporation into proteins by nonsense suppression has proven to be a valuable tool for structure-function studies. Using the *in vivo* nonsense suppression methodology, information on ligand binding and ion channel gating mechanisms has been obtained on a variety of ion channels. To date, such studies have been limited to the *Xenopus* oocyte heterologous expression system. There would be clear benefits to expanding the technology to a mammalian cell expression system. This would provide a more relevant environment for many proteins of mammalian origin and would allow for studies of cell-specific signal transduction pathways.

We describe here unnatural amino acid incorporation into channels and receptors expressed in mammalian cells. Presented is a general method to deliver mRNA or DNA that codes for a protein of interest, amber suppressor tRNA, and a reporter gene to mammalian cells. Chapter 2 describes in detail the screening of several suppressor tRNAs, as well as various transfection methods tested for tRNA delivery including electroporation, lipofection, peptide-mediated transfection and biolistics. It was found that electroporation was the best method to deliver tRNA to adherent cells, and that THG73 was the most efficient suppressor tRNA. Chapter 3 describes studies, aimed at optimizing the protocol, that involved co-electroporation of a human serine amber suppressor tRNA with the DNA or mRNA corresponding to the protein of interest into adherent cells. This leads to highly efficient delivery of these components and efficient nonsense suppression. We demonstrate this for both enhanced green fluorescent protein and nicotinic acetylcholine receptor expression in CHO-K1 cells. We also show that the

approach is successful in cultured hippocampal neurons. Finally, Chapter 4 demonstrates the application of the electroporation method to the delivery of aminoacyl-tRNA to cells for unnatural amino acid incorporation into the nicotinic acetylcholine receptor. When chemically aminoacylated with natural or unnatural amino acids, THG73 delivers the amino acid site-specifically into receptors expressed in CHO-K1 cells.

Electrophysiology clearly reveals the expected shift in dose-response relations, establishing that the desired unnatural amino acid has been incorporated. In conclusion, we describe the first general method for unnatural amino acid incorporation in mammalian cells.

## Table of Contents

Acknowledgements	iv
Abstract	vii
List of Figures	xiv
List of Tables	xviii

## Chapter 1

Introduction	1
1.1 The nonsense suppression methodology for unnatural amino acid incorporation	2
1.2 Nonsense suppression in mammalian cells	7
1.3 Delivery of aminoacyl-tRNA to mammalian cells	9
1.4 References	11

## Chapter 2

Developing a Mammalian Cell Expression System for Unnatural Amino Acid Incorporation: Screening Suppressor tRNAs and Transfection Methods	15
2.1 Introduction	16
2.2 Results and Discussion	17
2.2.1 Screening suppressor tRNAs in vitro	17

2.2.1.1	Results	19
2.2.1.2	Discussion	23
2.2.2	Electroporation of tRNA	23
2.2.2.1	Microelectroporation	24
2.2.2.1.1	Results	25
2.2.2.1.2	Discussion	31
2.2.2.2	Epizap	33
2.2.2.2.1	Results	33
2.2.2.2.2	Discussion	35
2.2.3	Peptide-mediated delivery of tRNA	36
2.2.3.1	Covalent coupling between the ANTP peptide and tRNA	37
2.2.3.1.1	Results	37
2.2.3.1.2	Discussion	46
2.2.3.2	Noncovalent coupling between the ANTP peptide and tRNA	47
2.2.3.2.1	Results	47
2.2.3.2.2	Discussion	51
2.2.4	Lipofection	51
2.2.4.1	Results	52
2.2.4.2	Discussion	57
2.2.5	Biolistics	58
2.2.5.1	Results	58
2.2.5.2	Discussion	59

2.3	Conclusions	60
2.4	Experimental methods and materials	61
2.4.1	Materials	61
2.4.2	Mutagenesis, mRNA and tRNA synthesis	62
2.4.3	Tissue culture	64
2.4.4	Microscopy	64
2.4.5	Electroporation	64
2.4.5.1	Microelectroporation	64
2.4.5.2	Epizap	65
2.4.6	In vitro protein synthesis	66
2.4.7	Peptide-oligonucleotide coupling reactions	66
2.4.8	Lipofection	69
2.4.8.1	Effectene	69
2.4.8.2	Polyfect	69
2.4.8.3	GeneJammer	70
2.4.8.4	Lipofectamine 2000	70
2.4.9	Biolistics	70
2.5	References	72

### **Chapter 3**

	The HSAS Assay: Optimizing tRNA Delivery to Mammalian Cells	77
3.1	Introduction	78
3.2	Results	82

3.2.1	Electroporation of tRNA into adherent CHO-K1 and HEK cells: EGFP expression by nonsense suppression	82
3.2.2	Nonsense suppression in hippocampal neurons	84
3.3	Discussion and Future Directions	86
3.4	Experimental methods and materials	90
3.4.1	Materials	90
3.4.2	Mutagenesis and tRNA synthesis	90
3.4.3	Tissue culture	91
3.4.4	Electroporation	91
3.4.5	Microscopy	92
3.5	References	93

## **Chapter 4**

### Natural and Unnatural Amino Acid Incorporation into Ion Channels

	Expressed in Mammalian Cells by Nonsense Suppression	96
4.1	Introduction	97
4.2	Results and Discussion	98
4.2.1	nAChR expression by HSAS suppression	98
	4.2.1.1 Results	99
	4.2.1.2 Discussion	102
4.2.2	nAChR expression by unnatural amino acid incorporation	102
	4.2.2.1 Results	103
	4.2.2.2 Discussion	106

4.2.3	Attempts at neuronal $\alpha 4\beta 2$ expression by nonsense suppression	107
4.2.3.1	Results	109
4.2.3.2	Disussion	111
4.2.4	NMDA receptor expression by nonsense suppression	112
4.2.4.1	Results	114
4.2.4.2	Discussion	118
4.3	Conclusions	120
4.4	Experimental methods and materials	122
4.4.1	Materials	122
4.4.2	Mutagenesis, mRNA and tRNA synthesis	122
4.4.3	Tissue culture	123
4.4.4	Electroporation	123
4.4.5	Microscopy	124
4.4.6	Electrophysiology	124
4.5	References	126

## List of Figures

Figure 1.1	Unnatural amino acids incorporated into proteins using the <i>Xenopus</i> oocyte expression system	3
Figure 1.2	Unnatural amino acid incorporation by nonsense suppression	5
Figure 2.1	Amber suppressor tRNAs tested in developing a mammalian cell expression system for unnatural amino acids.	19
Figure 2.2	Western blot demonstrating nonsense suppression by THG73-ValOH and HSAS in rabbit reticulocyte lysate.	20
Figure 2.3	Western blot demonstrating nonsense suppression by THG73-F <sub>2</sub> W and HSAS in rabbit reticulocyte lysate.	21
Figure 2.4	Western blot demonstrating that EQAS is not an efficient suppressor tRNA in rabbit reticulocyte lysate.	22
Figure 2.5	Western blot demonstrating that EAAS and EYAS are not efficient suppressor tRNAs in rabbit reticulocyte lysate	22
Figure 2.6	The microelectroporator used for transfecting adherent mammalian cells.	25
Figure 2.7	Wild-type EGFP expression in CHO-K1 cells by transfection with pCS2gapEGFP DNA.	26
Figure 2.8	Wild-type EGFP expression in CHO-K1 cells by transfection with pCS2gapEGFP mRNA.	26
Figure 2.9	Electroporation of rhodamine-green tRNA into CHO-K1 cells.	27
Figure 2.10	Testing the stability of tRNA-aa at pH 7.4 (10 minute incubation) by in vitro translation.	29
Figure 2.11	Testing the stability of THG73-Ala at pH 7.4 (≥ 1 hour incubation) by in vitro translation.	30
Figure 2.12	Testing the stability of THG73-ValOH at pH 7.4 (≥ 1 hour incubation) by in vitro translation	30
Figure 2.13	Testing the stability of THG73-aa in the presence of the CO <sub>2</sub> independent electroporation buffer by in vitro translation.	31

Figure 2.14	Electroporation of CHO-K1 cells using Epizap.	34
Figure 2.15	Electroporation of HEK cells using Epizap.	35
Figure 2.16	Agarose gel showing the results of TMR-MI coupling reactions with 5'-phosphorothioate labeled tRNA (tRNA-PO <sub>3</sub> S)	39
Figure 2.17	PAGE gel showing attempts to couple tRNA-PO <sub>3</sub> S to the ANTP peptide.	41
Figure 2.18	ANTP-tRNA coupling strategy.	42
Figure 2.19	PAGE gel showing the coupling reactions of HSAS 5'14mer to the ANTP peptide (PTD).	43
Figure 2.20	PAGE gel showing the coupling reactions of HSAS 5'14mer to the ANTP peptide (PTD), high salt conditions.	44
Figure 2.21	PAGE gel showing the coupling reactions between EQAS 14mer RNA, 5'thiol-modified, with the ANTP peptide (PTD).	45
Figure 2.22	PAGE gel showing the tRNA ligation reaction between HSAS 3'71mer and HSAS 5'14mer.	46
Figure 2.23	ANTP delivery of tRNA to CHO-K1 cells by non-covalent coupling, 30 minutes after transfection.	48
Figure 2.24	ANTP delivery of tRNA to CHO-K1 cells by non-covalent coupling, 24 hours after transfection.	49
Figure 2.25	Non-covalent delivery of HSAS tRNA to CHO-K1 cells by ANTP	50
Figure 2.26	Effectene transfection of CHO-K1 cells with EGFP DNA and HSAS tRNA.	53
Figure 2.27	Effectene transfection of HEK cells with EGFP DNA and HSAS tRNA.	54
Figure 2.28	Effectene transfection of COS1 cells with EGFP DNA and HSAS tRNA.	54
Figure 2.29	Polyfect transfection of CHO-K1 cells with EGFP DNA and HSAS tRNA.	55

Figure 2.30	GeneJammer transfection of CHO-K1 cells with EGFP DNA and HSAS tRNA.	56
Figure 2.31	Lipofectamine 2000 transfection of CHO-K1 cells with EGFP DNA and HSAS tRNA.	57
Figure 2.32	Transfection of CHO-K1 cells using biolistics.	59
Figure 2.33	Oligo design for tRNA gene construction.	63
Figure 3.1	The human serine amber suppressor tRNA (HSAS) primary and secondary structure.	81
Figure 3.2	The HSAS suppression assay.	81
Figure 3.3	EGFP (pCS2gapEGFP) expression in CHO-K1 cells by nonsense suppression using HSAS tRNA.	83
Figure 3.4	EGFP (pEGFP-F) expression in HEK cells by nonsense suppression using HSAS tRNA.	84
Figure 3.5	EGFP (pEGFP-F) expression in hippocampal neurons by nonsense suppression using HSAS tRNA.	85
Figure 4.1	nAChR expression in CHO-K1 cells by nonsense suppression using HSAS tRNA.	101
Figure 4.2	The $\alpha$ Trp149 of the muscle-type nAChR interacts with acetylcholine via a cation- $\pi$ type interaction.	103
Figure 4.3	Incorporation of natural and unnatural amino acids into the nAChR expressed in CHO-K1 cells by nonsense suppression using chemically aminoacylated THG73 tRNA.	105
Figure 4.4	The anomalous behavior of nicotine binding at the muscle-type nAChR.	108
Figure 4.5	A typical whole-cell patch clamp response from a CHO-K1 cell transfected with $\alpha$ 4 $\beta$ 2.	110
Figure 4.6	Expression of wt NMDA receptors in CHO-K1 cells.	115
Figure 4.7	Expression and Mg <sup>2+</sup> block (50 ms application) of wt NMDA receptors.	116

Figure 4.8	Expression and $Mg^{2+}$ block (1 s application) of wt NMDA receptors.	117
Figure 4.9	Expression of wt NMDA receptors in CHO-K1 cells by nonsense suppression.	118

**List of Tables**

Table 2.1	Attempts to recover EGFP using various tRNA-aa for nonsense suppression.	28
-----------	--	----

## **Chapter 1**

### Introduction

## 1.1 The nonsense suppression methodology for unnatural amino acid incorporation

Site-specific incorporation of unnatural amino acids into proteins has become an invaluable tool in protein structure function studies. Examples include studies of protein stability, enzyme mechanisms, the incorporation of biophysical probes (fluorescent amino acids and spin labels) and photoreactive side chains (caged amino acids), and backbone mutations [1-5]. This technique was first employed by the use of in vitro translation systems (*E. coli* and rabbit reticulocyte), where the labs of Schultz, Chamberlin and Hecht have studied a wide variety of proteins using these expression systems [6, 7]. The use of unnatural amino acids has since been expanded to a *Xenopus* oocyte in vivo translation system [8], which has been used by our lab to study ion channels and neuroreceptors. Although these expression systems have provided a wealth of information, they do have their limitations. Because *Xenopus* oocytes are intact cells, this translation system is more physiologically relevant than cell free systems. However, many of the proteins that are studied are of mammalian origin, and there are a growing number of examples addressing protein-protein interactions of mammalian cellular signaling pathways. Since proteins do not function as discrete entities within a cell, but rather in concert with many proteins, it would be more relevant to study these proteins in an expression system that more closely resembles their natural environment. Removing a protein from its natural environment limits any conclusions that can be drawn. This research report therefore addresses efforts to incorporate unnatural amino acids into proteins expressed in mammalian cells.



encoding for  $\beta$ -lactamase that contains a TAG codon in place of the Phe66 codon (via standard site directed mutagenesis). Because there are no endogenous tRNAs that recognize the TAG codon, only the unnatural amino acid on the amber suppressor tRNA was incorporated at that position of the protein. This was in competition with translation termination, so a mixture of truncated protein and full-length protein bearing the unnatural amino acid was generated. Importantly, while the yeast amber suppressor tRNA is recognized by the *E. coli* translational machinery, it is orthogonal to the aminoacyl synthetases. Therefore the unnatural amino acid was not replaced with Phe. Research in both the Schultz and Hecht labs has subsequently led to great success with unnatural amino acid incorporation using the yeast amber suppressor tRNA in in vitro translation systems [14-17], where as Chamberlin uses an *E. coli* tRNA<sup>Gly</sup>(CUA) amber suppressor [3, 6, 12, 18]. Since the development of the technique, Schultz has developed an improved amber suppressor tRNA - *E. coli* tRNA<sup>Asn</sup>(CUA) - that shows a higher ratio of full length protein to truncated in an *E. coli* expression system [19].

Sisido and coworkers have taken a different approach to unnatural amino acid incorporation into proteins. Rather than using suppressor tRNAs, they have designed tRNAs that read four-base [20, 21], or even five-base codons [22]. Multiple stop codons (just downstream of the four/five base codon) are engineered into the message if a frameshift occurs by an endogenous tRNA encoding for the first three nucleotides. This technique then allows for the incorporation of more than one unnatural amino acid [23], since each can have a unique four/five base codon.

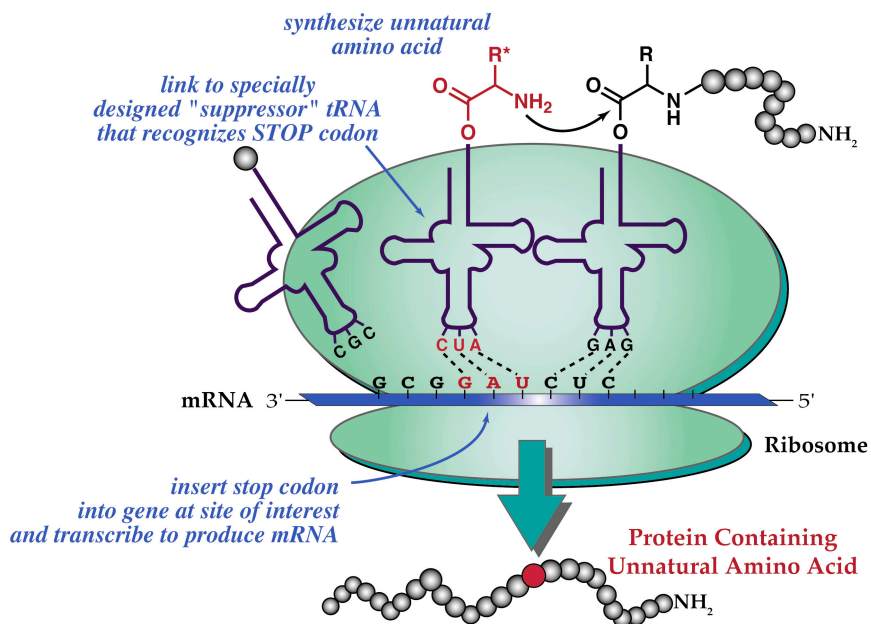


**Figure 1.2.** Unnatural amino acid incorporation by nonsense suppression. The unnatural amino acid is first synthesized, coupled to an in vitro transcribed suppressor tRNA, and incorporated into the desired expression system. Likewise, the mRNA encoding for the protein of interest is mutated to incorporate a TAG stop codon at the desired site of unnatural amino acid incorporation.

A limitation of the nonsense suppression methodology is that the aminoacylated tRNA is a stoichiometric reagent. To therefore generate enough protein for characterization, either the use of very large quantities of aminoacylated tRNA or a very sensitive assay is required. In our lab, the latter approach has been taken. An in vivo *Xenopus* oocyte expression system is used to study ion channels and neuroreceptors [8]. These proteins are ideal candidates for the unnatural amino acid technique. Membrane bound proteins are more difficult to study than soluble proteins in that they require cellular trafficking machinery and a membrane to fold and assemble correctly. They are also difficult to over-express, making it difficult to obtain crystal structures. The unnatural amino acid technique offers a convenient way to probe protein structure and function since they can be modified very specifically with unnatural amino acids, and

their function can be assayed by very sensitive electrophysiological techniques [4, 5]. Information on ligand binding and ion channel gating mechanisms has been obtained on a variety of ion channels using this method including the nicotinic acetylcholine receptor (nAChR) [24-29], the serotonin receptors 5-HT<sub>3A</sub> [30] and MOD-1 [31] (latter derived from *Caenorhabditis elegans*), and the Shaker [32] and Kir2.1 [33] potassium channels.

The *Xenopus* oocyte expression required the engineering of a new amber suppressor tRNA because Schultz's yeast amber suppressor was not orthogonal to this system. The first amber suppressor designed, MN3, was a modified version of the yeast tRNA<sup>Phe</sup>(CUA) [24]. There was poor orthogonality to this expression system, however. Subsequently an improved tRNA construct has been engineered, derived from *Tetrahymena thermophila*. This organism uses a nonstandard genetic code where TAG encodes for glutamine. U to G modification at position 73 reduced recognition by endogenous *Xenopus* glutamine synthetases, generating an amber suppressor superior to MN3 [34]. This is charged with unnatural amino acids, and is co-injected with mRNA encoding for the protein of interest into *Xenopus* oocytes.

The use of unnatural amino acids has evolved from in vitro translation systems to an in vivo translation system. The next challenge is to progress to a mammalian expression system. This would provide a more relevant model system when studying mammalian proteins.

## 1.2 Nonsense suppression in mammalian cells

Prior to 1982, nonsense suppression was studied in yeast and bacteria but not in mammalian cells [9, 10]. However, nonsense mutations are associated with some diseases, and it was thought that suppressor tRNAs could be used in genetic therapy. As a first effort toward this goal, RajBhandary and Sharp demonstrated that exogenous tRNAs could be properly spliced, processed and modified in transfected CV-1 (monkey kidney) cells that had been transfected with the tRNA<sup>Tyr</sup> gene. Their tRNA<sup>Tyr</sup> construct was derived from *Xenopus laevis*, and was aminoacylated by the endogenous CV-1 tyrosine synthetase (TyrRS) [35]. They subsequently mutated this tRNA to be an amber (UAG) suppressor which was still recognized by the CV-1 TyrRS. Suppression of amber nonsense mutant reporter genes by tRNA<sup>Tyr</sup>(UAG) was achieved in an in vitro reticulocyte translation system, as well as in cultured CV-1 cells by viral cotransfection [36] or microinjection of the tRNA<sup>Tyr</sup> gene (DNA) [37]. The suppression efficiencies ranged from 20 to 40% of wild-type protein expression. Interestingly, in the viral cotransfection studies it was determined that 24 to 48 hours between suppressor tRNA transfection and reporter gene transfection led to optimal suppression [38].

A new generation of suppressor tRNAs was later developed by RajBhandary, Sharp and Capone, derived from a human serine tRNA [39]. All three amber, opal and ochre suppressor tRNAs were made and virally transfected into CV-1 cells. The suppression efficiency of the amber mutant was found to be 25 to 30%, and the ochre ~15%. Suppression of the opal constructs was initially unsuccessful, but was later achieved in both CV-1 and mouse NIH3T3 cells [40]. In this latter report, it was shown

that the suppression efficiencies ranged from 10 to 50% of that of wild-type protein expression, was typically higher in CV-1 cells than NIH3T3 cells and ranked in the order amber > opal > ochre.

All of the above examples are of cells that continuously express both suppressor tRNA and nonsense mutant reporter genes. To harness control of nonsense suppression, such that it can be turned on and off, inducible amber suppressor systems have been developed. One example employed the use of a temperature-sensitive viral vector carrying the gene encoding for human tRNA<sup>Ser</sup>(UAG) in CV-1 cells [41]. At 39.5°C nonsense suppression was blocked, but at 33°C transcription of the suppressor tRNA was turned on. Alternatively, Capone and coworkers took advantage of the *lac* operator/repressor system in HeLa cells stably transfected with the human tRNA<sup>Ser</sup>(UAG) gene [42]. By the incorporation of the *lac* repressor upstream of the coding region, suppression was inhibited until the inducer IPTG was applied.

An elegant example of an inducible nonsense suppression system was developed by RajBhandary, and integrates almost 20 years of research. Because the inducible expression systems discussed above depend upon aminoacylation of the suppressor tRNAs by endogenous synthetases, there is read through observed and hence a background level of protein expression. RajBhandary and coworkers took a different approach by controlling the suppressor tRNA function rather than tRNA expression [43]. They reported the development of an *E. coli* tRNA<sup>Gln</sup>(UAG) amber suppressor that is orthogonal to the mammalian glutamine synthetase (GlnRS) of both CV-1 and COS-1 cells (monkey). Suppression was achieved when the amber suppressor tRNA was co-expressed with both a mutant CAT reporter gene and *E. coli* GlnRS, hence

aminoacylation of the suppressor tRNA was dependent upon its own synthetase. This was later fine tuned by placing the *E. coli* GlnRS gene under the control of the tetracycline regulatory element [44]. Both HeLa (human) and COS-1 cells were stably transfected with this gene, along with genes encoding for the *E. coli* tRNA<sup>Gln</sup>(UAG) amber suppressor and the mutant CAT reporter. Suppression was blocked in the presence, and initiated in the absence of tetracycline.

### **1.3 Delivery of aminoacyl-tRNA to mammalian cells**

To use unnatural amino acids in mammalian cells, a method must be devised for delivering charged tRNAs. This method must be capable of delivering large quantities of tRNA to the cells since aminoacyl-tRNAs are a stoichiometric reagent, and should also be able to deliver *both* aminoacyl-tRNA and the reporter gene (DNA or mRNA) to cells. Delivery should be rapid because of the susceptibility of the aminoacyl ester linkage to hydrolysis. Also, this method should not disrupt normal cell physiology, and should be applicable to a variety of cells lines. For the study of neuronal ion channels, it would be useful if the methodology could be easily transferred to neurons.

There are only a few examples of delivering exogenous tRNA to mammalian cells. Deutscher has reported aminoacyl-tRNA delivery by electroporation [45] and saponin mediated cell permeabilization [46]. In this example, total RNA from cell extracts were delivered to cells, rather than purified or in vitro transcribed aminoacyl tRNA. More recently, RajBhandary and coworkers have shown the delivery of both amber and ochre suppressor aminoacyl-tRNAs (purified from *E. coli*) to COS-1 cells

using the transfection reagent Effectene (Qiagen) [47]. They observed suppression of chloramphenicol acetyl transferase, mutated to contain the corresponding stop codon within the coding region. Lastly, Vogel and coworkers demonstrated nonsense suppression of EGFP with aminoacyl-tRNA [48]. They microinjected CHO cells with chemically aminoacylated in vitro transcribed amber suppressor tRNA. In none of these examples was an unnatural amino acid delivered to mammalian cells.

An alternate approach to site-specific unnatural amino acid incorporation was reported by Yokoyama and coworkers [49]. They expressed in CHO-Y cells a mutant *E. coli* tyrosine synthetase that aminoacylates *B. Stearothermophilus* amber suppressor tRNA with 3-iodo-L-tyrosine. This is significant work toward engineering cells with novel amino acids, but is complicated by the requirement that each new amino acid has a specific engineered synthetase and tRNA. For our purposes, chemical aminoacylation of tRNA has the distinct advantage of not being amino acid specific and no protein engineering is required, and therefore it is a more general technique.

It was our ultimate goal to develop a general method for unnatural amino acid incorporation into mammalian cells. Toward this goal, a variety of transfection methods were tested, including electroporation, lipofection, peptide-mediated delivery and biolistics. We also tested several suppressor tRNAs. By not being limited to the *Xenopus* oocyte expression system, the use of unnatural amino acids in studying protein structure-function relationships in cell-specific signaling cascades will be greatly expanded. This will advance our studies on neuronal ion channels, as well as making the use of unnatural amino acids more attainable to a broader cross-section of researchers.

## 1.4 References

1. Cornish, V.W., et al., *Site-specific incorporation of biophysical probes into proteins*. Proc Natl Acad Sci USA, 1994. **91**: p. 2910-2914.
2. Cornish, V.W., D. Mendel, and P.G. Schultz, *Probing protein structure and function with an expanded genetic code*. Angew Chem Int Ed Engl, 1995. **34**: p. 621-633.
3. Gillmore, M.A., L.E. Steward, and A.R. Chamberlin, *Incorporation of noncoded amino acids by in vitro protein biosynthesis*. Topics Curr Chem, 1999. **202**: p. 77-99.
4. Dougherty, D.A., *Unnatural amino acids as probes of protein structure and function*. Curr Opin Chem Biol, 2000. **4**(6): p. 645-52.
5. Beene, D.L., D.A. Dougherty, and H.A. Lester, *Unnatural amino acid mutagenesis in mapping ion channel function*. Curr Opin Neurobiol, 2003. **13**(3): p. 264-70.
6. Steward, L.E. and A.R. Chamberlin, *Protein engineering with nonstandard amino acids*. Methods Mol Biol, 1998. **77**: p. 325-54.
7. Thorson, J.S., et al., *A biosynthetic approach for the incorporation of unnatural amino acids into proteins*. Methods Mol Biol, 1998. **77**: p. 43-73.
8. Nowak, M.W., et al., *In vivo incorporation of unnatural amino acids into ion channels in a Xenopus oocyte expression system*. Methods Enzymol., 1998. **293**: p. 504-529.
9. Piper, P.W., *Characterisation and sequence analysis of nonsense suppressor tRNAs from Saccharomyces cerevisiae*, in *Nonsense mutations and tRNA suppressors*, J.E. Celis and J.D. Smith, Editors. 1979, Academic Press: London. p. 155-172.
10. Smith, J.D., *Suppressor tRNAs in prokaryotes*, in *Nonsense mutations and tRNA suppressors*, J.E. Celis and J.D. Smith, Editors. 1979, Academic Press: London. p. 109-126.
11. Noren, C.J., et al., *A general method for site-specific incorporation of unnatural amino acids into proteins*. Science, 1989. **244**(4901): p. 182-8.
12. Bain, J.D., et al., *Biosynthetic site-specific incorporation of a non-natural amino acid into a polypeptide*. J. Am. Chem. Soc., 1989. **111**: p. 8013-8014.

13. Heckler, T.G., et al., *T4 RNA ligase mediated preparation of novel "chemically misacylated" tRNAPheS*. *Biochemistry*, 1984. **23**(7): p. 1468-73.
14. Arslan, T.S., et al., *Structurally modified firefly luciferase. Effects of amino acid substitution at position 286*. *J. Am. Chem. Soc.*, 1997. **119**(45): p. 10877-10887.
15. Karginov, A.V., M. Lodder, and S.M. Hecht, *Facile characterization of translation initiation via nonsense codon suppression*. *Nucleic Acids Res.*, 1999. **27**(16): p. 3283-3290.
16. Karginov, V.A., et al., *Probing the role of an active site aspartic acid in dihydrofolate reductase*. *J. Am. Chem. Soc.*, 1997. **119**: p. 8166-8176.
17. Karginov, V.A., S.V. Mamaev, and S.M. Hecht, *In vitro suppression as a tool for the investigation of translation initiation*. *Nucleic Acids Res*, 1997. **25**(19): p. 3912-6.
18. Steward, L.E., et al., *In vitro site-specific incorporation of fluorescent probes into  $\beta$ -galactosidase*. *J. Am. Chem. Soc.*, 1997. **119**: p. 6-11.
19. Cload, S.T., et al., *Development of improved tRNAs for in vitro biosynthesis of proteins containing unnatural amino acids*. *Chem Biol*, 1996. **3**(12): p. 1033-8.
20. Hohsaka, T. and M. Sisido, *Incorporation of non-natural amino acids into proteins*. *Curr Opin Chem Biol*, 2002. **6**(6): p. 809-15.
21. Hohsaka, T., et al., *Incorporation of nonnatural amino acids into proteins by using various four-base codons in an Escherichia coli in vitro translation system*. *Biochemistry*, 2001. **40**(37): p. 11060-11064.
22. Hohsaka, T., et al., *Five-base codons for incorporation of nonnatural amino acids into proteins*. *Nucleic Acids Research*, 2001. **29**(17): p. 3646-3651.
23. Hohsaka, T., et al., *Incorporation of two different nonnatural amino acids independently into a single protein through extension of the genetic code*. *J. Am. Chem. Soc.*, 1999. **121**: p. 12194-12195.
24. Nowak, M.W., et al., *Nicotinic receptor binding site probed with unnatural amino acid incorporation in intact cells*. *Science*, 1995. **268**(5209): p. 439-42.
25. Li, L.T., et al., *The tethered agonist approach to mapping ion channel proteins toward a structural model for the agonist binding site of the nicotinic acetylcholine receptor*. *Chemistry & Biology*, 2001. **8**(1): p. 47-58.
26. Petersson, E.J., et al., *A perturbed pK(a) at the binding site of the nicotinic acetylcholine receptor: Implications for nicotine binding*. *J Am Chem Soc*, 2002. **124**(43): p. 12662-12663.

27. Kearney, P.C., et al., *Determinants of nicotinic receptor gating in natural and unnatural side chain structures at the M2 9' position*. *Neuron*, 1996. **17**(6): p. 1221-9.
28. Miller, J.C., et al., *Flash decaging of tyrosine sidechains in an ion channel*. *Neuron*, 1998. **20**(4): p. 619-24.
29. Zhong, W., et al., *From ab initio quantum mechanics to molecular neurobiology: A cation- $\pi$  binding site in the nicotinic receptor*. *Proc Natl Acad Sci USA*, 1998. **95**: p. 12088-12093.
30. Beene, D., et al., *Cation- $\pi$  interactions in ligand recognition by serotonergic (5-HT<sub>3A</sub>) and nicotinic acetylcholine receptors: The anomalous binding properties of nicotine*. *Biochemistry*, 2002. **41**(32): p. 10262-10269.
31. Mu, T.W., H.A. Lester, and D.A. Dougherty, *Different Binding Orientations for the Same Agonist at Homologous Receptors: A Lock and Key or a Simple Wedge?* *J. Am. Chem. Soc.*, 2003. **125**(23): p. 6850-6851.
32. England, P.M., et al., *Site-specific, photochemical proteolysis applied to ion channels in vivo*. *Proc Natl Acad Sci USA*, 1997. **94**(20): p. 11025-30.
33. Tong, Y.H., et al., *Tyrosine decaging leads to substantial membrane trafficking during modulation of an inward rectifier potassium channel*. *J Gen Physiol*, 2001. **117**(2): p. 103-118.
34. Saks, M.E., et al., *An engineered Tetrahymena tRNA<sup>Gln</sup> for in vivo incorporation of unnatural amino acids into proteins by nonsense suppression*. *J Biol Chem*, 1996. **271**(23169-23175): p. 23169-23175.
35. Laski, F.A., et al., *Expression of a X. laevis tRNA<sup>Tyr</sup> gene in mammalian cells*. *Nucleic Acids Res*, 1982. **10**(15): p. 4609-26.
36. Laski, F.A., et al., *An amber suppressor tRNA gene derived by site-specific mutagenesis: cloning and function in mammalian cells*. *Proc Natl Acad Sci U S A*, 1982. **79**(19): p. 5813-7.
37. Hudziak, R.M., et al., *Establishment of mammalian cell lines containing multiple nonsense mutations and functional suppressor tRNA genes*. *Cell*, 1982. **31**(1): p. 137-46.
38. Summers, W.P., et al., *Functional suppression in mammalian cells of nonsense mutations in the herpes simplex virus thymidine kinase gene by suppressor tRNA genes*. *J Virol*, 1983. **47**(2): p. 376-9.
39. Capone, J.P., P.A. Sharp, and U.L. RajBhandary, *Amber, ochre and opal suppressor tRNA genes derived from a human serine tRNA gene*. *Embo J*, 1985. **4**(1): p. 213-21.

40. Capone, J.P., et al., *Introduction of UAG, UAA, and UGA nonsense mutations at a specific site in the Escherichia coli chloramphenicol acetyltransferase gene: use in measurement of amber, ochre, and opal suppression in mammalian cells*. Mol Cell Biol, 1986. **6**(9): p. 3059-67.
41. Sedivy, J.M., et al., *An inducible mammalian amber suppressor: propagation of a poliovirus mutant*. Cell, 1987. **50**(3): p. 379-89.
42. Syroid, D.E., R.I. Tapping, and J.P. Capone, *Regulated expression of a mammalian nonsense suppressor tRNA gene in vivo and in vitro using the lac operator/repressor system*. Mol Cell Biol, 1992. **12**(10): p. 4271-8.
43. Drabkin, H.J., H.J. Park, and U.L. RajBhandary, *Amber suppression in mammalian cells dependent upon expression of an Escherichia coli aminoacyl-tRNA synthetase gene*. Mol Cell Biol, 1996. **16**(3): p. 907-13.
44. Park, H.J. and U.L. RajBhandary, *Tetracycline-regulated suppression of amber codons in mammalian cells*. Mol Cell Biol, 1998. **18**(8): p. 4418-25.
45. Negrutskii, B.S. and M.P. Deutscher, *Channeling of aminoacyl-tRNA for protein synthesis in vivo*. Proc Natl Acad Sci U S A, 1991. **88**(11): p. 4991-5.
46. Negrutskii, B.S., R. Stapulionis, and M.P. Deutscher, *Supramolecular organization of the mammalian translation system*. Proc Natl Acad Sci U S A, 1994. **91**(3): p. 964-8.
47. Kohrer, C., et al., *Import of amber and ochre suppressor tRNAs into mammalian cells: a general approach to site-specific insertion of amino acid analogues into proteins*. Proc Natl Acad Sci U S A, 2001. **98**(25): p. 14310-5.
48. Ilegems, E., H.M. Pick, and H. Vogel, *Monitoring mis-acylated tRNA suppression efficiency in mammalian cells via EGFP fluorescence recovery*. Nucleic Acids Res, 2002. **30**(23): p. e128.
49. Sakamoto, K., et al., *Site-specific incorporation of an unnatural amino acid into proteins in mammalian cells*. Nucleic Acids Res, 2002. **30**(21): p. 4692-9.

## **Chapter 2**

Developing a Mammalian Cell Expression System for Unnatural Amino  
Acid Incorporation: Screening Suppressor tRNAs and Transfection Methods

## 2.1 Introduction

Unnatural amino acid incorporation into proteins by nonsense suppression has proven to be a valuable tool for structure-function studies [1-5]. Using the *in vivo* nonsense suppression methodology [6], information on ligand binding and ion channel gating mechanisms has been obtained on a variety of ion channels including the nicotinic ACh receptor (nAChR) [7-12], 5-HT<sub>3A</sub> receptor [13], and the Shaker [14] and Kir2.1 [15] potassium channels. To date, such studies have been limited to the *Xenopus* oocyte heterologous expression system. There would be clear benefits to expanding the technology to a mammalian cell expression system. This would provide a more relevant environment for many proteins of mammalian origin and would allow for studies of cell-specific signal transduction pathways.

When developing a new expression system for unnatural amino acid incorporation, there are many variables to be considered. Importantly, a suppressor tRNA needs to be identified. This tRNA must be orthogonal to the endogenous tRNA synthetases, yet still be recognized by the translational machinery of the cell. For the *Xenopus* oocyte expression system, a tRNA derived from *Tetrahymena thermophilus* has been optimized for unnatural amino acid delivery, THG73 [16]. This tRNA is an obvious candidate to test in mammalian cells, but is not necessarily the best suppressor tRNA. For this reason, several suppressor tRNAs - including tRNAs specifically designed for mammalian expression systems - must be tested. These include the human serine amber suppressor (HSAS) [17], the *E. coli* alanine amber suppressor (EAAS) [18], *E. coli* glutamine amber suppressor (EQAS) [19, 20] and the *E. coli* tyrosine amber suppressor (EYAS) [21].

A variety of methods to deliver tRNA to mammalian cells must also be explored. One needs to deliver enough aminoacyl-tRNA to each cell in order to generate a detectable amount of protein. One of the greatest challenges in developing a mammalian cell expression system for unnatural amino acid incorporation arises from the fact that the aminoacyl-tRNA is a stoichiometric reagent. The amount of protein made containing the unnatural amino acid is limited by the amount of aminoacyl-tRNA that can be delivered to the cell. Because of the relatively small size of mammalian cells (10 - 30  $\mu\text{M}$  in width) in comparison to *Xenopus* oocytes (diameter  $\sim$  1 mm), much less aminoacyl-tRNA can be delivered to the former, hence less protein can be made.

Initial experiments by Dr. Pamela England involved microinjection into mammalian cells. These experiments were unfortunately unsuccessful. Several factors may have accounted for this, one being clogging of the pipette due to high concentrations of aminoacyl-tRNA used. Microinjection is a tedious transfection method, so rather than pursuing this method further we set out to develop a transfection technique that would be efficient, easy and general. We explored a variety of techniques including electroporation, peptide-mediated transfection, lipofection, and biolistics.

## **2.2 Results and Discussion**

### **2.2.1 Screening suppressor tRNAs in vitro**

For the *Xenopus* oocyte expression system, the suppressor tRNA THG73 was optimized to maximize protein expression while maintaining orthogonality to the endogenous synthetases. THG73 is an obvious candidate to test for a mammalian

expression system, however there are other amber suppressor tRNAs that have been used successfully in mammalian expression systems (Figure 2.1). The human serine amber suppressor HSAS is a tRNA that is recognized and aminoacylated by endogenous mammalian serine synthetases, and is therefore not suitable for unnatural amino acid delivery [17]. However, HSAS is a useful tool for optimizing DNA delivery to mammalian cells (discussed in detail in Chapter 3). Importantly, there have been examples of orthogonal amber suppressor tRNAs used for nonsense suppression in mammalian cells. For example, Vogel and co-workers recently described successful EGFP fluorescence recovery by nonsense suppression by microinjection of aminoacyl-EAAS (*E. coli* alanine amber suppressor tRNA) into CHO cells [18]. RajBhandary demonstrated suppression of chloramphenicol acetyl-transferase (CAT) using the transfection reagent Effectene (Qiagen) to deliver aminoacyl-EYAS (*E. coli* tyrosine amber suppressor tRNA) [21]. An older example of nonsense suppression in mammalian cells also comes from the labs of RajBhandary. They found that the EQAS (*E. coli* glutamine amber suppressor) tRNA was orthogonal to COS1 and CV1 cells. Expression of the CAT gene by nonsense suppression was dependent on the co-expression of the *E. coli* glutamine amber suppressor tRNA gene and the *E. coli* glutamine synthetase [19, 20]. Although in this latter example the EQAS was expressed and aminoacylated by the cells, rather than being delivered after in vitro transcription, these experiments still demonstrate that EQAS is a functional and orthogonal amber suppressor tRNA that may be useful for unnatural amino acid incorporation. Because of their success in various expression systems, all of these tRNAs were tested for unnatural amino acid delivery into mammalian cells.

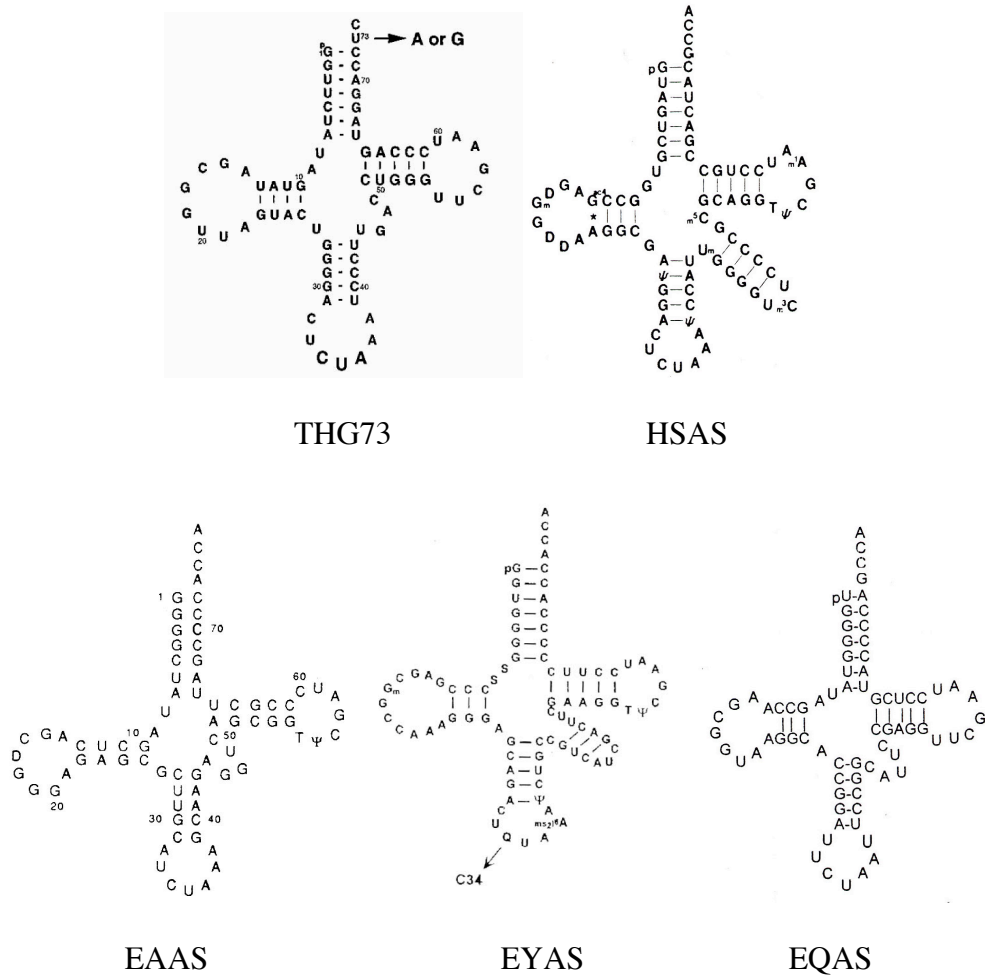
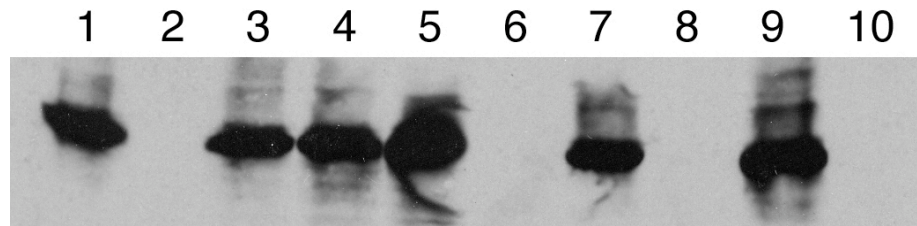


**Figure 2.1.** Amber suppressor tRNAs tested in developing a mammalian cell expression system for unnatural amino acids. THG73 (derived from *Tetrahymena thermophilus*); HSAS (human serine amber suppressor); EAAS (*E. coli* alanine amber suppressor); EYAS (*E. coli* tyrosine amber suppressor); EQAS (*E. coli* glutamine amber suppressor). In vitro transcribed tRNAs do not contain modified bases.

### 2.2.1.1 Results

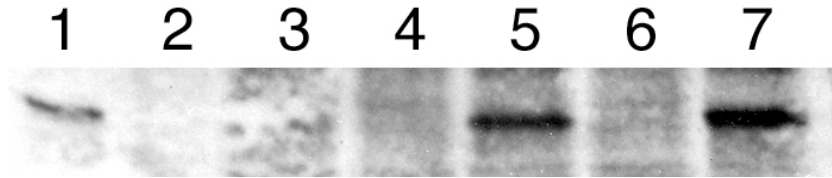
An in vitro transcription system was used to initially screen the amber suppressor tRNAs of interest. Rabbit reticulocyte lysate was used to approximate a mammalian cell expression system. mRNA encoding for the  $\alpha$  subunit of the muscle-type nAChR was used in all of the in vitro translation reactions, because it contained an HA epitope for use

in Western blots. As can be seen in Figure 2.2 and 2.3, both aminoacyl-THG73 and HSAS suppress several TAG mutants very efficiently, when compared to wild-type expression. In the case of THG73, efficient suppression is seen for both an amino acid (5,7-difluorotryptophan F<sub>2</sub>W) as well as an alpha-hydroxy acid (valine hydroxy acid ValOH). Importantly, no read-through is observed in the absence of aminoacyl-THG73.



1. wt alphaHA
2. Rainbow ladder
3. Ala122TAG + HSAS
4. Leu146TAG + HSAS
5. Tyr127TAG + HSAS
6. Ala122TAG + THG73 (74mer)
7. Ala122TAG + THG-ValOH
8. Tyr127TAG + THG73 (74mer)
9. Tyr127TAG + THG-ValOH
10. Blank (rabbit reticulocyte only)

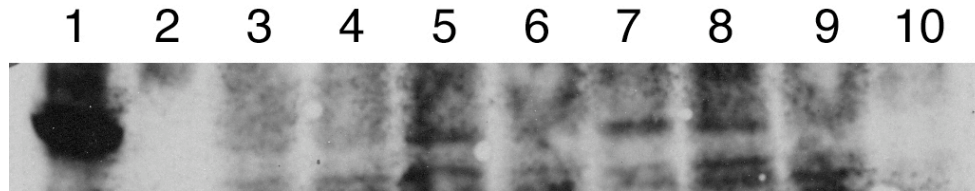
**Figure 2.2.** Western blot demonstrating nonsense suppression by THG73-ValOH and HSAS in rabbit reticulocyte lysate. The major band observed in each lane is the  $\alpha$  subunit of the muscle-type nAChR, and contains an HA epitope. Suppression by aminoacyl-THG73 was achieved using the valine alpha-hydroxy acid (ValOH).



1. wt alphaHA
2. Rainbow ladder
3. Blank (rabbit reticulocyte only)
4. Leu146TAG
5. Leu146TAG + HSAS
6. Leu146TAG + THG73 (74mer)
7. Leu146TAG + THG-F<sub>2</sub>W

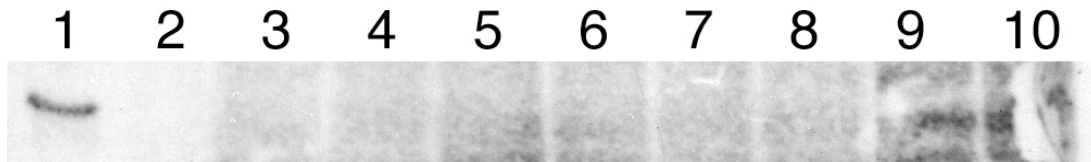
**Figure 2.3.** Western blot demonstrating nonsense suppression by THG73-F<sub>2</sub>W and HSAS in rabbit reticulocyte lysate. The major band observed in each lane is the  $\alpha$  subunit of the muscle-type nAChR, and contains an HA epitope. Suppression by aminoacyl-THG73 was achieved using the amino acid 5,7-difluorotryptophan (F<sub>2</sub>W).

The suppressor tRNAs EQAS, EAAS and EYAS were also tested in vitro. As shown in Figure 2.4, expression levels above background by EQAS suppression were not observed. EAAS also did not show any sign of suppression at all, and EYAS only resulted in a band that was slightly stronger than background (Figure 2.5).



1. wt alphaHA
2. rainbow ladder
3. Ala122TAG
4. Leu146TAG
5. Tyr127TAG
6. Ala122TAG + EQAS
7. Ala122TAG + EQAS-ValOH
8. Tyr127TAG + EQAS
9. Tyr127TAG + EQAS-ValOH
10. Blank (rabbit reticulocyte only)

**Figure 2.4.** Western blot demonstrating that EQAS is not an efficient suppressor tRNA in rabbit reticulocyte lysate. The major band observed in lane 1 is the  $\alpha$  subunit of the muscle-type nAChR, containing an HA epitope. Suppression was tested using EQAS aminoacylated with valine alpha-hydroxy acid (ValOH).



1. wt alphaHA
2. Rainbow ladder
3. Blank (rabbit reticulocyte only)
4. Leu146TAG
5. Leu146TAG + EAAS
6. Leu146TAG + EAAS-Ala
7. Leu146TAG + EAAS-Ala
8. Leu146TAG + EYAS
9. Leu146TAG + EYAS-Ala
10. Leu146TAG + EYAS-Ala

**Figure 2.5.** Western blot demonstrating that EAAS and EYAS are not efficient suppressor tRNAs in rabbit reticulocyte lysate. The major band observed in lane 1 is the  $\alpha$  subunit of the muscle-type nAChR, containing an HA epitope. Suppression was tested using EAAS or EYAS aminoacylated with alanine.

### 2.2.1.2 Discussion

From the data shown, it is clear that in rabbit reticulocyte THG73 and HSAS are the most efficient suppressor tRNAs tested. Furthermore, it is demonstrated that in this expression system THG73 is fully orthogonal to the endogenous synthetases and efficiently delivers amino acids and alpha-hydroxy acids. It is somewhat surprising that EQAS, EAAS and EYAS all functioned so poorly in our hands, since they have been used successfully in other labs. In the cases of EQAS and EYAS, RajBhandary and co-workers used the highly sensitive CAT assay, and this may explain the difference. It is more difficult to explain why EAAS did not work at all for us, since the assay used by Vogel and co-workers was to rescue wild-type EGFP in CHO cells, certainly not significantly more sensitive than our in vitro assay. We speculated that rabbit reticulocyte may not be an appropriate mimic of a mammalian cell, and decided that it was still worth testing these amber suppressor tRNAs in mammalian cells.

### 2.2.2 Electroporation of tRNA

Electroporation is a common method used to deliver many different types of macromolecules to cells, and is generally a favoured DNA transfection technique [22, 23]. It is operationally easy, reproducible, and works for many cell types including cultured neurons. Furthermore, cells that are either attached or in suspension can be transfected by electroporation. In essence, the application of an electric field to a population of cells results in reversible membrane breakdown, and the formation of large pores that allow the passage of macromolecules. The basic steps of electroporation include (i) electric field generation, (ii) polarization of the outer membrane, (iii) pore

formation, (iv) transmembrane transport and (v) electropore resealing. The mechanism of pore formation and resealing is not known. Another advantage to this technique is that there are many parameters to control for optimization, including electric field strength, pulse duration and the number of pulses applied. A disadvantage is that there is no standard protocol, so optimization must be done for each individual system studied. Finally, electroporation has been used to successfully deliver aminoacyl-tRNA (rabbit liver tRNA) to CHO cells, although in this report the tRNA was found to not be functional within the cells [24]. Because of its generality, electroporation was tested as a method to deliver tRNA to adherent mammalian cells.

#### 2.2.2.1 Microelectroporation

It can be imagined that electroporation of a large population of cells would require very large quantities of aminoacyl-tRNA. This can be circumvented using a "microporator" designed by Teruel and Meyer (Figure 2.6) [25, 26]. This electroporation device allows for the transfection of a small area of attached cells (10 mm<sup>2</sup>), using only a small volume of solution ( $\geq 1 \mu\text{l}$ ). They have demonstrated successful transfection using both DNA and mRNA, with over 90% cell survivability and over 50% transfection efficiency in rat basophilic leukemia cells, neocortical neuroblastoma cells and hippocampal neurons.

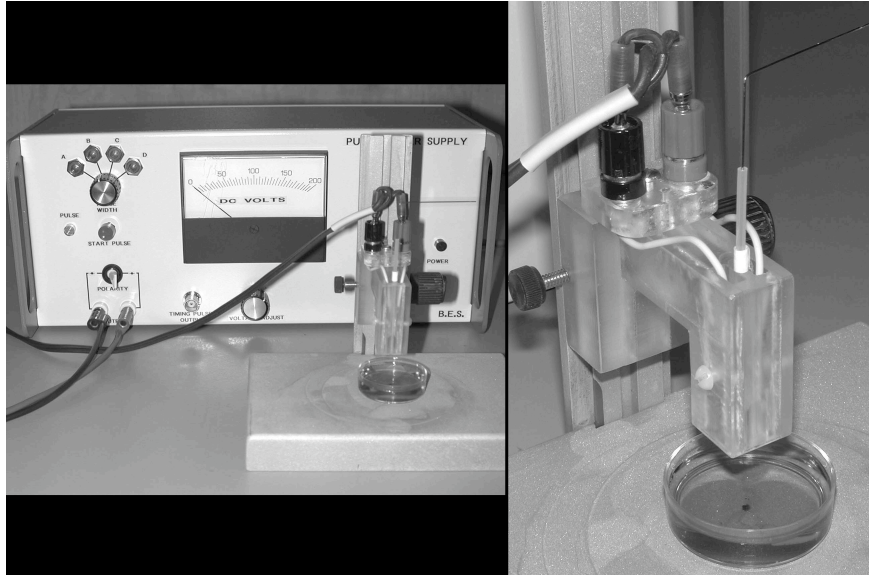


**Figure 2.6.** The microelectroporator used for transfecting adherent mammalian cells. A 35 mm dish is shown for scale. The power supply (left) can deliver up to 150 V, using 25, 50, 100 or 200 ms square pulses. The electrode holder (right) is lowered into a 35 mm dish of cultured cells, placing the electrodes 300  $\mu\text{M}$  above the adherent cells.

#### 2.2.2.1.1 Results

Electroporation of wild-type EGFP DNA and mRNA led to successful EGFP expression in CHO-K1 cells as shown in Figures 2.7 and 2.8. Transfections with DNA typically led to higher expression of EGFP, and expression could be seen as soon as 2 hours after transfection.

In order to determine if tRNA can be successfully delivered to cells using the microelectroporator, a fluorescently labeled tRNA was made. This was done by including rhodamine green-UTP (RhG-UTP) in the THG73 tRNA in vitro transcription reaction, at a ratio of 3 UTP to 1 RhG-UTP. The RhG-labeled tRNA was dialyzed to ensure that no free RhG-UTP was left when electroporating the cells. As can be seen in Figure 2.9, fluorescent tRNA was successfully delivered to CHO-K1 cells. Because it

was not possible to determine how many fluorophores were incorporated per tRNA molecule, the amount of tRNA delivered to each cell could not be quantified.

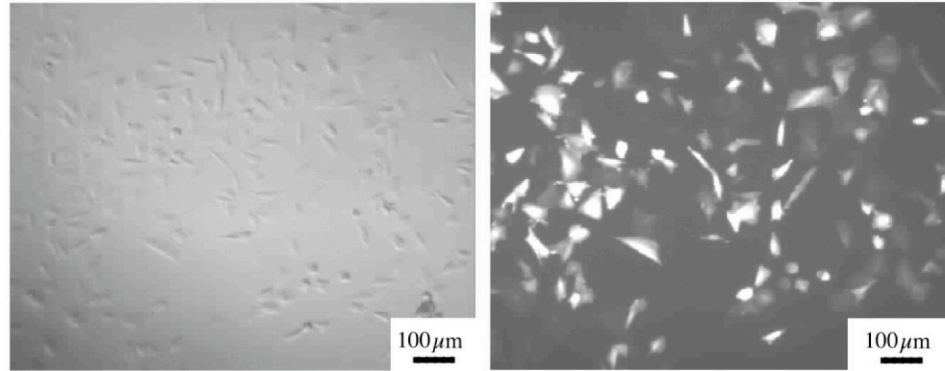


**Figure 2.7.** Wild-type EGFP expression in CHO-K1 cells by transfection with pCS2gapEGFP DNA. The cells were transfected with a 5  $\mu$ l solution containing 2.5  $\mu$ g/ $\mu$ l DNA, applying four 120 V, 50 ms pulses. The bright field (left) and fluorescence images (right) were taken 2 hours after transfection.

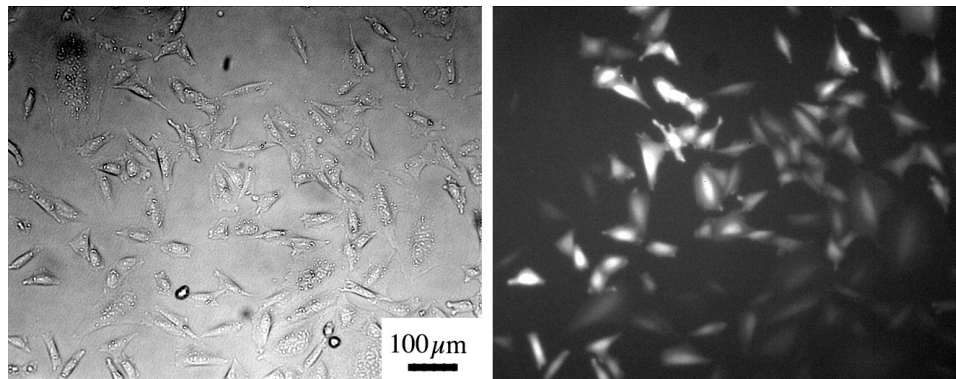


**Figure 2.8.** Wild-type EGFP expression in CHO-K1 cells by transfection with pCS2gapEGFP mRNA. The cells were transfected with a 10  $\mu$ l solution containing 3  $\mu$ g/ $\mu$ l DNA, applying four 120 V, 50 ms pulses. The bright field (left) and fluorescence images (right) were taken 3 hours after transfection.

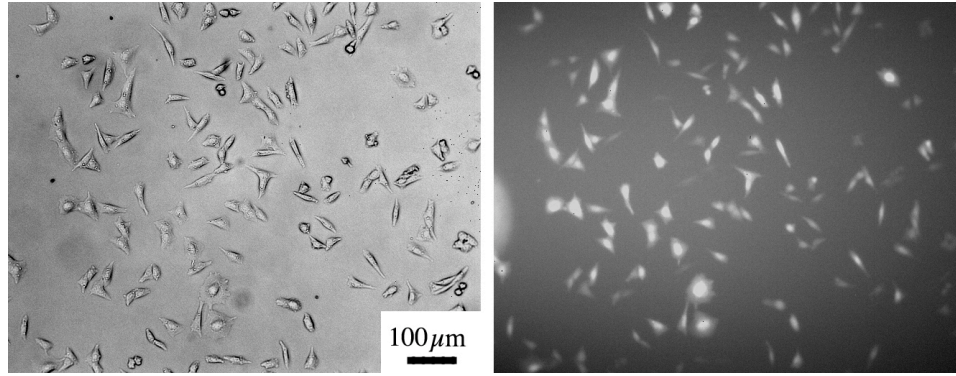


**Figure 2.9.** Electroporation of Rhodamine-Green tRNA into CHO-K1 cells. The cells were transfected with a 4  $\mu\text{l}$  solution of 1  $\mu\text{g}/\mu\text{l}$  RhG-tRNA (dialyzed), applying four 120 V, 50 ms pulses. The bright field (left) and fluorescence images (right) were taken immediately after transfection.

Given that the above results demonstrate that DNA, mRNA and tRNA can all be efficiently delivered to mammalian cells by electroporation, we wanted to next test the delivery of aminoacyl-tRNA (see Chapter 3 for detailed description of HSAS suppression of EGFP by electroporation). Toward this goal, we designed an EGFP assay. We made the EGFP mutants Ala37TAG, and Tyr66TAG to be co-electroporated with tRNA-Ala, or tRNA-Tyr, respectively. It was hoped that wild-type EGFP recovery would be observed in these experiments, while no EGFP expression would be observed in the absence of aminoacyl-tRNA. The mutant Val55TAG was also made for co-electroporation with tRNA-ValOH (valine alpha-hydroxy acid). The aminoacyl-linkage of alpha-hydroxy acids on tRNA is less susceptible to hydrolysis than for amino acids, so they can be easier to work with. Finally, we obtained the pT7EGFP Leu64TAG construct from the labs of Horst Vogel. They observed wild-type EGFP recovery using EAAS-Leu(4PO) for nonsense suppression by microinjection, therefore we wanted to test the electroporation method using these same constructs.

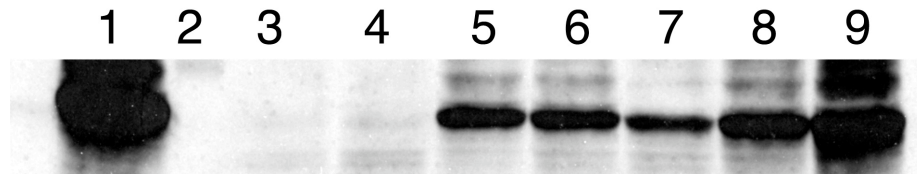
The results from these experiments are summarized in Table 2.1. In essence, EGFP recovery by nonsense suppression was not observed for any of the aminoacyl-tRNAs tested. Only HSAS suppression of Ser29TAG ever worked using EGFP recovery as an assay (see Chapter 3).

Amino Acid	tRNA Species					EGFP mutant
	THG73	HSAS	EQAS	EAAS	EYAS	
Ala(NVOC)	✘		✘	✘	✘	A37TAG
ValOH	✘		✘			V55TAG
Tyr(NVOC)	✘	✘				Y66TAG
Leu(4PO)				✘		L64TAG*
		✓				S29TAG

**Table 2.1** Attempts to recover EGFP using various tRNA-aa for nonsense suppression. The tRNAs THG73, HSAS, EQAS, EAAS and EYAS were aminoacylated with wild-type Ala or Tyr (NVOC protected), wild-type Leu (4PO protected) or with the valine alpha hydroxy acid (ValOH), and were tested for nonsense suppression using the various EGFP mutants shown. An "✘" represents failed experiments, i.e., no EGFP expression by nonsense suppression was observed using the corresponding tRNA-aa and EGFP mutant. A "✓" represents successful EGFP expression by nonsense suppression. An empty box represents combinations that were not attempted. \* pT7EGFP Leu64TAG was obtained from the Horst Vogel lab [18].

Because nonsense suppression was not observed for any tRNAs studied, including THG73 which has been shown to work very well in Rabbit Reticulocyte, we next sought out to ensure that amino acid wasn't hydrolyzing off of the tRNA during the electroporation protocol. Mammalian cells must be electroporated at physiological pH, but the aminoacyl-ester bond between the tRNA and the amino acid is more labile at higher pHs (we normally keep tRNA-aa at pH 4.5 for the *Xenopus* oocyte methodology). A solution of tRNA-aa at pH 4.5 or 7.4 was allowed to sit at room temperature for 10

minutes (Figure 2.10), or  $\geq 1$  hour (Figures 2.11 and 2.12), and added to an in vitro transcription reaction. This was done using both protected (NVOC) and photo-deprotected THG73-Ala, as well the valine alpha-hydroxy acid ValOH. It can be seen in Figure 2.10 that a 10-minute incubation of tRNA-aa at room temperature, pH 7.4, has minimal impact on suppression, implying that the aminoacyl-ester bond between the amino acid and tRNA is stable under these conditions. Only for longer incubations of  $\geq 1$  hour does the alphaHA band appear weaker, presumably due to reduced amounts of functional aminoacyl-tRNA. This is observed for both THG73-Ala (Figure 2.11) and THG73-ValOH (Figure 2.12).



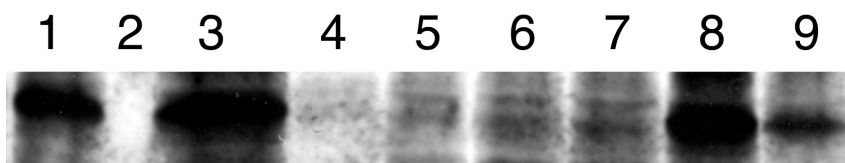
1. wt alphaHA
2. Rainbow ladder
3. Ala122TAG
4. Ala122TAG + THG73 74mer
5. Ala122TAG + THG73-Ala(NVOC) pH 7.4, photo-deprotected 10 minute, at room temperature, prior to translation reaction assembly
6. Ala122TAG + THG73-Ala(NVOC) pH 4.5, translation reaction assembled immediately
7. Ala122TAG + THG73-Ala(NVOC) pH 4.5, translation reaction assembled immediately
8. Ala122TAG + THG73-ValOH pH 7.4, sat for 10 minutes prior to assembly of translation reaction
9. Ala122TAG + THG73-ValOH pH 4.5, sat for 10 minutes prior to assembly of translation reaction

**Figure 2.10.** Testing the stability of tRNA-aa at pH 7.4 (10 minute incubation) by in vitro translation. The major band observed in all lanes is the  $\alpha$  subunit of the muscle-type nAChR, containing an HA epitope.



1. wt alphaHA
2. Ala122TAG + HSAS
3. Ala122TAG
4. Ala122TAG + THG73-Ala(NVOC), remained protected pH 7.4,  $\geq$  1 hour, deprotected immediately immediately prior to translation reaction assembly
5. Ala122TAG + THG73-Ala(NVOC), pH 7.4, photo-deprotected  $\geq$  1 hour prior to translation reaction assembly

**Figure 2.11.** Testing the stability of THG73-Ala at pH 7.4 ( $\geq$  1 hour incubation) by in vitro translation. The major band observed in all lanes is the  $\alpha$  subunit of the muscle-type nAChR, containing an HA epitope.

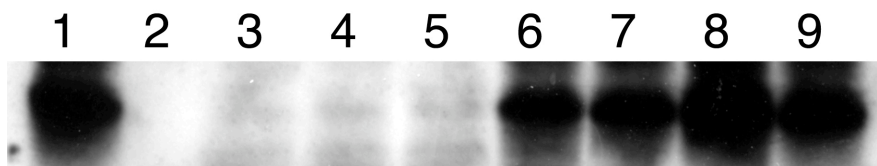


1. Ala122TAG + THG73-Ala(NVOC)
2. Rainbow ladder
3. Ala123TAG + HSAS
4. Blank
5. Ala122TAG
6. Ala122TAG + THG73 76mer (dCA)
7. Ala122TAG + THG73 74mer
8. Ala122TAG + THG73-ValOH, translation reaction assembled immediately
9. Ala122TAG + THG73-ValOH, sat at pH 7.4  $\geq$  1 hour prior to assembly of translation reaction

**Figure 2.12.** Testing the stability of THG73-ValOH at pH 7.4 ( $\geq$  1 hour incubation) by in vitro translation. The major band observed in all lanes is the  $\alpha$  subunit of the muscle-type nAChR, containing an HA epitope.

Lastly, we wanted to ensure that there were no components in the CO<sub>2</sub> independent electroporation buffer that may cause hydrolysis of the amino acid. The recipe for this buffer is proprietary, so we simply added the buffer to an in vitro transcription reaction to ensure that the tRNA-aa was still functional. As can be seen in

Figure 2.13, the presence of the electroporation buffer did not appear to compromise the integrity of the aminoacyl-tRNA.



1. wt alphaHA
2. Rainbow ladder
3. Ala122TAG
4. Ala122TAG + THG73 74mer
5. Ala122TAG + THG73 76mer (dCA)
6. Ala122TAG + THG73-ValOH
7. Ala122TAG + THG73-Ala(NVOC)
8. Ala122TAG + THG73-ValOH in CO<sub>2</sub> independent electroporation buffer
9. Ala122TAG + THG73-Ala(NVOC) in CO<sub>2</sub> independent electroporation buffer

**Figure 2.13.** Testing the stability of THG73-aa in the presence of the CO<sub>2</sub> independent electroporation buffer by in vitro translation. The major band observed in all lanes is the  $\alpha$  subunit of the muscle-type nAChR, containing an HA epitope.

#### 2.2.2.1.2 Discussion

It was somewhat discouraging that no sign of EGFP expression by nonsense suppression was observed for any of the aminoacyl-tRNAs tested, given the HSAS (Chapter 3) and RhG-tRNA experiments demonstrating that tRNA is efficiently delivered to cells by electroporation. Particularly surprising was that EAAS failed in our hands, since Vogel and co-workers found this to be a functional suppressor tRNA in CHO cells. The main difference between their experiments and ours was that they microinjected EAAS-Leu, rather than using electroporation. Perhaps microinjection simply delivers more material than microelectroporation. When the in vitro experiments are considered (2.2.1) it may not be surprising that HSAS works in mammalian cells while EQAS,

EAAS and EYAS do not, since this was true of rabbit reticulocyte, which is also a mammalian expression system. From all the data obtained, we therefore felt that EQAS, EAAS and EYAS would not be efficient suppressor tRNAs for unnatural amino acid incorporation using our methodology.

The fact that THG73 worked so well in vitro and seemingly not at all in cells led us to do a series of experiments examining the stability of the tRNA-aminoacyl linkage. We wanted to ensure that the amino acid was not hydrolyzing off of the tRNA at any point during the electroporation protocol. These experiments included incubating aminoacyl-tRNA at room temperature, pH 7.4, for 10 minutes to  $\geq 1$  hour. Although the  $\sim 1$ -hour room temperature incubations at pH 7.4 did lead to less efficient nonsense suppression by the aminoacyl-tRNA, the 10-minute incubations had minimal effect. Experimentally, it takes less than 10 minutes from the time the aminoacyl-tRNA is photodeprotected to the time that it is electroporated into the mammalian cells. Therefore, it seems unlikely that aminoacyl-tRNA hydrolysis is a concern. Furthermore, the CO<sub>2</sub> independent electroporation buffer also did not seem to interfere with the aminoacyl-tRNA.

From the data presented above, it seemed that functional aminoacyl-tRNA should be getting into adherent mammalian cells by electroporation, and that THG73 should be a functional amber suppressor tRNA in a mammalian cell expression system. By deduction, we were left with the possibility that not enough aminoacyl-tRNA was getting into the cells for us to actually observe suppression, and that we were operating below the EGFP detection limit. For this reason we abandoned the EGFP assay and moved on to a more sensitive assay, electrophysiology (see Chapter 4).

#### 2.2.2.2 Epizap

The Epizap is a commercially available electroporator, designed for transfecting adherent cells [27]. The cells are grown on optically transparent indium-tin oxide (ITO) coated glass slides. This electrically conductive surface acts as the anode of the electroporator. One advantage we thought that Epizap would have over our microelectroporator is that prior to electroporation, all of the growth media is removed from the cells (on the glass slide) and replaced with a minimum volume of 17  $\mu$ l of electroporation solution. Although the microelectroporator uses smaller volumes, we were concerned that the media remaining in the tissue culture dish was diluting the electroporation solution. We therefore hoped that a higher concentration of electroporation solution could be delivered using Epizap.

##### 2.2.2.2.1 Results

Electroporation of both CHO-K1 cells and HEK cells was tested using the Epizap, using either wild-type EGFP DNA or Ser29TAG DNA and HSAS tRNA (Figures 2.14 and 2.15). In general, it was found that the electroporation efficiency was on occasion similar to, but usually worse than, the microelectroporator. Furthermore, it took longer for EGFP expression to be observed when compared to the microelectroporator. One complication that arose was that the cell health seemed to be compromised when grown on the ITO surface. At least half of the experiments failed because of massive cell death, even after several attempts to optimize the electroporation conditions by modifying the voltage and capacitance. Basically there was a lot of variability and it was difficult to reproduce the experiments that actually did work well.

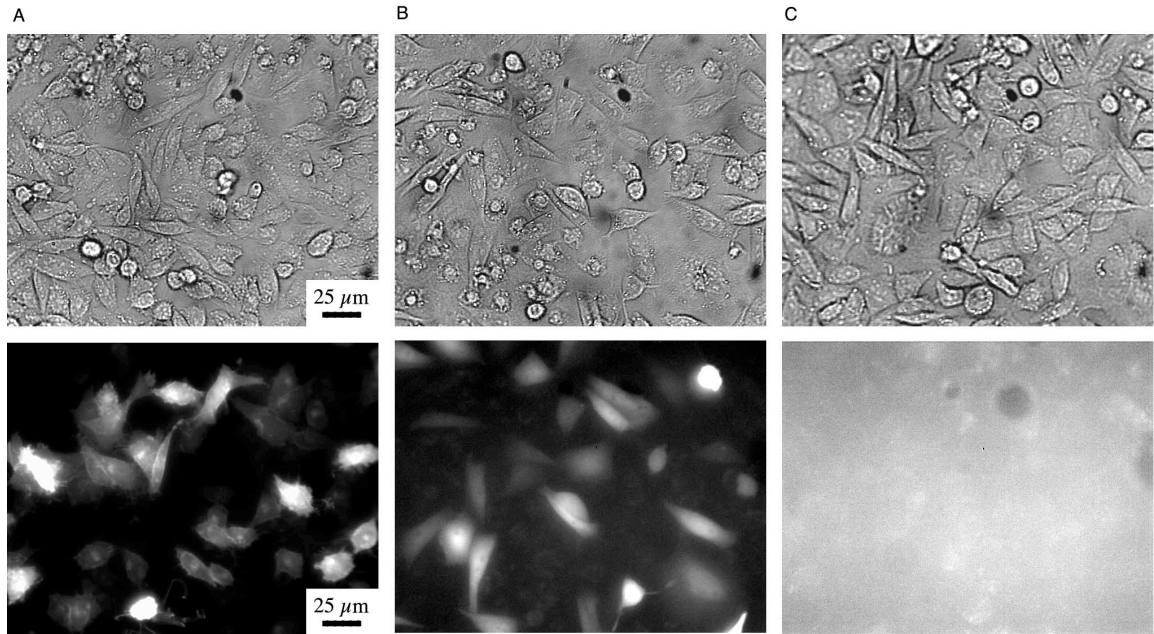


**Figure 2.14.** Electroporation of CHO-K1 cells using Epizap. The bright field (upper) and fluorescence images were taken 7 hours after transfection. (A) Cells were electroporated with a 17  $\mu\text{l}$  solution of wild-type pCS2gapEGFP DNA (2  $\mu\text{g}/\mu\text{l}$ ). (B) Cells were electroporated with a 17  $\mu\text{l}$  solution of HSAS tRNA (4  $\mu\text{g}/\mu\text{l}$ ) and pCS2EGFP Ser29TAG DNA (2  $\mu\text{g}/\mu\text{l}$ ). (C) Cells were electroporated with a 17  $\mu\text{l}$  solution of pCS2EGFP Ser29TAG DNA (2  $\mu\text{g}/\mu\text{l}$ ). For all cases, four 45 V, 1.0  $\mu\text{F}$  pulses were delivered to the cells. The fluorescent image in (C) was taken with four times the exposure length as in (A) and (B).

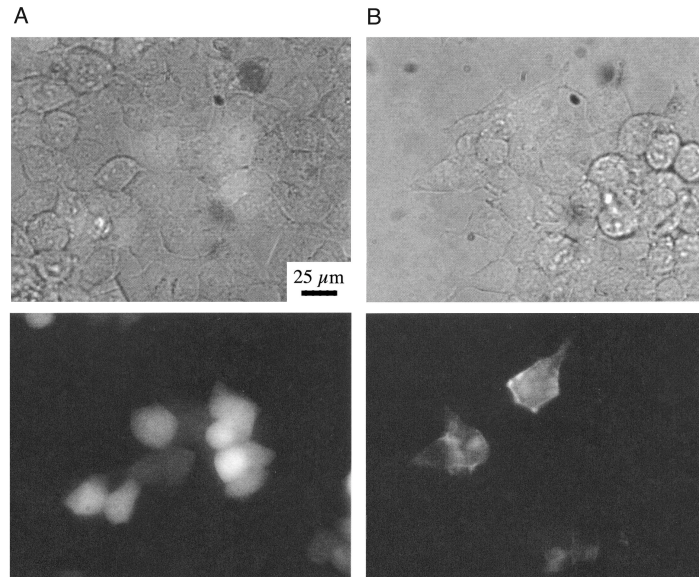


**Figure 2.15.** Electroporation of HEK cells using Epizap. The bright field (upper) and fluorescence images were taken 7 hours after transfection. (A) Cells were electroporated with a 17  $\mu\text{l}$  solution of wild-type pCS2EGFP DNA (2  $\mu\text{g}/\mu\text{l}$ ). (B) Cells were electroporated with a 17  $\mu\text{l}$  solution of HSAS tRNA (4  $\mu\text{g}/\mu\text{l}$ ) and pCS2gapEGFP Ser29TAG DNA (2  $\mu\text{g}/\mu\text{l}$ ). For all cases, four 30 V, 10  $\mu\text{F}$  pulses were delivered to the cells. The fluorescent images were taken with the same exposure length.

#### 2.2.2.2.2 Discussion

It can be concluded that the Epizap did not work well in our hands. Most of the time there was so much cell death that the experiments were a total loss. There was also a great deal of variability, and it was therefore very difficult to reproduce any experiments that worked well. These issues, along with the fact that the Epizap consumed much more material (aminoacyl-tRNA in particular) than the microelectroporator, brought us to the conclusion that it wasn't really worth pursuing further.

### 2.2.3 Peptide-mediated delivery of tRNA

Another method to incorporate tRNA into mammalian cells that was explored took advantage of a class of peptides that have the unique ability to drag cargo across cell membranes, protein transduction domains (PTD). The most efficient of these are the ANTP peptide (antenopedia, isolated from *Drosophila*, also known as Penetratin), the Tat peptide (isolated from HIV-1) and VP22 (isolated from herpes simplex virus). These peptides can transport cargo across a cell membrane when fused to proteins (up to 120 kDa) or oligonucleotides (up to 55mer) at either their C or N terminus. Transport occurs with equal efficiency at 4°C as it does at 37°C suggesting that it is not receptor or transporter mediated, and nonendocytotic. This phenomenon is independent of the cell line used, and works for neuronal cultures, suggesting that transport is due to a direct interaction with the cellular membrane. In fact, the ANTP peptide was shown to cross a synthetic bilayer [28]. Maximal intracellular concentrations are achieved on the order of minutes and are dependent upon the extracellular PTD concentration. These peptides have been reviewed in detail [29-39].

The third helix of the ANTP homeoprotein contains the minimal domain required for transport across a biological membrane. This domain consists of 16 amino acids, (RQIKIWFQNRRMKWKK) and has been shown to successfully transport oligonucleotide cargos [40-43]. Therefore, we attempted to couple this peptide to tRNA for transport into mammalian cells.

### 2.2.3.1 Covalent coupling between the ANTP peptide and tRNA

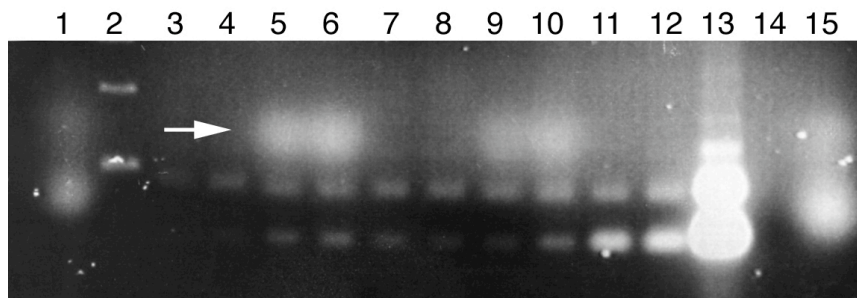
Initial experiments were designed to covalently couple the ANTP peptide to tRNA. Although this may render the tRNA nonfunctional in an expression system, we were more interested in seeing if these peptides could transport tRNA across a cell membrane. Therefore, our primary strategy focussed on reacting maleimide functionalized ANTP peptides with phosphorothioate or thiol modified RNAs.

#### 2.2.3.1.1 Results

Our initial coupling strategy consisted of labeling the 5'-end of the tRNA with a phosphorothioate group, which would be reactive toward a maleimide-functionalized ANTP peptide. Phosphorothioate labeling can be achieved using the KinaseMax kit (Ambion). When tRNA is combined with ATP- $\gamma$ -phosphorothioate (ATP- $\gamma$ -S), a T4 kinase-catalyzed exchange reaction occurs, replacing the 5'-phosphate with a phosphorothioate (tRNA- PO<sub>3</sub>S). We performed both 16-hour and 20-hour exchange reactions, and then monitored the reaction by coupling to maleimide-functionalized tetramethyl-rhodamine (TMR-MI).

The results from the TMR-MI coupling experiments are shown in Figure 2.16. The coupling reactions between tRNA- PO<sub>3</sub>S and TMR-MI are in lanes 5, 6, 9 and 10, and the rest of the lanes are controls. The white arrow indicates a unique band observed for the experimental coupling reactions, which may be the coupled product. The two major bands below this (observed in lanes 3 - 13) are THG73 tRNA, which runs in multiple conformations in agarose. Identification of the coupled product is not clear because of the result seen in lane 15. When ATP- $\gamma$ -S is reacted with TMR-MI and run on

the same agarose gel, it can be seen that there is a band that runs at the same position as the putative tRNA-TMR coupled product, in addition to a stronger band that runs faster (lane 15). However, when this ATP- $\gamma$ -S/TMR-MI reaction mixture is run through a nucleotide removal column, both bands disappear (lane 14). Since all the tRNA coupling reactions were run through nucleotide removal columns, then one would presume the free ATP- $\gamma$ -S to be gone, and not available to react with TMR-MI. So although it is suspicious that the band thought to be coupled tRNA product runs the same as one of the bands seen in lane 15, we presumed to have successfully made tRNA-  $\text{PO}_3\text{S}$ , and went ahead and tried to couple it to the ANTP peptide.

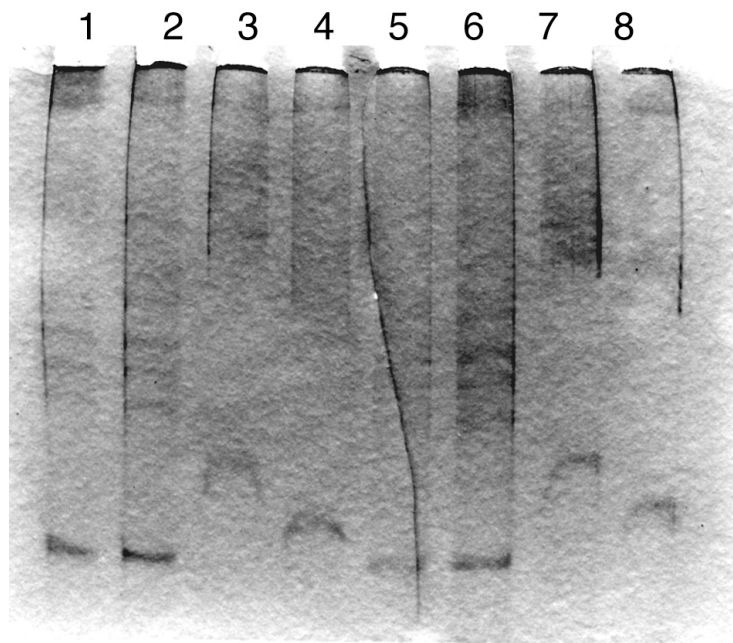


1. ATP-γ-S + TMR-MI, 2 hr
2. 100 base-pair ladder
3. ATP, 20 hr exchange + TMR-MI, 2 hr
4. ATP, 20 hr exchange + TMR-MI, 1 hr
5. ATP-γ-S, 20 hr exchange + TMR-MI, 2 hr
6. ATP-γ-S, 20 hr exchange + TMR-MI, 1 hr
7. ATP, 16 hr exchange + TMR-MI, 2 hr
8. ATP, 16 hr exchange + TMR-MI, 1 hr
9. ATP-γ-S, 16 hr exchange + TMR-MI, 2 hr
10. ATP-γ-S, 16 hr exchange + TMR-MI, 1 hr
11. 74mer THG73 + TMR-MI, 2 hr
12. 74mer THG73 + TMR-MI, 1 hr
13. 74mer
14. ATP-γ-S + TMR-MI, run through nucleotide removal column
15. ATP-γ-S + TMR-MI, 1 hr

**Figure 2.16.** Agarose gel showing the results of TMR-MI coupling reactions with 5'-phosphorothioate labeled THG73 tRNA (tRNA- PO<sub>3</sub>S). Coupling reactions to TMR-MI were done with tRNA- PO<sub>3</sub>S that had undergone 16-hour (lanes 9, 10) or 20-hour (lanes 5, 6) exchange reactions with ATP-γ-S. Controls included reacting TMR-MI with tRNA that had undergone exchange reactions with ATP (lanes 3, 4, 7, 8); reacting TMR-MI with 74mer tRNA (no exchange reaction, lanes 11, 12); reacting ATP-γ-S with TMR-MI (lanes 1, 15); and reacting ATP-γ-S with TMR-MI, then running the reaction through a nucleotide removal column (lane 14). Also shown is a 100-base pair ladder (lane 2) and 74mer tRNA only (lane 13). The white arrow indicates the band suspected to be tRNA-TMR coupled product. A 100 μl reaction mixture contained 5 μg tRNA, 20-fold excess TMR-MI, with 10% DMSO in a HEPES buffered solution (pH 7.5), incubated for 2 hours at room temperature.

In order to covalently couple the ANTP peptide to tRNA, we obtained an N-terminus maleimide-functionalized ANTP peptide (PTD-mal). A variety of conditions were tested for coupling tRNA- PO<sub>3</sub>S to the ANTP peptide. In most cases when tRNA was combined with ANTP and loaded onto a gel, it was observed that nothing in the reaction mixture entered the gel; everything just remained in the wells. There was also

some precipitation observed in the reaction mixtures. To reduce any nonspecific electrostatic interactions between these two species, the reaction was done under high salt conditions (1 M NaCl). This is shown in Figure 2.17. Unfortunately, it can be seen that there is no difference between the experimental tRNA- PO<sub>3</sub>S and PTD-mal coupling reaction and any of the control reactions. Interestingly, whenever PTD was present (with or without the maleimide) the tRNA ran slower on the gel than in the absence of PTD. This suggests that even in high salt conditions, there is still a nonspecific electrostatic interaction between the ANTP peptide and tRNA. Therefore it is impossible to say whether or not the coupling reaction was successful, based on the data shown.



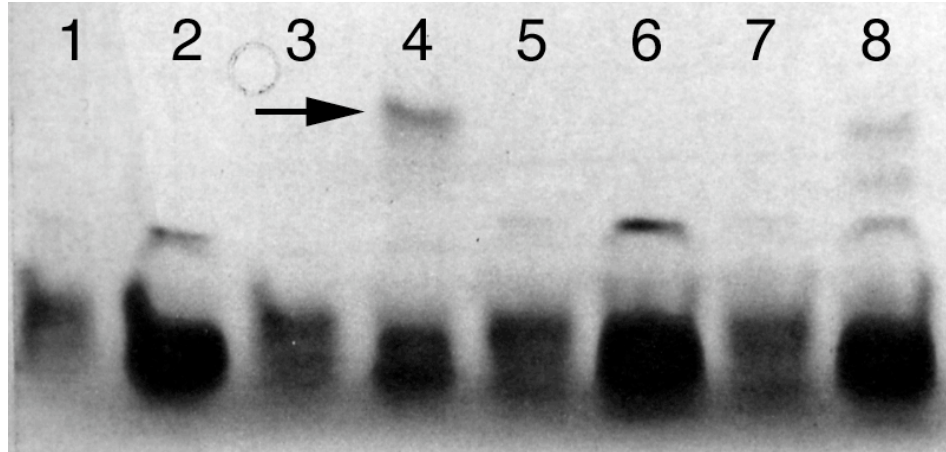
1. HSAS-PO<sub>4</sub>
2. HSAS-PO<sub>4</sub> + TMR-MI
3. HSAS-PO<sub>4</sub> + PTD
4. HSAS-PO<sub>4</sub> + PTD-mal
5. HSAS-PO<sub>3</sub>S
6. HSAS-PO<sub>3</sub>S + TMR-MI
7. HSAS-PO<sub>3</sub>S + PTD
8. HSAS-PO<sub>3</sub>S + PTD-mal

**Figure 2.17.** PAGE gel showing attempts to couple tRNA- PO<sub>3</sub>S to the ANTP peptide. Lanes 1 - 4 are reactions between unlabeled HSAS tRNA (HSAS-PO<sub>4</sub>) and TMR-MI (lane 2), non-functionalized PTD (lane 3) and PTD-mal (lane 4). Lanes 5 - 8 are reactions between HSAS- PO<sub>3</sub>S and TMR-MI (lane 6), non-functionalized PTD (lane 7) and PTD-mal (lane 8). A 20  $\mu$ l reaction contained 2  $\mu$ g tRNA, 10-100 fold excess PTD, 1 M NaCl, 10% DMSO, was phosphate buffered (pH 7.5), and incubated for 2 hours at room temperature.

ANTP is thought to be an alpha helix that interacts with the minor-groove of DNA helices. Therefore, the ANTP peptide may have been binding to double-helical structures of the tRNA, leading to the nonspecific interactions observed. For this reason, an alternate strategy for coupling the ANTP peptide to tRNA was pursued. A 14mer RNA molecule was made, that corresponds to the 14 nucleotides found at the 5'-end of

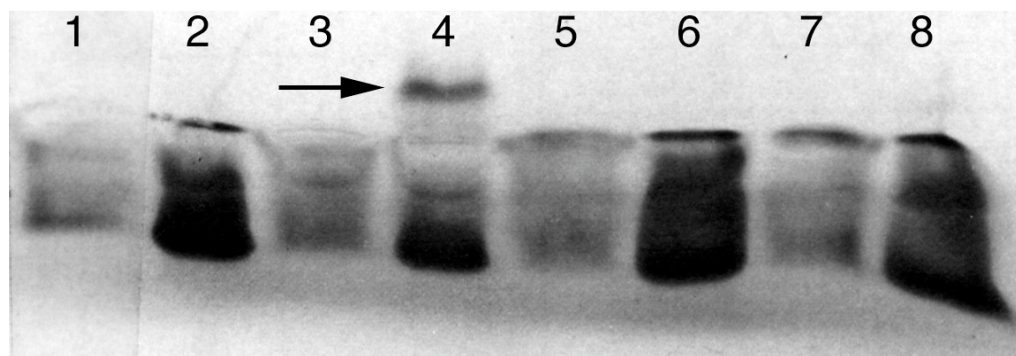


the reactions are far from completion since the unreacted RNA band is much more intense.



1. HSAS + PTD (20  $\mu\text{g}$ )
2. HSAS- $\text{PO}_3\text{S}$  + PTD (20  $\mu\text{g}$ )
3. HSAS + PTD-mal (20  $\mu\text{g}$ )
4. HSAS- $\text{PO}_3\text{S}$  + PTD-mal (20  $\mu\text{g}$ )
5. HSAS + PTD (2  $\mu\text{g}$ )
6. HSAS- $\text{PO}_3\text{S}$  + PTD (2  $\mu\text{g}$ )
7. HSAS + PTD-mal (2  $\mu\text{g}$ )
8. HSAS- $\text{PO}_3\text{S}$  + PTD-mal (2  $\mu\text{g}$ )

**Figure 2.19.** PAGE gel showing the coupling reactions of HSAS 5'14mer to the ANTP peptide (PTD). 14mer RNA was labeled with phosphorothioate using ATP- $\gamma$ -S and T4 kinase (KinaseMax kit, as described for tRNA labeling). A 100-fold excess (lanes 1 - 4) or 10-fold excess (lanes 5 - 8) of PTD was included. Reactions between HSAS- $\text{PO}_3\text{S}$  + PTD-mal are shown in lanes 4 and 8. Controls included reactions with unlabeled RNA (lanes 1, 3, 5, 7) and nonfunctionalized PTD (lanes 1, 2, 5, 6). A 10  $\mu\text{l}$  reaction contained 5  $\mu\text{g}$  RNA, 2 or 20  $\mu\text{g}$  PTD, 20 mM  $\text{MgCl}_2$ , was buffered by PBS (pH 7.4), and was incubated for 2 hours at 37°C.



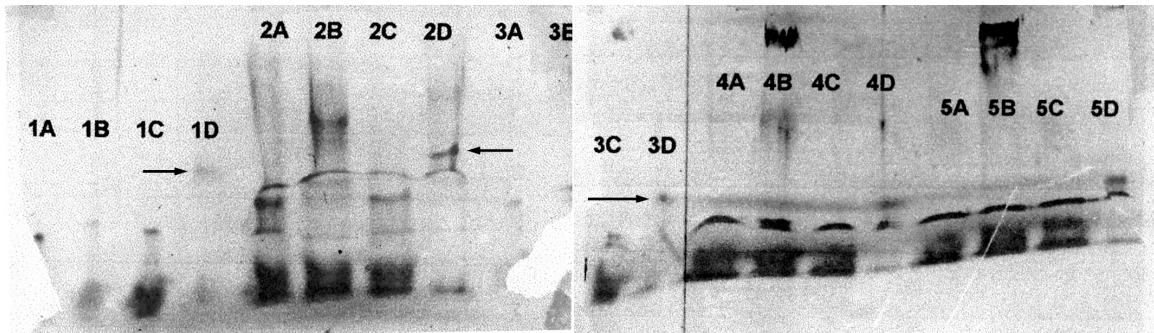
1. HSAS + PTD (20  $\mu\text{g}$ )
2. HSAS- $\text{PO}_3\text{S}$  + PTD (20  $\mu\text{g}$ )
3. HSAS + PTD-mal (20  $\mu\text{g}$ )
4. HSAS- $\text{PO}_3\text{S}$  + PTD-mal (20  $\mu\text{g}$ )
5. HSAS + PTD (2  $\mu\text{g}$ )
6. HSAS- $\text{PO}_3\text{S}$  + PTD (2  $\mu\text{g}$ )
7. HSAS + PTD-mal (2  $\mu\text{g}$ )
8. HSAS- $\text{PO}_3\text{S}$  + PTD-mal (2  $\mu\text{g}$ )

**Figure 2.20.** PAGE gel showing the coupling reactions of HSAS 5'14mer to the ANTP peptide (PTD), high salt conditions. 14mer RNA was labeled with phosphorothioate using ATP- $\gamma$ -S and T4 kinase (KinaseMax kit, as described for tRNA labeling). A 100-fold excess (lanes 1 - 4) or 10-fold excess (lanes 5 - 8) of PTD was included. Reactions between HSAS- $\text{PO}_3\text{S}$  + PTD-mal are shown in lanes 4 and 8. Controls included reactions with unlabeled RNA (lanes 1, 3, 5, 7) and nonfunctionalized PTD (lanes 1, 2, 5, 6). A 10  $\mu\text{l}$  reaction contained 5  $\mu\text{g}$  RNA, 2 or 20  $\mu\text{g}$  PTD, 20 mM  $\text{MgCl}_2$ , 1 M NaCl, was buffered by PBS (pH 7.4), and incubated for 2 hours at 37°C.

The ATP- $\gamma$ -S exchange reaction with oligonucleotides usually does not go to completion. This would explain why the reactions between HSAS- $\text{PO}_3\text{S}$  14mer RNAs and PTD-mal also did not go to completion. To remedy this, 5'thiol-modified 14mer RNAs were synthesized. Therefore all of the RNA molecules should be reactive toward the PTD-mal, and should also be more reactive than the phosphorothioate group.

These experiments were done when we thought that the EQAS tRNA would still be useful for unnatural amino acid incorporation, so we designed an EQAS 5'thiol modified 14mer RNA. Coupling reactions were done using a variety of conditions [44-49], however none of these gave promising results (Figure 2.21). The gels for these

reactions were very messy, and difficult to interpret. It is possible that the deprotection steps for the RNA 2'OH and the 5'thiol compromised the integrity of the RNA. The arrows in Figure 2.21 indicate bands that were unique to the coupling reactions, not observed in the control reactions, but it is certainly difficult to identify these bands as coupled product with any certainty.

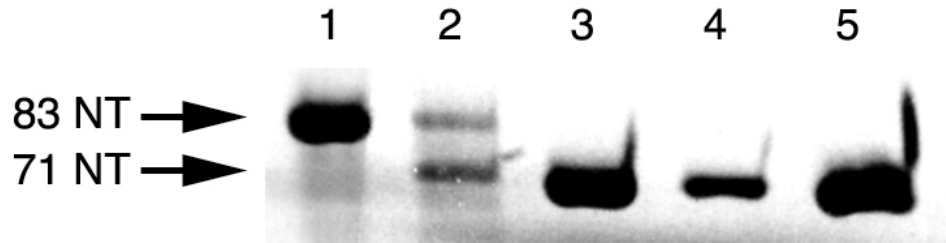


1. Water only
  2. 2 M NaCl, HEPES
  3. 50% acetonitrile, TEAA
  4. TEAA
- A. EQAS + PTD
  - B. EQAS-SH + PTD
  - C. EQAS + PTD-mal
  - D. EQAS-SH + PTD-mal

**Figure 2.21.** PAGE gel showing the coupling reactions between EQAS 14mer RNA, 5'thiol modified, with the ANTP peptide (PTD). The coupling reactions were done in (1) water, (2) 2 M NaCl, HEPES buffered, (3) 50% acetonitrile, TEAA buffered (4) TEAA buffered solutions. The control reactions are shown (A - C), and the EQAS-SH/PTD-mal coupling reactions are shown in D. A 10  $\mu$ l reaction contained 4  $\mu$ g RNA, 20  $\mu$ g PTD, and was incubated at 37°C for 4 hours. Arrows indicate bands that may be the coupled RNA-peptide product.

While the ANTP-RNA coupling reactions were being worked out, so was the ligation reaction between the HSAS 5'14mer and HSAS 3'71mer RNA. Several failed attempts of this ligation using a variety of conditions [50-53] were done before realizing that the 5'-end of the HSAS 3'71mer tRNA was not a monophosphate. In vitro

transcription yields a 5'-triphosphate, which needs to be phosphatased off, followed by reaction with T4 kinase to put on a single phosphate group. This tRNA could then be successfully ligated to the 14mer RNA, as seen in Figure 2.22, although under the conditions used the reaction did not go to completion.



1. HSAS 83mer
2. HSAS 71mer + 14mer ligation reaction
3. HSAS 71mer
4. HSAS 71mer, alkaline phosphatase
5. HSAS 71mer

**Figure 2.22.** PAGE gel showing the tRNA ligation reaction between HSAS 3'71mer and HSAS 5'14mer. The HSAS 3'71mer tRNA had to be first reacted with alkaline phosphatase, followed by T4 kinase, before ligation to the HSAS 5'14mer RNA. The 83mer indicated by the arrow is full length HSAS, and the 71mer is the truncated HSAS tRNA.

#### 2.2.3.1.2 Discussion

At the time these experiments were in progress we decided to focus our attention on the electroporation protocol, which was proving to be more promising. However, the data suggest that the ANTP coupling to the 14mer RNAs was working, as well as the HSAS 3'71mer/5'14mer ligations. Although some optimization of these reactions is required, the next step would be to ligate the 14mer-ANTP coupled product to the 3'71mer tRNA, and see if it goes into mammalian cells. The easiest way to do this would be to make rhodamine green-labeled tRNA, since the tRNA may not be functional with

the ANTP peptide coupled to it. It would also be interesting to design a system whereby the ANTP was coupled to the tRNA via a disulphide bond. Upon entry into a cell, the ANTP would be released from the tRNA by reduction of the disulphide bond, rendering a functional tRNA. Using HSAS tRNA would be the most convenient tRNA for optimizing such experiments since it is aminoacylated by the cell, and hence does not require chemical aminoacylation.

#### 2.2.3.2 Non-covalent coupling between the ANTP peptide and tRNA

It was discovered when trying to covalently couple ANTP to tRNA that there was a very strong non-covalent interaction between these two species, most likely due to electrostatics (Figure 2.17). Although there are no examples of ANTP transporting cargo across a biological membrane via a non-specific, non-covalent complex, we thought it would be worth exploring all the same.

##### 2.2.3.2.1 Results

The ANTP peptide was mixed as a 1 to 1 ratio with rhodamine green-labeled tRNA (RhG-tRNA), and applied to adherent CHO-K1 cells. As can be seen in Figures 2.23 and 2.24, only cells that were treated with both ANTP and RhG-tRNA are fluorescent. This was true 30 minutes after transfection (Figure 2.23), as well as 24 hours after transfection (Figure 2.24).

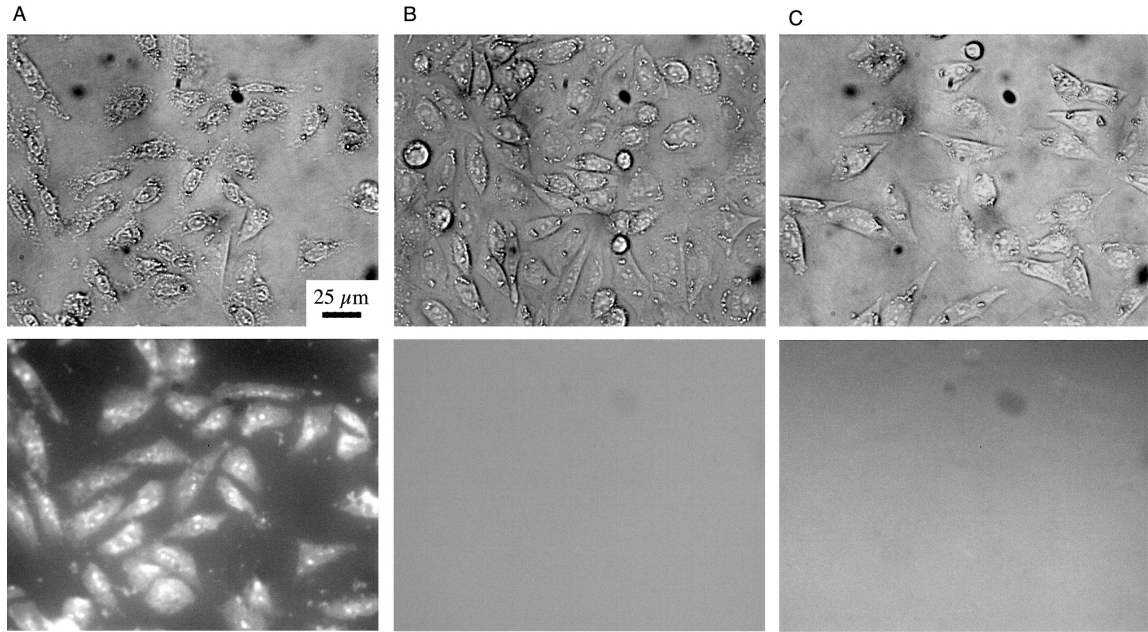


**Figure 2.23.** ANTP delivery of tRNA to CHO-K1 cells by non-covalent coupling, imaged 30 minutes after transfection (upper images bright field, lower fluorescent). (A) A 1:1 ratio of tRNA and ANTP ( $5 \mu\text{g}$  and  $30 \mu\text{g}$ , respectively) were mixed in  $50 \mu\text{l}$  of Ham's F12 growth media, added to CHO-K1 cells, and incubated for 30 minutes at  $37^\circ\text{C}$ . The media was then swapped to L15 for imaging. (B) ANTP peptide only. (C) RhG-tRNA only. The fluorescent images were taken with the same exposure length.

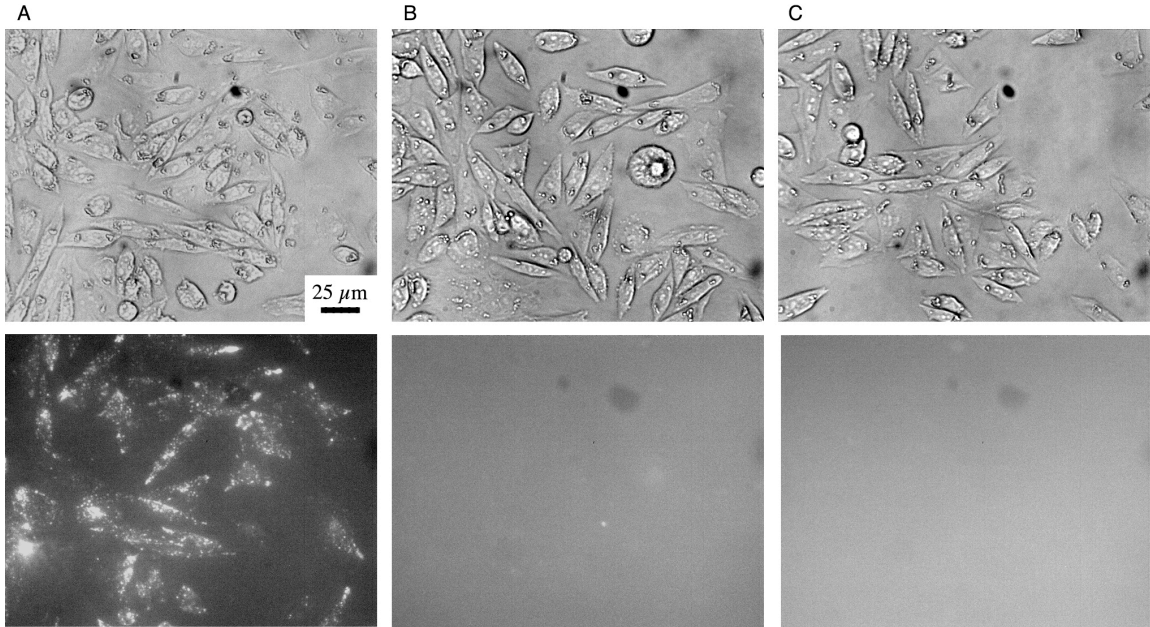


**Figure 2.24.** ANTP delivery of tRNA to CHO-K1 cells by non-covalent coupling, imaged 24 hours after transfection (upper images bright field, lower fluorescent). (A) A 1:1 ratio of tRNA and ANTP ( $5 \mu\text{g}$  and  $30 \mu\text{g}$  respectively) were mixed in  $50 \mu\text{l}$  of Ham's F12 growth media, added to CHO-K1 cells, and incubated for 30 minutes at  $37^\circ\text{C}$ . The media was swapped to L15 for imaging. (B) ANTP peptide only. (C) RhG-tRNA only. The fluorescent images were taken with the same exposure length.

Although these data were promising, it is possible that the ANTP-tRNA complex was simply stuck to the surface of the cells (possibly through electrostatics) rather than having been transported inside the cells. To test for tRNA transport, the Ser29TAG EGFP DNA was electroporated into CHO-K1 cells 30 minutes prior to application of an ANTP/HSAS mixture. The results from these experiments are shown in Figure 2.25. It can be seen that there is a fair amount of background expression in the negative controls (C - E), which is typical when imaging 24 hours after transfection. Cells transfected with Ser29TAG followed by ANTP/HSAS application demonstrated slightly higher expression than the negative controls (F), but not nearly as high expression as cells that were co-electroporated with both DNA and tRNA (B).

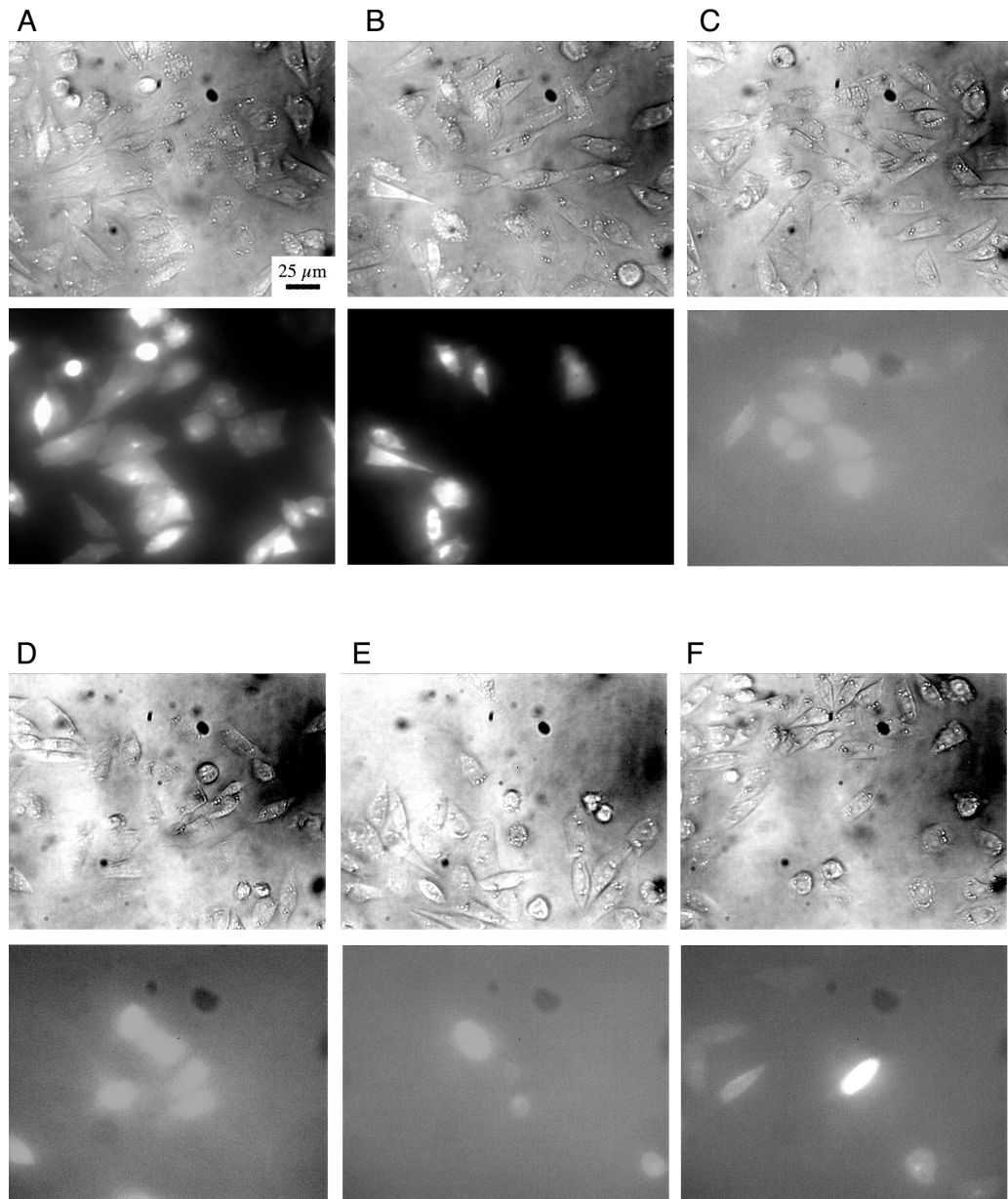


**Figure 2.25.** Non-covalent delivery of HSAS tRNA to CHO-K1 cells by ANTP. CHO-K1 cells were electroporated first with DNA, either wild-type EGFP or Ser29TAG ( $4 \mu\text{l}$ ,  $2.5 \mu\text{g}/\mu\text{l}$ ). The cells were then incubated for 1 hour at  $37^\circ\text{C}$ . A  $500 \mu\text{l}$  solution of ANTP ( $300 \mu\text{g}$ ) and/or HSAS tRNA ( $50 \mu\text{g}$ ) was then added, and the cells were incubated for a further 30 minutes.  $1.5 \text{ ml}$  of fresh media was added, and the media was totally replaced after 5 hours. (A) wt EGFP DNA electroporated, flu exposure 1 s. (B) Ser29TAG DNA ( $2.5 \mu\text{g}/\mu\text{l}$ ) + HSAS ( $4 \mu\text{g}/\mu\text{l}$ ), co-electroporated, flu exposure 0.3 s. (C) Ser29TAG DNA electroporated, flu exposure 4 s. (D) Ser29TAG DNA electroporated, HSAS added to media 30 minutes later, flu exposure 7 s. (E) Ser29TAG DNA electroporated, ANTP added to media 30 minutes later, flu exposure 4 s. (F) Ser29TAG DNA electroporated, HSAS + ANTP added to media 30 minutes later, flu exposure 4 s. The bright field (upper) and fluorescence (lower) images were taken 24 hours after transfection.

#### 2.2.3.2.2 Discussion

Delivery of tRNA by non-covalent coupling to the ANTP peptide does not seem to be nearly as efficient as microelectroporation. Although these are only preliminary results, it is not obvious how one would optimize this method. Also, it could be tricky to optimize this for delivery of aminoacyl-tRNA. Incubation of aminoacyl-tRNA in cell growth media at 37°C may hydrolyze the amino acid off of the tRNA. Electroporation delivers aa-tRNA in seconds, whereas the time scale of ANTP delivery by non-covalent coupling is uncertain. Although the above results are interesting, microelectroporation seems superior to ANTP-mediated delivery of tRNA to cells, therefore the latter may not be worth pursuing further.

#### 2.2.4 Lipofection

Lipid-mediated transfection was also tested for aminoacyl-tRNA delivery to mammalian cells. This method of transfection traditionally involves the loading of DNA into phospholipid vesicles that fuse with the cellular plasma membrane. Transfection with the use of synthetic cationic lipids is termed lipofection. There are many commercially available lipofection reagents that exhibit efficient transfection using DNA. One disadvantage of using lipofection is that the transfection protocol varies significantly between cell types. Another drawback is that the cationic lipids used are usually toxic to cells, and therefore compromise cell health. Furthermore, lipofection has not traditionally been used for RNA delivery to cells [25]. However, RajBhandary and co-workers have recently demonstrated delivery of aminoacyl-tRNA (EYAS-Tyr) using the lipofection reagent Effectene (Qiagen) [21]. They observed suppression of

chloramphenicol acetyl transferase (CAT) in COS1 cells. Although their protein expression levels were very low (they did not see expression at the single cell level, but rather had to harvest many cells for their assay) we felt it was worth exploring this method all the same, to compare it to microelectroporation. We decided to test the lipofection reagents Effectene (Qiagen), Polyfect (Qiagen), GeneJammer (Stratagene) and Lipofectamine 2000 (Invitrogen).

#### 2.2.4.1 Results

Because we want to observe protein expression at a single cell level, we used our EGFP assay rather than the CAT assay used by RajBhandary. A new EGFP construct was used for some of these experiments, pEGFP-N1-G2. This EGFP had an N-terminal handle added to the EGFP gene consisting of 40 amino acids, including a 6-His tag. This construct was made to introduce TAG stop codons in the N-terminal handle, such that any unnatural amino acid could be incorporated. This would allow us to test a variety of unnatural amino acids (such as alpha-hydroxy acids which are more stable than amino acids) without compromising the EGFP structure itself. Therefore the TAG mutant Leu28TAG (within the N-terminal handle) was made for this purpose.

Effectene was used to test delivery of aminoacyl-tRNA to CHO-K1, HEK and COS1 cells (Figures 2.26, 2.27 and 2.28). Figures 2.26 and 2.27 show that there is a high level of background expression for the pEGFP-N1-G2 Leu28TAG mutant, much higher than that observed for the pCS2gapEGFP Ser29TAG transfection in COS1 cells (Figure 2.28). However, wild-type expression was significantly higher than read-through expression. Unfortunately, HSAS suppression, which is usually comparable to wild-type

expression, did not lead to expression higher than background. Finally, poor cell health was observed in most cases, when compared to electroporation.

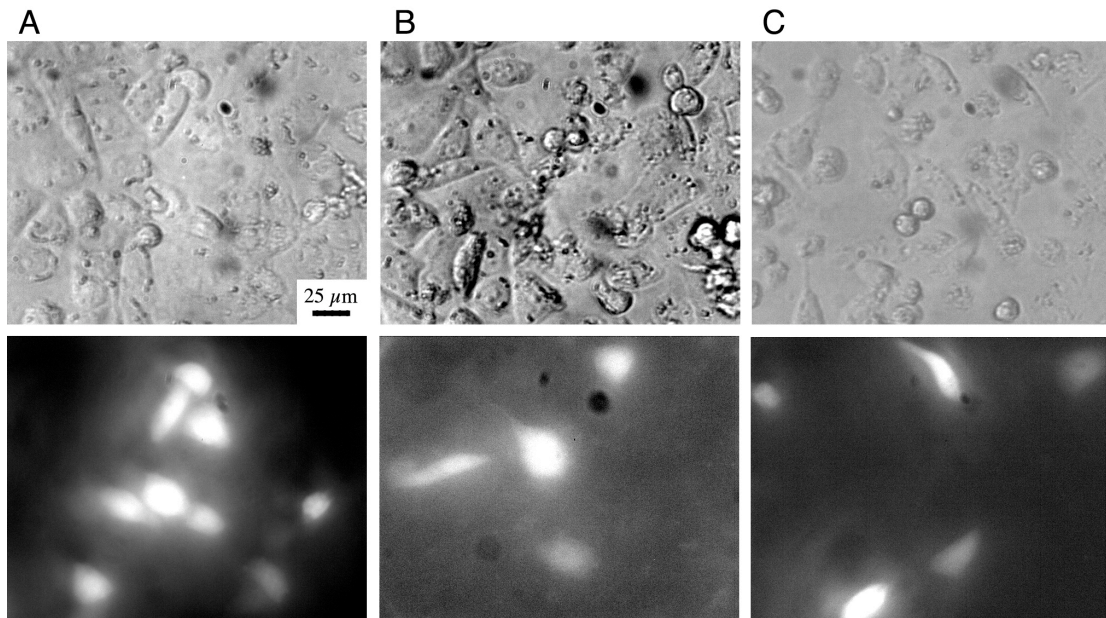


**Figure 2.26.** Effectene transfection of CHO-K1 cells with EGFP DNA and HSAS tRNA. (A) Wild-type pEGFP-N1-G2, fluorescence exposure 1 s. (B) Leu28TAG DNA only, fluorescence exposure 10 s. (C) Leu28TAG DNA and HSAS tRNA, fluorescence exposure 2 s. The bright field (upper) and fluorescence (lower) images were taken 24 hours after transfection.

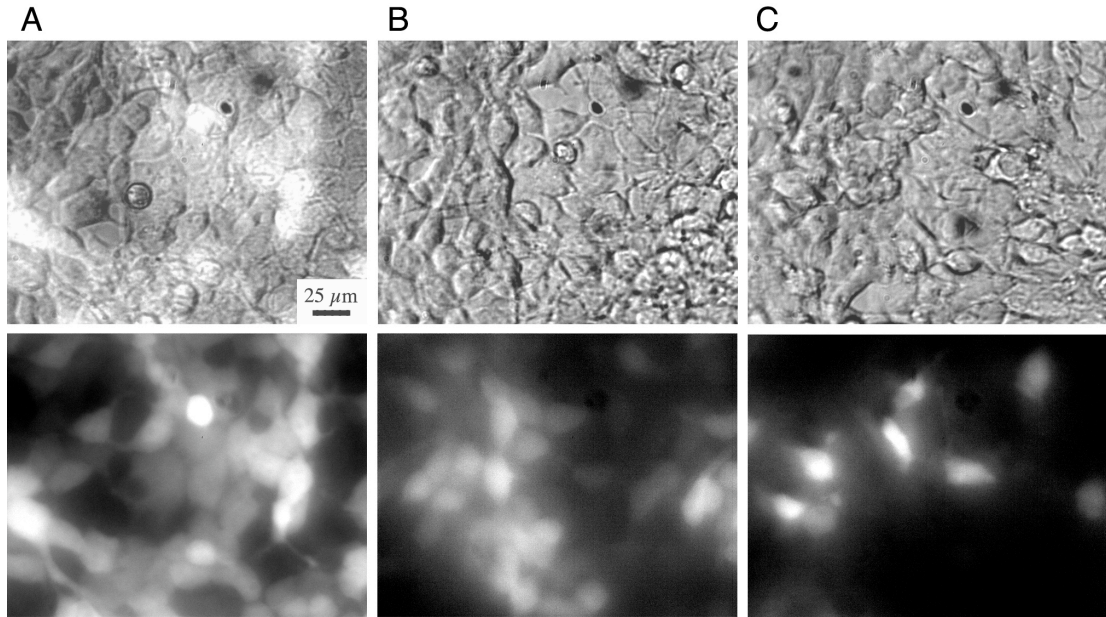


**Figure 2.27.** Effectene transfection of HEK cells with EGFP DNA and HSAS tRNA. (A) Wild-type EGFP-N1-G2 DNA, fluorescence exposure 0.1 s. (B) Leu28TAG DNA only, fluorescence exposure 1 s. (C) Leu28TAG DNA + HSAS, fluorescence exposure 1 s. The bright field (upper) and fluorescence (lower) images were taken 24 hours after transfection.

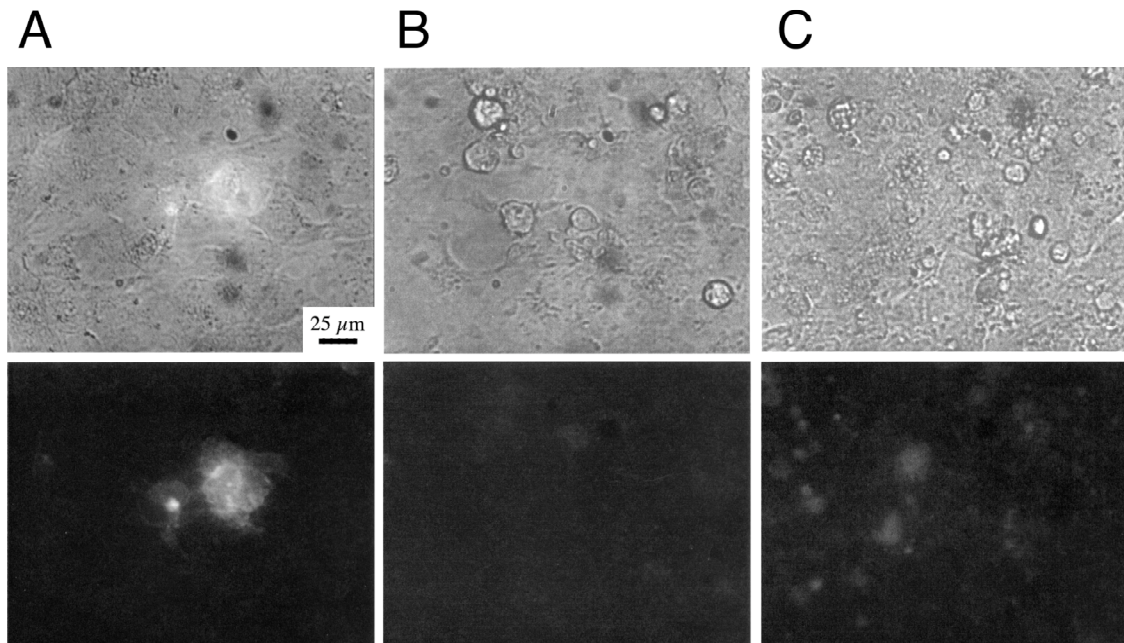


**Figure 2.28.** Effectene transfection of COS1 cells with EGFP DNA and HSAS tRNA. (A) Wild-type pCS2gapEGFP, fluorescence exposure 5 s. (B) Ser29TAG DNA only, fluorescence exposure 5 s. (C) Ser29TAG DNA + HSAS, fluorescence exposure 5 s. The bright field (upper) and fluorescence (lower) images were taken 24 hours after transfection.

Polyfect was also tested for tRNA delivery to CHO-K1 cells. It can be seen in Figure 2.29 that there is again read-through of the Leu28TAG mutant. In this case HSAS suppression resulted in higher expression than background, much closer to wild-type expression levels than were observed when using Effectene. However, like Effectene a lot of cell death was apparent after Polyfect transfection.

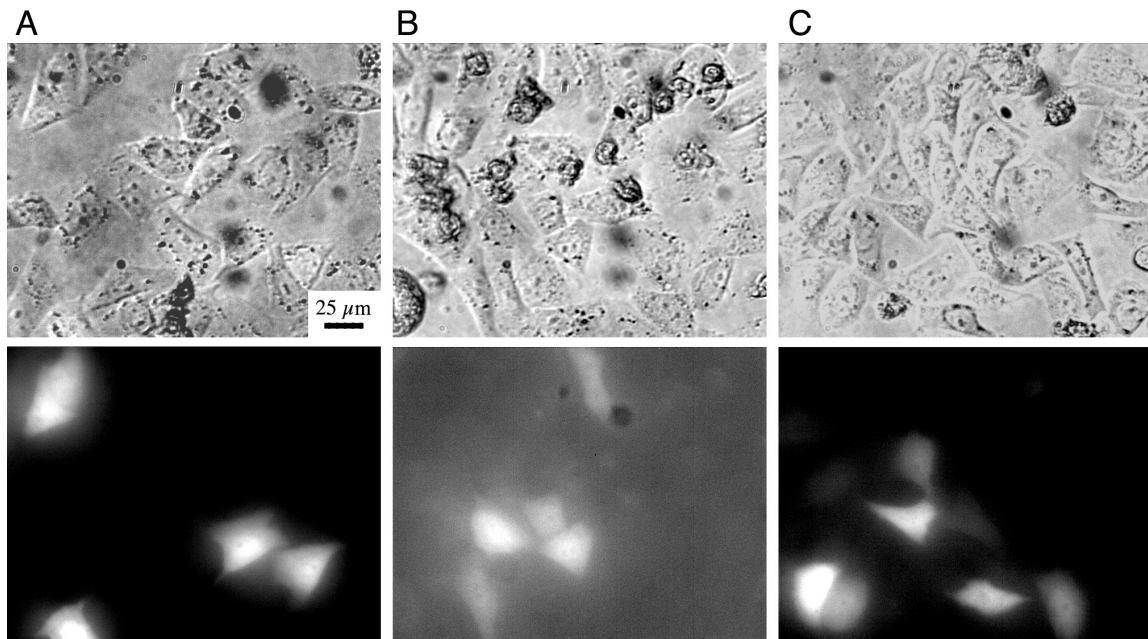


**Figure 2.29.** Polyfect transfection of CHO-K1 cells using EGFP DNA and HSAS tRNA. (A) Wild-type pEGFP-N1-G2, fluorescence exposure 0.5 s. (B) Leu28TAG DNA only, fluorescence exposure 5 s. (C) Leu28TAG + HSAS, fluorescence exposure 1 s. The bright field (upper) and fluorescence (lower) images were taken 24 hours after transfection.

We next tested the lipofection reagent GeneJammer. In these experiments we also co-electroporated a dish with TAG mutant DNA and HSAS tRNA to compare the efficiency of lipofection to electroporation. As can be seen in Figure 2.30, there is little background expression of the pCS2gapEGFP mutant. When electroporation of HSAS and Ser29TAG is compared to GeneJammer transfection, the expression levels were

comparable in some cases (Figure 2.30 C and D). However, in most cases electroporation was still more efficient, and expression was observed within a few hours where as expression with GeneJammer transfection was not observed until the next day. There was also a lot of cell death with this lipofection reagent, as observed for the others examined.

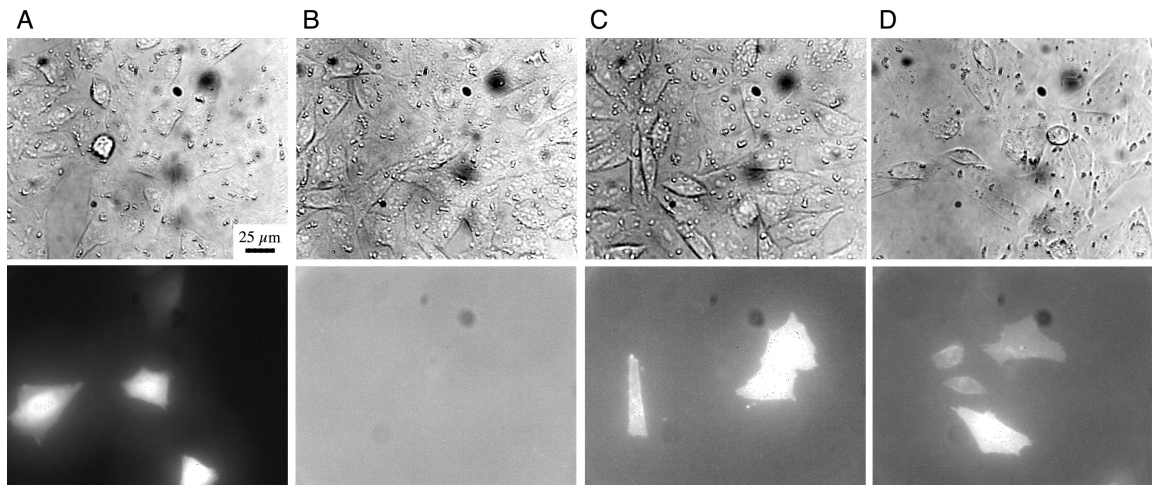


**Figure 2.30.** GeneJammer transfection of CHO-K1 cells using EGFP DNA and HSAS tRNA. (A) Wild-type pCS2EGFP DNA, fluorescence exposure 5 s. (B) Ser29TAG DNA only, fluorescence exposure 7 s. (C) Ser29TAG + HSAS tRNA, co-electroporation control, fluorescence exposure 7 s (four 120 V, 50 ms pulses, 4  $\mu$ l of 2  $\mu$ g/ $\mu$ l each DNA and tRNA). (D) Ser29TAG DNA + HSAS tRNA (GeneJammer), fluorescence exposure 7 s. The bright field (upper) and fluorescence (lower) images were taken 24 hours after transfection.

Lastly, we tested the lipofection reagent Lipofectamine 2000. These experiments were a bit different, in that we first transfected the cells with DNA using Lipofectamine 2000, followed by electroporation of HSAS tRNA. The rational was to see if the cells would tolerate a combination of transfection techniques, so that we could increase the concentration of tRNA in the electroporation solution. The results from these experiments are shown in Figure 2.31. Electroporation of empty buffer into cells

transfected with wild-type EGFP DNA did compromise cell health to some extent, as a lot of cell death was apparent. Electroporation of HSAS tRNA into cells transfected with Ser29TAG DNA did lead to expression, although it was lower than wild-type expression and the cells were unhealthy.

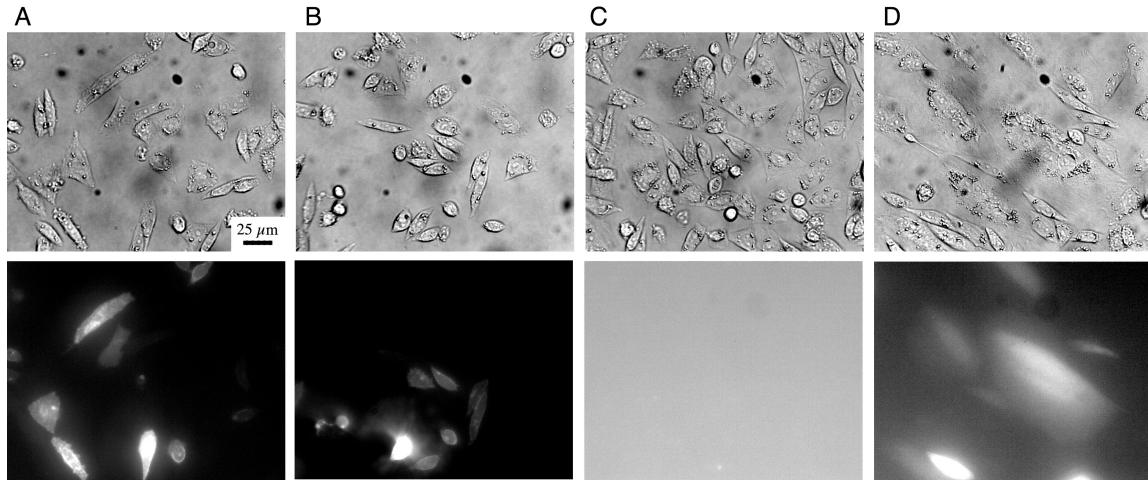


**Figure 2.31.** Lipofectamine 2000 transfection of CHO-K1 cells using HSAS tRNA, following electroporation of EGFP DNA. (A) Wild-type pCS2gapEGFP, delivered using lipofectamine 2000, fluorescence exposure 4 s. (B) Wild-type pCS2gapEGFP DNA, delivered using lipofectamine 2000 followed by electroporation of empty buffer (four 120 V, 50 ms pulses), fluorescence exposure 4 s. (C) Ser29TAG DNA only, delivered with lipofectamine 2000, fluorescence exposure 7 s. (D) Ser29TAG DNA delivered with lipofectamine, followed by electroporation of a 4  $\mu$ l solution of HSAS (2  $\mu$ g/ $\mu$ l, four 120 V, 50 ms pulses). The bright field (upper) and fluorescence (lower) images were taken 24 hours after transfection.

#### 2.2.4.2 Discussion

In general, it can be summarized that lipofection offers no real advantage over microelectroporation. The cells were typically quite unhealthy after transfection, apparent from the amount of cellular detachment and debris in the tissue culture dishes. Furthermore, EGFP expression was not observed until the day after transfection whereas

electroporation leads to expression within a few hours. These observations were true for all of the reagents tested, and were important factors to consider for future experiments. Lipofection reagents exhibit a lot of variability between cell types and do not work for transfection of neurons, a limitation we want to avoid. It was our ultimate goal to study ion channel expression in a variety of mammalian cells by electrophysiology, and the cells must be healthy enough for whole-cell patch clamping. Given that most of the cells transfected with lipofection reagents were detached the next day, this is most likely not the best transfection method for our purposes.

### 2.2.5 Biolistics

A final method that we explored for tRNA delivery to mammalian cells was biolistics [21]. The main reason we wanted to try this method is because it is a fairly general transfection technique that works on many cell types including neuronal cultures. Furthermore, RNA has been successfully delivered to cells using biolistics [54, 55], one of the few transfection techniques to do so.

#### 2.2.5.1 Results

Precipitation of wild-type EGFP DNA, or co-precipitation of EGFP TAG mutants and tRNA onto gold microcarriers was done prior to transfection. The EGFP mutants included Val55TAG DNA with THG73-ValOH (alpha-hydroxy acid), and Ala37TAG DNA with THG73-Ala. The TAG mutants were also delivered to cells alone, or with 74mer tRNA. These experiments were done before developing the HSAS assay, so HSAS suppression was unfortunately not examined. Figure 2.32 shows CHO-K1 cells

transfected with wild-type DNA. There was good transfection efficiency, and the cells appeared quite healthy after transfection. Unfortunately, no expression was observed for any of the other experiments.

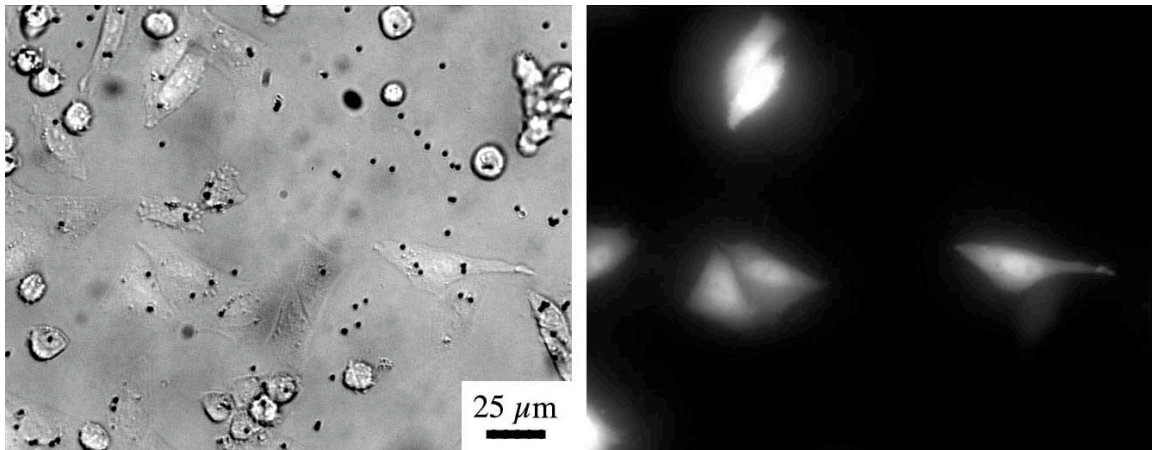


**Figure 2.32.** Transfection of CHO-K1 cells using biolistics. Wild-type EGFP DNA was precipitated onto gold microcarriers for transfection. The bright field (left) and fluorescence (right) images were taken 24 hours after transfection.

#### 2.2.5.2 Discussion

The biolistics experiments were not explored to their full potential. Transfection with wild-type EGFP DNA gave good expression, and the cells were in good health. It is not surprising that suppression of the EGFP TAG mutants was not observed, similar to electroporation. These experiments were unfortunately done before the HSAS assay was developed, and it would be interesting compare biolistics to electroporation using this assay. However, biolistics is an expensive transfection technique, in that it requires not only a gene-gun, but also fresh gold microcarriers for each experiment. So although this method may be a general mammalian cell transfection method, it may not be the most practical.

## 2.3 Conclusions

Of all the transfection methods tested, the microelectroporator is by far the most efficient. It is the most general (also see Chapter 3), leads to the least amount of cell death, and protein expression can be observed as soon as two hours after transfection. One disadvantage of this method is that it does consume large quantities of aminoacyl-tRNA, in comparison to the *Xenopus* oocyte method. Only a small percentage of the tRNA applied to the cells actually goes inside the cells, and the vast majority is thrown away. This is an area that needs optimization. As an alternative electroporation strategy, single-cell electroporation is now being explored by Dr. Rigo Pantoja. This method has the advantage of requiring significantly less material than the microelectroporator. A micropipette is filled with a small volume (hundreds of nanoliters) of transfection solution, and this can be used to transfect hundreds of cells in multiple dishes. In summary, electroporation is an optimal way to deliver DNA, mRNA and tRNA to mammalian cells for unnatural amino acid incorporation.

## 2.4 Experimental Methods and Materials

### 2.4.1 Materials

Synthetic DNA oligonucleotides were synthesized on an ABI 394 DNA Synthesizer on site. Peptides were synthesized on an ABI 433A Peptide Synthesizer and stored as a lyophilized powder. Restriction enzymes and T4 RNA ligase were purchased from New England Biolabs (Beverly, MA). Rhodamine Green-UTP and tetramethylrhodamine-maleimide (TMR-MI) were purchased from Molecular Probes (Eugene, OR). Slide-A-Lyzer was purchased from Pierce (Rochford, IL). ATP- $\gamma$ -S was purchased from Boehringer Mannheim (Indianapolis, IN). Polyfect and Effectene were purchased from Qiagen (Valencia, CA), GeneJammer from Stratagene (La Jolla, CA), and Lipofectamine 2000 from Invitrogen (Carlsbad, CA). Gold microcarriers and tubing for biolistics were purchased from Bio-Rad (Hercules, CA). Stains-All was purchased from Aldrich (Milwaukee, WI). The monoclonal antibody mouse anti-HA was purchased from Covance Research Products (Denver, PA), and the monoclonal antibody anti-mouse was purchased from Jackson ImmunoResearch (West Grove, PA). The ECL reagents for chemiluminescent visualization of western blots were purchased from Amersham Biosciences (Piscataway, NJ). The GFP mammalian expression vectors pCS2gapEGFP (membrane-localized) and pCS2EGFP were obtained from Jack Horne (Caltech). pEGFP-F (membrane-localized) and pEGFP-N1 (soluble EGFP construct) were purchased from BD Biosciences Clontech (Palo Alto, CA). The KinaseMax kit, mMessage mMachine and MegaShortScript in vitro transcription kits were purchased from Ambion (Austin, TX). Maxiprep kits used for plasmid isolation, and nucleotide

removal kits were purchased from Qiagen (Valencia, CA). The Rabbit Reticulocyte in vitro protein translation system was purchased from Promega (Madison, WI). Ham's F12 tissue culture media and DMEM were purchased from Irvine Scientific (Santa Ana, CA), and CO<sub>2</sub> independent media was purchased from GIBCO Invitrogen Corporation (Carlsbad, CA). The microelectroporator was built on site. Epizap and indium-tin oxide coated plates were purchased from ASK Science Products (Kingston, ON). The Helios GeneGun system from Bio-Rad (Hercules, CA) was used for biolistics.

#### 2.4.2 Mutagenesis, mRNA and tRNA synthesis

The tRNA genes EQAS, EAAS, EYAS, HSAS 3'71 and EQAS 3'61 were constructed as follows: Two complementary synthetic oligonucleotides encoding for the T7 promoter, the tRNA gene, and the Fok I restriction site were synthesized, annealed and ligated into the EcoR I and BamH I restriction sites of pUC19. After linearization of the DNA with Fok I, in vitro transcription with the MegShortScript kit (Ambion) yields the corresponding tRNA (Figure ). All mRNA was synthesized using the mMessage mMachine kit (Ambion) with linearized template DNA.

```
oligo 1: 5'-AATTCGTAATACGACTCACTATA-tRNAgene-TGAGACCCATCCG-3'
oligo 2: 3'-GCATTATGCTGAGTGATAT-tRNAgene-ACTCTGGGTAGGCCTAG-5'
```

**Figure 2.33.** Oligo design for tRNA gene construction. The tRNA sequence is inserted where indicated. The T7 promoter is shown in bold on the sense-strand. The sticky ends AATT and CTAG correspond to Eco RI and Bam HI respectively, for insertion into pUC19.

To synthesize Rhodamine green labeled tRNA, the Ambion protocol was modified as follows. A three-to-one mixture of UTP and rhodamine green-UTP (RhG-

UTP), respectively, was added to the transcription reaction, with a final total concentration of 2.4 mM. The other nucleotides had a final concentration of 3 mM (total volume of 25  $\mu$ l). After a 2 hour incubation at 37°C, tRNA was isolated by PCI extraction and NH<sub>4</sub>OH/isopropanol precipitation. The tRNA was resuspended in 100  $\mu$ l of RNase free water, and dialyzed (Slide-A-Lyzer, molecular weight cut off of 3500) in 1800 ml of millipore purified water at 4°C for 16 hours to eliminate any unincorporated RhG-UTP. For a RhG-UTP control, 20  $\mu$ g of THG73 tRNA was mixed with an equivalent amount of RhG-UTP as used in the transcription reaction to a total volume of 25  $\mu$ l, and worked up as described.

All EGFP mutants (TAG 29, TAG37, TAG55, TAG66) were made following the Quickchange mutagenesis protocol (Stratagene). The pEGFP-N1-G2 construct (wild-type and Leu28TAG) was made by inserting an N-terminal handle on the EGFP-N1 construct (Clontech). This construct was made to introduce TAG stop codons in the N-terminal handle, such that any unnatural amino acid could be incorporated. This would allow us to test a variety of unnatural amino acids (such as alpha-hydroxy acids which are more stable than amino acids) without compromising the EGFP structure itself. The DNA sequence inserted

(atgcgcggcagccaccaccaccaccacggcatggccggatccagctccatgaccggcggccagcagatgggcccgcg

acctgtacgacgacgacgacaaggaccccccgccgagttc) corresponds to the peptide sequence

MRGSHHHHHHGMAGSSSMTGGQMGRDLYDDDDKDPPAEF. To remove the

original kozak sequence and initiator methionine (which was causing a lot of read-

through of the TAG28 mutant), the EGFP gene with the N-terminal handle was cut out of

the original vector (using Not I and Eco RI) and subcloned into the corresponding sites of the pGEM-11Zf(+) vector.

#### 2.4.3 Tissue culture

CHO cells were grown in Ham's F12 media, and HEK and COS1 cells were grown in DMEM, at 37°C and 5% CO<sub>2</sub>, enriched with glutamine, fetal bovine serum (FBS, 10 %), penicillin, and streptomycin. One to two days prior to electroporation, the cells were passaged onto 35 mm tissue culture dishes such that confluency was typically 50% or less at the time of transfection.

#### 2.4.4 Microscopy

Cells were visualized with an inverted microscope (Olympus IMT2), a 250 W Hg/Xe lamp operating at 150 W, a GFP filter set (Chroma, model 41017) with an excitation band pass of 450 to 490 nm and an emission band pass of 500 to 550 nm, 10x/0.25NA or 40x/1.3NA lens, and a Photometrix Quantix CCD camera running Axon Imaging Workbench 4.0.

#### 2.4.5 Electroporation

##### 2.4.5.1 Microelectroporation

The DNA, mRNA or tRNA to be electroporated into mammalian cells was precipitated alone or as co-precipitates in ethanol and ammonium acetate, and left at -20°C for at least 1 hour. For tRNA-aa, the amino acids have an o-nitroveratryloxycarbonyl (NVOC), or a 4-pentenoyl (4-PO) protecting group at the N-

terminus. Deprotection of NVOC consisted of irradiating a 15  $\mu$ l solution of tRNA-aa (1  $\mu$ g/ $\mu$ l) in 1 mM NaOAc (pH 4.5) for 6 minutes, using a 1000 W Hg/Xe arc lamp (Oriol, Stratford, CT) operating at 400 W, equipped with WG355 and UG11 filters (Schott, Duryea, PA). Deprotection of the 4-PO consisted of mixing a 15  $\mu$ l solution of tRNA-aa with 15  $\mu$ l of a saturated iodine solution, and allowing it to sit at room temperature for 10 minutes. Reporter EGFP DNA and the AChR subunit mRNA or NMDA subunit DNA were then combined with this and precipitated with ammonium acetate and ethanol. This was then microcentrifuged at 15,000 rpm, 4°C for 15 minutes, vacuum dried for 5 minutes, and resuspended in CO<sub>2</sub> independent medium to the desired final concentration. Immediately prior to electroporation, the cell tissue culture media was swapped to CO<sub>2</sub> independent media (with no glutamine, FBS or antibiotics). Approximately 5  $\mu$ l of the electroporation solution was applied to the cells, followed by application of electrical pulses. This was typically four 120 V pulses of 50 ms duration. The CO<sub>2</sub> independent media was immediately replaced with fresh growth media, and the cells were placed back into the 37°C incubator.

#### 2.4.5.2 Epizap

The day prior to electroporation, cells were passaged onto indium-tin oxide coated glass slides (ASK Science Products) such that confluency was typically 50% or less at the time of transfection. The DNA or tRNA to be electroporated was precipitated alone or as coprecipitates in ethanol and ammonium acetate, and left at -20°C for at least 1 hour.

This was then microcentrifuged at 15,000 rpm, 4°C for 15 minutes, vacuum dried for 5 minutes, and resuspended in CO<sub>2</sub> independent medium to the desired final concentration.

The cells were typically transfected with EGFP DNA at a concentration of  $2.5 \mu\text{g}/\mu\text{l}$ , with or without HSAS tRNA at a concentration of  $4 \mu\text{g}/\mu\text{l}$ . Immediately prior to electroporation, the cell tissue culture media was removed from the glass slides. Approximately  $17 \mu\text{l}$  of the electroporation solution was applied to the cells, followed by application of electrical pulses. This was typically four 30 - 50 V pulses, 1.0 - 10  $\mu\text{F}$ . Fresh growth media was applied, and the cells were placed back into the  $37^\circ\text{C}$  incubator. Imaging of EGFP was done as soon as 2 hours after transfection.

#### 2.4.6 In vitro protein synthesis

Various amber suppressor tRNAs were tested using a Rabbit Reticulocyte expression system (Promega), according to the manufacture's instructions. Typically  $1 \mu\text{g}$  of mRNA and 1 - 3  $\mu\text{g}$  of tRNA would be added to the lysate mixture along with the amino acid mix. This sat at  $30^\circ\text{C}$  for 90 minutes, and was then run on a 10% Tris-Cl polyacrylamide gel in an SDS/Tris/Glycine running buffer. All of the mRNAs used (alpha subunit of the muscle-type nAChR receptor) contained a HA-epitope. The bands were transferred to nitrocellulose, and labeled with monoclonal mouse anti-HA (Covance), followed by monoclonal anti-mouse antibodies coupled to horseradish peroxidase (Jackson) for visualization by chemiluminescence (ECL reagents, Amersham Biosciences).

#### 2.4.7 Peptide-oligonucleotide coupling reactions

5'phosphorothioate labeling of tRNA was achieved by an in vitro T4 kinase exchange reaction, according to the Ambion KinaseMax kit protocol. Briefly, a typical

reaction consisted of 10  $\mu\text{g}$  of tRNA, 80-fold excess of ATP- $\gamma$ -S and 2  $\mu\text{l}$  of T4 kinase (20 units) with a total reaction volume of 10  $\mu\text{l}$ . Reactions were incubated for 16 or 20 hours at 37°C, and purified with a Qiagen nucleotide removal kit.

tRNA-PO<sub>3</sub>S was assayed by reaction with tetramethylrhodamine-5-maleimide (TMR-MI). A typical reaction (100  $\mu\text{l}$ ) consisted of combining 5  $\mu\text{g}$  of tRNA-PO<sub>3</sub>S with a 20-fold excess of TMR-MI in 10% DMSO, pH 7.5 (HEPES). The reaction was allowed to proceed for 2 hours at room temperature and was then loaded directly onto a 3% agarose gel, run at 50 V for 3-4 hours. A band shift was used to identify tRNA-PO<sub>3</sub>S, as interpreted by a reaction with TMR-MI (ethidium bromide stained gel). Control reactions using unlabeled tRNA were also done.

Reactions of tRNA-PO<sub>3</sub>S with N-terminal maleimide functionalized ANTP peptides (PTD-mal) were also attempted. A typical reaction consisted of combining 2  $\mu\text{g}$  of tRNA-PO<sub>3</sub>S with ~ 10-100-fold excess PTD-mal in a 1 M NaCl, 10% DMSO, phosphate buffered solution (pH 7.5) to a total volume of 20  $\mu\text{l}$ . Control reactions with unlabeled tRNA, and with the PTD lacking the reactive maleimide were also performed. After reacting for 2 hours at room temperature, the reaction mixture was loaded onto a 12% PAGE gel (19:1, 7M urea, 1 x TBE, running buffer 1 x TBE and 0.1 % SDS), and run at 170 V for 30 minutes. Bands were visualized by treatment with Stains-All.

Synthetic 14mer RNAs had to undergo 2'OH deprotection (silyl) before use. Typically, 1  $\mu\text{mol}$  of RNA was mixed with 300  $\mu\text{l}$  of 1 M TBAF for 24 hours. The volume was reduced by vacuum, and brought up to 500  $\mu\text{l}$  using a 50 % acetonitrile solution. This was purified using a NAP-25 column (Amersham), following the manufacturer's instructions. The eluant was reduced in volume by vacuum, then

precipitated using a 1/10 volume of 1 M  $\text{NH}_4\text{OH}$ , 1 mM spermidine, and 1 volume of isopropanol.

The 5'thiol modified 14mer RNAs had to undergo deprotection of the thiol (trityl) before use. This was done using the Glen Research protocol. Briefly, 15  $\mu\text{l}$  of a 1 M  $\text{AgNO}_3$  solution was added to a 50  $\mu\text{l}$  solution of 14mer in 0.1 M TEAA. After sitting at room temperature for 30 minutes, 20  $\mu\text{l}$  of 1 M DTT was added. This was centrifuged, the pellet washed with 100  $\mu\text{l}$  of 0.1 M TEAA, the supernatants combined, and brought up to 500  $\mu\text{l}$  with 50% acetonitrile. This was desalted on a NAP-25 column (Amersham) according to the manufacturer's instructions. The final eluant was lyophilized to dryness, and stored as a powder.

Coupling reactions between 5'thiol-modified 14mer, 5'phosphorothioate labeled 14mer RNA and PTD-mal were done under a variety of conditions. A typical reaction was done using 5  $\mu\text{g}$  of 14mer RNA, with 2 - 20  $\mu\text{g}$  of PTD-mal, in 10  $\mu\text{l}$  total volume. These were done at room temperature, typically for  $\sim$  2 hours. A variety of buffers and salt concentrations were tested (see results section).

Ligation of the HSAS 3'71mer to the HSAS 5'14mer was done using the following protocol. The HSAS 3'71 was reacted with alkaline phosphatase, cleaned up by PCI extraction, and then reacted with polynucleotide kinase (PNK) and again cleaned up by PCI extraction. 50  $\mu\text{g}$  of this tRNA was mixed with 50  $\mu\text{g}$  of the 14mer RNA in 180  $\mu\text{l}$ , and heated to 90°C for 2 minutes. Separately, a solution of 200 mM  $\text{MgCl}_2$  and 400 mM HEPES were heated to 90°C. 40  $\mu\text{l}$  of each of these solutions was added to the hot RNA solution. This was cooled to room temperature, and 80  $\mu\text{l}$  of a 5x ligation buffer was added, as well as 40  $\mu\text{l}$  DMSO and 20  $\mu\text{l}$  of RNA ligase. This was then

incubated at 15°C overnight. The 5x ligation buffer consisted of 20  $\mu$ l 100mM DTT, 7.5  $\mu$ l 10 mM ATP, 20  $\mu$ l 20mg/ml BSA-Ac, 50.5  $\mu$ l water and 2  $\mu$ l RNase inhibitor.

## 2.4.8 Lipofection

### 2.4.8.1 Effectene

Cells were transfected following the manufacturer's instructions (Qiagen). Briefly, 1.7  $\mu$ g of DNA, with or without 3.5  $\mu$ g of HSAS tRNA, was combined with 85  $\mu$ l of the provided EC buffer and incubated for 5 minutes. 5.1  $\mu$ l of Enhancer was added and incubated for a further 5 minutes. 10.2  $\mu$ l of Effectene was added to this, incubated for 10 minutes and diluted to 600  $\mu$ l with prewarmed DMEM (10% FBS, including antibiotics). This was added to the cells, followed by 1.5 ml of fresh media and incubated overnight.

### 2.4.8.2 Polyfect

Cells were transfected following the manufacturer's instructions (Qiagen). Briefly, 3  $\mu$ g of DNA with or without 7  $\mu$ g of HSAS tRNA was diluted to 150  $\mu$ l using serum free media. 15  $\mu$ l of the Polyfect reagent was added to this, and incubated for 10 minutes. Fresh media (1 ml) containing serum and antibiotics was added to the cells, and 1 ml of fresh media was added to the Polyfect complex, the latter of which was also applied to the cells. This was incubated overnight.

#### 2.4.8.3 GeneJammer

Cells were transfected following the manufacturer's instructions (Stratagene). Briefly, 6  $\mu$ l of the GeneJammer reagent was added to 100  $\mu$ l of serum-free media, and incubated for 10 minutes. 1  $\mu$ g of DNA with or without 5  $\mu$ g of HSAS tRNA was added to this and incubated for a further 10 minutes. 900  $\mu$ l of fresh serum containing media was added to the cells, and the transfection mix was added to this drop-wise. The cells were incubated for 3 hours, 1 ml of fresh media was then added, and the cells were further incubated overnight.

#### 2.4.8.4 Lipofectamine 2000

Cells were transfected following the manufacturer's instructions (Invitrogen). Briefly, 1  $\mu$ g of DNA was added to 250  $\mu$ l of serum-free media. Separately, 3  $\mu$ l of the Lipofectamine 2000 reagent was added to 250  $\mu$ l of serum-free media and incubated for 5 minutes. The DNA and Lipofectamine solutions were combined and incubated for 20 minutes. 2 ml of fresh serum containing media was added to the cells, followed by addition of the 500  $\mu$ l DNA/Lipofectamine complex solution. This was incubated for 4 hours, at which point the media was replaced with fresh growth media.

#### 2.4.9 Biolistics

Preparation of the DNA/tRNA coated gold microcarriers was done according to the Bio-Rad protocol. Briefly, 17.5 mg of 1.6  $\mu$ m gold beads were weighed out. 50  $\mu$ l of a 50 mM spermidine solution was added to the beads, and sonicated for 5 minutes. 25  $\mu$ g of DNA with or without 50  $\mu$ g of tRNA was added, and the mixture was vortexed. While

vortexing, 50  $\mu$ l of a 1 M CaCl<sub>2</sub> solution was added drop-wise. The suspension was incubated at room temperature for 10 minutes, with vortexing every 2 minutes. This was then centrifuged, washed three times with 100% ethanol, and resuspended in 300  $\mu$ l PVP/ethanol solution (0.02 mg/ml PVP in ethanol) with vortexing. This was transferred to a 15 ml conical tube, and diluted to 3.5 ml with the PVP/ethanol solution. The gold-coat tubing was then prepared as described by the Bio-Rad Helios Gene Gun protocol.

## 2.5 References

1. Cornish, V.W., et al., *Site-specific incorporation of biophysical probes into proteins*. Proc Natl Acad Sci USA, 1994. **91**: p. 2910-2914.
2. Cornish, V.W., D. Mendel, and P.G. Schultz, *Probing protein structure and function with an expanded genetic code*. Angew Chem Int Ed Engl, 1995. **34**: p. 621-633.
3. Dougherty, D.A., *Unnatural amino acids as probes of protein structure and function*. Curr Opin Chem Biol, 2000. **4**(6): p. 645-52.
4. Gillmore, M.A., L.E. Steward, and A.R. Chamberlin, *Incorporation of noncoded amino acids by in vitro protein biosynthesis*. Topics Curr Chem, 1999. **202**: p. 77-99.
5. Beene, D.L., D.A. Dougherty, and H.A. Lester, *Unnatural amino acid mutagenesis in mapping ion channel function*. Curr Opin Neurobiol, 2003. **13**(3): p. 264-70.
6. Nowak, M.W., et al., *In vivo incorporation of unnatural amino acids into ion channels in a Xenopus oocyte expression system*. Methods Enzymol., 1998. **293**: p. 504-529.
7. Nowak, M.W., et al., *Nicotinic receptor binding site probed with unnatural amino acid incorporation in intact cells*. Science, 1995. **268**(5209): p. 439-42.
8. Li, L.T., et al., *The tethered agonist approach to mapping ion channel proteins toward a structural model for the agonist binding site of the nicotinic acetylcholine receptor*. Chemistry & Biology, 2001. **8**(1): p. 47-58.
9. Petersson, E.J., et al., *A perturbed pK(a) at the binding site of the nicotinic acetylcholine receptor: Implications for nicotine binding*. J Am Chem Soc, 2002. **124**(43): p. 12662-12663.
10. Kearney, P.C., et al., *Determinants of nicotinic receptor gating in natural and unnatural side chain structures at the M2 9' position*. Neuron, 1996. **17**(6): p. 1221-9.
11. Miller, J.C., et al., *Flash decaging of tyrosine sidechains in an ion channel*. Neuron, 1998. **20**(4): p. 619-24.
12. Zhong, W., et al., *From ab initio quantum mechanics to molecular neurobiology: A cation- $\pi$  binding site in the nicotinic receptor*. Proc Natl Acad Sci USA, 1998. **95**: p. 12088-12093.

13. Beene, D., et al., *Cation- $\pi$  interactions in ligand recognition by serotonergic (5-HT<sub>3A</sub>) and nicotinic acetylcholine receptors: The anomalous binding properties of nicotine*. *Biochemistry*, 2002. **41**(32): p. 10262-10269.
14. England, P.M., et al., *Site-specific, photochemical proteolysis applied to ion channels in vivo*. *Proc Natl Acad Sci U S A*, 1997. **94**(20): p. 11025-30.
15. Tong, Y.H., et al., *Tyrosine decaging leads to substantial membrane trafficking during modulation of an inward rectifier potassium channel*. *J Gen Physiol*, 2001. **117**(2): p. 103-118.
16. Saks, M.E., et al., *An engineered Tetrahymena tRNA<sup>Gln</sup> for in vivo incorporation of unnatural amino acids into proteins by nonsense suppression*. *J Biol Chem*, 1996. **271**(23169-23175): p. 23169-23175.
17. Capone, J.P., P.A. Sharp, and U.L. RajBhandary, *Amber, ochre and opal suppressor tRNA genes derived from a human serine tRNA gene*. *Embo J*, 1985. **4**(1): p. 213-21.
18. Ilegems, E., H.M. Pick, and H. Vogel, *Monitoring mis-acylated tRNA suppression efficiency in mammalian cells via EGFP fluorescence recovery*. *Nucleic Acids Res*, 2002. **30**(23): p. e128.
19. Drabkin, H.J., H.J. Park, and U.L. RajBhandary, *Amber suppression in mammalian cells dependent upon expression of an Escherichia coli aminoacyl-tRNA synthetase gene*. *Mol Cell Biol*, 1996. **16**(3): p. 907-13.
20. Park, H.J. and U.L. RajBhandary, *Tetracycline-regulated suppression of amber codons in mammalian cells*. *Mol Cell Biol*, 1998. **18**(8): p. 4418-25.
21. Kohrer, C., et al., *Import of amber and ochre suppressor tRNAs into mammalian cells: a general approach to site-specific insertion of amino acid analogues into proteins*. *Proc Natl Acad Sci U S A*, 2001. **98**(25): p. 14310-5.
22. Bobanovic, F., *Electroporation: A method for introduction of non-permeable molecular probes*, in *Biological Techniques: Fluorescent and luminescent probes for biological activity*, W.T. Mason, Editor. 1999, Academic Press: San Diego. p. 82-93.
23. Keown, W.A., C.R. Campbell, and R.S. Kucherlapati, *Methods for introducing DNA into mammalian cells*. *Methods Enzymol*, 1990. **185**: p. 527-37.
24. Negrutskii, B.S. and M.P. Deutscher, *Channeling of aminoacyl-tRNA for protein synthesis in vivo*. *Proc Natl Acad Sci U S A*, 1991. **88**(11): p. 4991-5.
25. Teruel, M.N., et al., *A versatile microporation technique for the transfection of cultured CNS neurons*. *J Neurosci Meth*, 1999. **93**: p. 37-48.

26. Teruel, M.N. and T. Meyer, *Electroporation-induced formation of individual calcium entry sites in the cell body and processes of adherent cells*. Biophys J, 1997. **73**: p. 1785-1796.
27. Raptis, L., et al., *In Situ electroporation for the study of signal transduction*, in *Cell Biology: A laboratory handbook*, J.E. Celis Editor. 198, Academic Press: San Diego. p. 75-87.
28. Terrone, D., et al., *Penetratin and related cell-penetrating cationic peptides can translocate across lipid bilayers in the presence of a transbilayer potential*. Biochemistry, 2003. **42**(47): p. 13787-99.
29. Kabouridis, P.S., *Biological applications of protein transduction technology*. Trends Biotechnol, 2003. **21**(11): p. 498-503.
30. Nakanishi, M., et al., *Basic peptides as functional components of non-viral gene transfer vehicles*. Curr Protein Pept Sci, 2003. **4**(2): p. 141-50.
31. Matsui, H., et al., *Protein Therapy: in vivo protein transduction by polyarginine (11R) PTD and subcellular targeting delivery*. Curr Protein Pept Sci, 2003. **4**(2): p. 151-7.
32. Bogoyevitch, M.A., et al., *Taking the cell by stealth or storm? Protein transduction domains (PTDs) as versatile vectors for delivery*. DNA Cell Biol, 2002. **21**(12): p. 879-94.
33. Ford, K.G., et al., *Protein transduction: an alternative to genetic intervention?* Gene Ther, 2001. **8**(1): p. 1-4.
34. Fernandez, T. and H. Bayley, *Ferrying proteins to the other side*. Nat. Biotech., 1998. **16**: p. 418-421.
35. Bayley, H., *Protein therapy-delivery guaranteed*. Nat. Biotech., 1999. **17**: p. 1066-1067.
36. Schwarze, S.R., et al., *In vivo protein transduction: delivery of a biologically active protein into the mouse*. Science, 1999. **285**(3): p. 1569-1572.
37. Schwarze, S.R. and S.F. Dowdy, *In vivo protein transduction: intracellular delivery of biologically active proteins, compounds and DNA*. Trends. Pharm. Sci., 2000. **21**: p. 45-48.
38. Lindgren, M., et al., *Translocation properties of novel cell penetrating transportan and penetratin analogues [In Process Citation]*. Bioconjug Chem, 2000. **11**(5): p. 619-26.
39. Lindgren, M., et al., *Cell-penetrating peptides*. Trends Pharm. Sci., 2000. **21**: p. 99-103.

40. Derossi, D., G. Chassaing, and A. Prochiantz, *Trojan peptides: the penetratin system for intracellular delivery*. Trends Cell Biol, 1998. **8**(2): p. 84-7.
41. Derossi, D., et al., *The third helix of the Antennapedia homeodomain translocates through biological membranes*. J Biol Chem, 1994. **269**(14): p. 10444-50.
42. Chatelin, L., et al., *Transcription factor hoxa-5 is taken up by cells in culture and conveyed to their nuclei*. Mech Dev, 1996. **55**(2): p. 111-7.
43. Derossi, D., et al., *Cell internalization of the third helix of the Antennapedia homeodomain is receptor-independent*. J Biol Chem, 1996. **271**(30): p. 18188-93.
44. Allinquant, B., et al., *Downregulation of amyloid precursor protein inhibits neurite outgrowth in vitro*. J. Cell Biol., 1995. **128**(5): p. 919-927.
45. Troy, C.M., et al., *Downregulation of Cu/Zn superoxide dismutase leads to cell death via the nitric oxide-peroxynitrite pathway*. J Neurosci, 1996. **16**(1): p. 253-61.
46. Ede, N.J., G.W. Tregear, and J. Haralambidis, *Routine preparation of thiol oligonucleotides: Application to the synthesis of oligonucleotide-peptide hybrids*. Bioconjugate Chem., 1994. **5**: p. 373-378.
47. Eritja, R., et al., *Synthesis of defined peptide-oligonucleotide hybrids containing a nuclear transport signal sequence*. Tetrahedron, 1991. **47**(24): p. 4113-4120.
48. Arar, K., M. Nomsigny, and R. Mayer, *Synthesis of oligonucleotide-peptide conjugates containing a KDEL signal sequence*. Tetrahedron Lett., 1993. **34**(50): p. 8087-8090.
49. Wu, C.W., et al., *Kinetics of coupling reactions that generate monothiophosphate disulfides: implications for modification of RNAs*. Bioconjug Chem, 2001. **12**(6): p. 842-4.
50. Wolfson, A.D., J.A. Pleiss, and O.C. Uhlenbeck, *A new assay for tRNA aminoacylation kinetics*. Rna, 1998. **4**(8): p. 1019-23.
51. Pan, T., R.R. Gutell, and O.C. Uhlenbeck, *Folding of circularly permuted transfer RNAs*. Science, 1991. **254**(5036): p. 1361-4.
52. Stello, T., M. Hong, and K. Musier-Forsyth, *Efficient aminoacylation of tRNA(Lys,3) by human lysyl-tRNA synthetase is dependent on covalent continuity between the acceptor stem and the anticodon domain*. Nucleic Acids Res, 1999. **27**(24): p. 4823-9.
53. Hou, Y.M., R.S. Lipman, and J.A. Zarutskie, *A tRNA circularization assay: evidence for the variation of the conformation of the CCA end*. Rna, 1998. **4**(7): p. 733-8.

54. Qiu, P., et al., *Gene gun delivery of mRNA in situ results in efficient transgene expression and genetic immunization*. *Gene Ther*, 1996. **3**(3): p. 262-8.
55. Davis, R.E., et al., *Transient expression of DNA and RNA in parasitic helminths by using particle bombardment*. *Proc Natl Acad Sci U S A*, 1999. **96**(15): p. 8687-92.

## **Chapter 3**

### **The HSAS Assay: Optimizing tRNA Delivery to Mammalian Cells**

### 3.1 Introduction

Unnatural amino acid incorporation into proteins by nonsense suppression has proven to be a valuable tool for structure-function studies [1-5]. Using the *in vivo* nonsense suppression methodology [6], information on ligand binding and ion channel gating mechanisms has been obtained on a variety of ion channels including the nicotinic ACh receptor (nAChR) [7-12], 5-HT<sub>3A</sub> receptor [13], and the Shaker [14] and Kir2.1 [15] potassium channels. To date, such studies have been limited to the *Xenopus* oocyte heterologous expression system. There would be clear benefits to expanding the technology to a mammalian cell expression system. This would provide a more relevant environment for many proteins of mammalian origin and would allow for studies of cell-specific signal transduction pathways.

When developing a new translation system for unnatural amino acid incorporation, there are many variables to be considered. Importantly, one needs to deliver enough aminoacyl-tRNA to each cell in order to generate a detectable amount of protein. One of the greatest challenges in developing a mammalian cell expression system for unnatural amino acid incorporation arises from the fact that the aminoacyl-tRNA is a stoichiometric reagent. The amount of protein made containing the unnatural amino acid is limited by the amount of aminoacyl-tRNA that can be delivered to the cell. Because of the relatively small size of mammalian cells (10 - 30  $\mu$ M in diameter) in comparison to *Xenopus* oocytes (diameter  $\sim$  1 mm), much less aminoacyl-tRNA can be delivered to the former, hence less protein can be made.

Electroporation is a common method used to deliver many different types of macromolecules to cells, and is generally a favoured DNA transfection technique [16, 17]. It is operationally easy, reproducible, and works for many cell types including cultured neurons. Furthermore, cells that are either attached or in suspension can be transfected by electroporation. In essence, the application of an electric field to a population of cells results in reversible membrane breakdown, and the formation of large pores that allow the passage of macromolecules. The basic steps of electroporation include (i) electric field generation, (ii) polarization of the outer membrane, (iii) pore formation, (iv) transmembrane transport and (v) electropore resealing. The mechanism of pore formation and resealing is not known. Another advantage to this technique is that there are many parameters to control for optimization, including electric field strength, pulse duration and the number of pulses applied. A disadvantage is that there is no standard protocol, so optimization must be done for each individual system studied. Finally, electroporation has been used to successfully deliver aminoacyl-tRNA (rabbit liver tRNA) to CHO cells, although in this report the tRNA was found to not be functional within the cells [18]. Because of its generality, electroporation was tested as a method to deliver tRNA to adherent mammalian cells.

In order to minimize the amount of material required to transfect the cells, a "microporator" designed by Teruel and Meyer was used [19, 20]. This electroporation device allows for the transfection of a small area of attached cells ( $\sim 1 \text{ cm}^2$ ), requiring small volumes of electroporation solution (1 - 10  $\mu\text{l}$ ). Teruel and Meyer have demonstrated successful transfection using both DNA and mRNA, with over 90% cell

survivability and over 50% transfection efficiency in rat basophilic leukemia cells, neocortical neuroblastoma cells and hippocampal neurons.

There are other variables that need to be considered. It has to be established that the mammalian cell translational machinery will recognize *in vitro* transcribed tRNA, while maintaining orthogonality to the endogenous synthetases. Also, one has to minimize hydrolysis of the aminoacyl-ester bond, which is labile at physiological pH, i.e. the required working pH when handling mammalian cells. Finally, it has to be determined if the tRNA THG73 - optimized for *Xenopus* oocyte nonsense suppression [21] - is functional in a mammalian expression system.

The HSAS assay described here was developed to reduce these variables, and to optimize tRNA delivery by electroporation. This assay involves the suppression of EGFP by a human serine amber suppressor tRNA (HSAS) first described by RajBhandary and coworkers [22] (Figure 3.1). They mutated the anticodon of the human serine tRNA to read the amber stop codon TAG. Because the tRNA anticodon is not a serine synthetase recognition element, this tRNA is still recognized and serylated in cultured mammalian cells. In our assay, HSAS was made by *in vitro* transcription. Likewise, the codon for Ser29 of EGFP was mutated to a TAG stop codon. It was hoped that when HSAS and Ser29TAG EGFP DNA were co-electroporated into mammalian cells, the HSAS would first be aminoacylated by the serine synthetase, and then used for nonsense suppression of EGFP. Electroporation of Ser29TAG mutant EGFP in the absence of HSAS tRNA would produce truncated non-functional protein (Figure 3.2). The advantage of this assay is that it allowed us to test for tRNA delivery to cells and to see if *in vitro* transcribed tRNA is functional in mammalian cells, without worrying about



## 3.2 Results

### 3.2.1 Electroporation of tRNA into adherent CHO-K1 and HEK cells: EGFP expression by nonsense suppression

The mutated EGFP construct Ser29TAG was combined with *in vitro* transcribed HSAS tRNA to a volume of 5  $\mu$ l. A microelectroporator was used to transfect adherent mammalian cells with tRNA and DNA. The electroporator was designed to transfect a small section ( $\sim 1 \text{ cm}^2$ ) of cells in a 35 mm dish, and therefore requires only small volumes of the transfection solution. Transfection was achieved by applying this solution to adherent CHO-K1 cells or HEK cells and applying four 120 V, 50 ms square wave pulses.

As shown in Figure 3.3, 2 hours after transfection there is high EGFP expression in CHO-K1 cells transfected with either wild-type EGFP or mutant Ser29TAG EGFP DNA and HSAS. When only the Ser29TAG mutant DNA is transfected without HSAS, no EGFP expression is observed in CHO-K1 cells. This demonstrates that both DNA and tRNA can be coelectroporated into cells with high efficiency; *in vitro* transcribed HSAS is aminoacylated by the endogenous CHO-K1 synthetase; and HSAS then functions as a suppressor tRNA in mammalian cells.

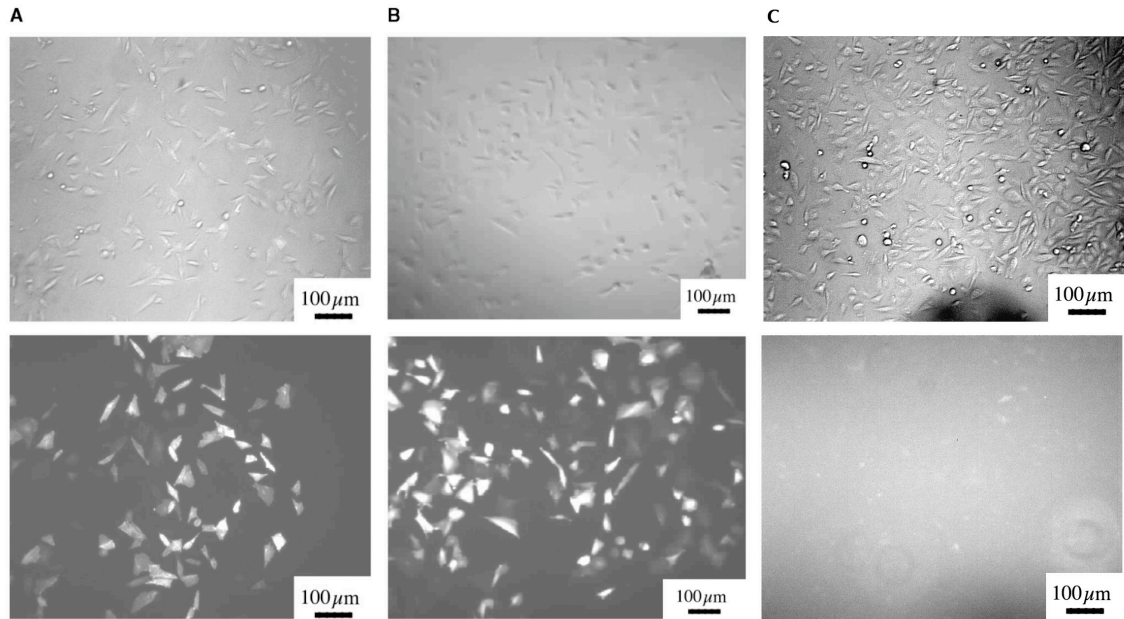


**Figure 3.3.** EGFP (pCS2gap EGFP) expression in CHO-K1 cells by nonsense suppression using HSAS tRNA. (A) CHO-K1 cells were electroporated with a 5  $\mu$ l solution of HSAS (4  $\mu$ g/ $\mu$ l) and Ser29TAG EGFP DNA (2.5  $\mu$ g/ $\mu$ l). (B) CHO-K1 cells were electroporated with wt EGFP DNA (2.5  $\mu$ g/ $\mu$ l). (C) CHO-K1 cells were electroporated with Ser29TAG EGFP DNA only (2.5  $\mu$ g/ $\mu$ l). For all cases, four 120 V, 50 ms pulses were delivered to the cells. The bright-field (upper) and fluorescent (lower) images were taken 2 hr after transfection. The fluorescent image in (C) was taken with twice the exposure length as in (A) and (B).

In the case of HEK cells, lower expression was observed when compared to CHO-K1 cells. For this reason imaging of the cells was done 20 hours after transfection. Expression levels of the wild-type EGFP were similar to the HSAS suppressed EGFP, but there is more background signal evident in cells that were transfected with only the Ser29TAG DNA.

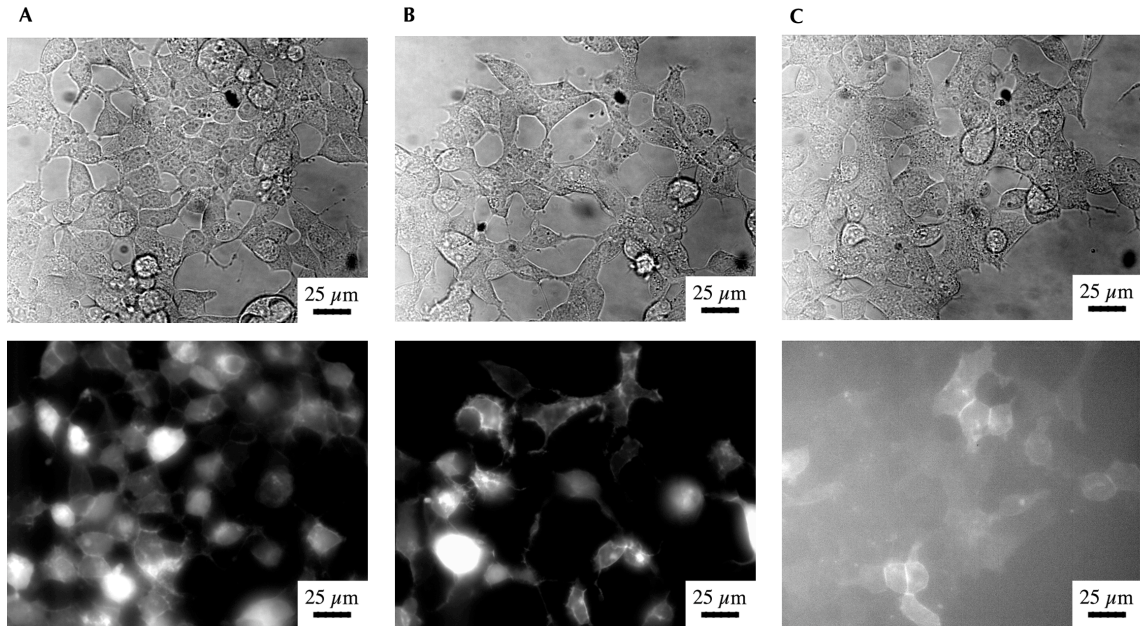


**Figure 3.4.** EGFP (pEGFP-F) expression in HEK cells by nonsense suppression using HSAS tRNA. (A) HEK cells were electroporated with wt EGFP DNA ( $2.5 \mu\text{g}/\mu\text{l}$ ). (B) HEK cells were electroporated with a  $5 \mu\text{l}$  solution of HSAS ( $4 \mu\text{g}/\mu\text{l}$ ) and Ser29TAG EGFP DNA ( $2.5 \mu\text{g}/\mu\text{l}$ ). (C) HEK cells were electroporated with Ser29TAG EGFP DNA only ( $2.5 \mu\text{g}/\mu\text{l}$ ). For all cases, four 120 V, 50 ms pulses were delivered to the cells. The bright-field (upper) and fluorescent (lower) images were taken 20 hr after transfection. The fluorescent image in (C) was taken with four times the exposure length as in (A) and (B).

### 3.2.2 Nonsense suppression in hippocampal neurons

In order to determine the generality of this method, we tested the EGFP suppression assay in neurons. As with CHO and HEK cell transfection, HSAS tRNA and Ser29TAG EGFP DNA were coelectroporated into E18 rat hippocampal neurons (5 days in culture). As can be seen in Figure 3.5, 24 hours after transfection EGFP suppression by HSAS leads to comparable expression levels as electroporation of wild-type EGFP DNA. This demonstrates that electroporation also efficiently delivers tRNA and DNA to neurons and that the neurons also readily use in vitro transcribed tRNA for nonsense

suppression. As shown in Figure 3.5 (C), only low levels of fluorescence were detected when no tRNA is added, indicating that minimal read-through of the Ser29TAG construct occurred.

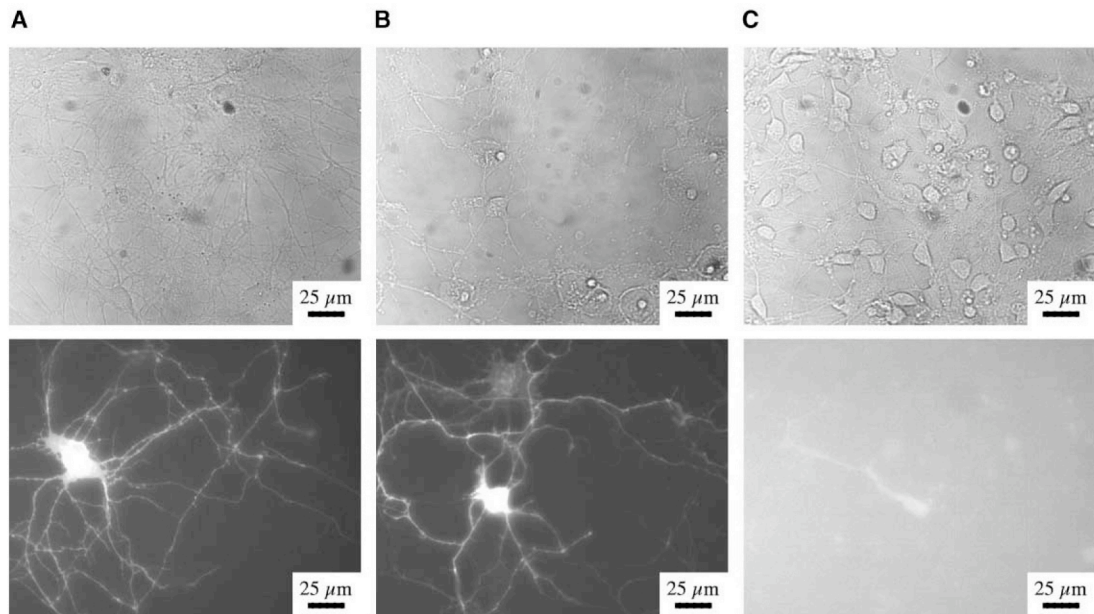


**Figure 3.5.** EGFP (pEGFP-F) expression in hippocampal neurons by nonsense suppression using HSAS tRNA. E18 rat hippocampal neurons (5 days in culture) were electroporated with a 5  $\mu\text{l}$  solution of (A) HSAS (4  $\mu\text{g}/\mu\text{l}$ ) and Ser29TAG EGFP DNA (2.5  $\mu\text{g}/\mu\text{l}$ ); (B) wt EGFP DNA (2.5  $\mu\text{g}/\mu\text{l}$ ); (C) Ser29TAG EGFP DNA in the absence of HSAS tRNA. In all cases, four 160 V, 25 ms pulses were delivered to the cells. The bright-field (upper) and fluorescent (lower) images were taken 24 hr after transfection. The fluorescence image in (C) was taken with twice the exposure as (A) and (B).

### 3.3 Discussion and Future Directions

Presented is a general microelectroporation method to transfect mammalian cells with amber suppressor tRNA and DNA simultaneously. CHO-K1 cells, HEK cells and hippocampal neurons readily aminoacylate in vitro transcribed human amber suppressor tRNA (HSAS), and this tRNA is efficiently used by the translational machinery of these cells. The levels of HSAS suppressed EGFP expression all appear to be similar to the levels of wild-type EGFP expression. This suggests that enough HSAS tRNA is getting into the cells to not be a limiting factor for EGFP expression. However, it is important to note that HSAS suppression is most likely catalytic, in that each HSAS tRNA can be serylated and used for nonsense suppression multiple times.

Our results with the HSAS assay tRNA appear to contradict early reports by Deutscher and coworkers, who found that exogenous tRNA was not used by the translational machinery of mammalian cells [18]. They concluded that tRNA is "channeled" within the cell and that exogenous tRNA cannot enter the translational apparatus. Although their experimental design differed somewhat from ours (their tRNA was isolated from rabbit liver), the reason our results differ so significantly is unclear. What is clear from our results is that exogenous tRNA can easily enter into the protein synthesis pathway.

There are many advantages to the HSAS assay. One in particular is that it allowed for the optimization of tRNA delivery, without consuming large quantities of aminoacyl-tRNA, which is chemically prepared and difficult to obtain in large amounts. Another advantage of the HSAS assay is that it can be used to test other methods of

tRNA delivery to mammalian cells. In addition to electroporation, we investigated several other transfection techniques including the commercially available transfection reagents Effectene and Polyfect (Qiagen), GeneJammer (Stratagene), Lipofectamine (Invitrogen), as well as microinjection and biolistics. All of these approaches resulted in lower DNA delivery, with no convincing evidence of tRNA delivery (discussed in greater detail in Chapter 2).

In our hands, microelectroporation proved to be the most effective method for tRNA delivery to mammalian cells. First, it is highly general since many types of cells can be electroporated with equal efficiency and low cell mortality. Second, the method and instrumentation are very simple. The microelectroporator is easily built, is small and portable, and is easy to use [19]. Electroporation of adherent cells can be done on the benchtop or in a biological safety cabinet, and hundreds of cells can be transfected in a matter of seconds. Furthermore, protein expression is observable as soon as 2 hours after transfection.

The HSAS assay is now being used to test single cell electroporation [23-27], by Dr. Rigo Pantoja in the Lester lab. This method has the advantage of requiring significantly less material than the microelectroporator. Although the microelectroporator only uses 5 to 6  $\mu$ l of transfection solution, the vast majority of this goes to waste since only a small percentage ( $\leq 1\%$ ) of the material applied actually gets inside the cells. With single cell electroporation, a micropipette is filled with a small volume (hundreds of nanoliters) of transfection solution, and this can be used to transfect hundreds of cells in multiple dishes. This method is being developed and optimized by delivery of Ser29TAG EGFP mutant DNA and HSAS tRNA.

Another application of the HSAS assay that is currently in progress is the optimization of the nonsense suppression method using siRNA directed toward the eukaryotic release factor eRF1, by Joanne Xiu in the Dougherty lab. This is based on a previous report that demonstrated increased read-through of stop codons when siRNA designed to recognize eRF1 was delivered to HEK cells [28]. We believe that eRF1 may compete with our nonsense suppressor tRNAs and unnatural amino acid incorporation. Therefore if we can reduce the amount of eRF1 present in either *Xenopus* oocytes or mammalian cells, we may be able to increase the efficiency of unnatural amino acid incorporation. Miss Xiu is using the HSAS assay to look for enhanced suppression with the addition of siRNA in a variety of expression systems.

Another spin off of the HSAS assay involves mutation of the HSAS tRNA to remove the synthetase recognition elements, so that this tRNA can be used for unnatural amino acid incorporation. This approach is being pursued by Dr. Fraser Moss in the Lester lab. Because HSAS suppression is so efficient in all the cell lines tested, the translational machinery of the cell must efficiently recognize this tRNA even though it is generated by in vitro transcription and hence lacks all the post-transcriptional modifications that most tRNAs possess. If appropriately modified such that it is no longer serylated, but still recognized by the translational machinery, this may prove to be an effective tRNA for unnatural amino acid delivery in mammalian cells. The serine synthetase recognition elements have been identified for the human serine tRNA [29-36], and based on these a variety of modified HSAS tRNAs are being prepared and tested in vitro and in cell culture.

In conclusion, the HSAS assay has proved to be quite valuable in optimizing tRNA delivery to mammalian cells by electroporation. It has also become a routine assay for exploring other methods of tRNA delivery, as well as optimization of existing methods.

## 3.4 Experimental Methods and Materials

### 3.4.1 Materials

Synthetic DNA oligonucleotides were synthesized on an ABI 394 DNA Synthesizer on site. Restriction enzymes and T4 RNA ligase were purchased from New England Biolabs (Beverly, MA). The mMessage mMachine and MegaShortScript in vitro transcription kits were purchased from Ambion (Austin, TX). Maxiprep kits used for plasmid isolation were purchased from Qiagen (Valencia, CA). Two membrane-localized GFP mammalian expression vectors were used, pCS2gapEGFP (Jack Horne, Caltech) and pEGFP-F (BD Biosciences Clontech, Palo Alto, CA). pEGFP-N1, a soluble EGFP construct was also purchased from BD Biosciences Clontech (Palo Alto, CA). Ham's F12 tissue culture media and DMEM were purchased from Irvine Scientific (Santa Ana, CA), and CO<sub>2</sub> independent and Neurobasal Media were purchased from GIBCO Introgen Corporation (Carlsbad, CA). The microelectroporator was built on site.

### 3.4.2 Mutagenesis and tRNA synthesis

The HSAS gene was constructed as follows: Two complementary synthetic oligonucleotides encoding for the T7 promoter, the HSAS gene, and the Fok I restriction site were annealed and ligated into the EcoR I and BamH I restriction sites of pUC19. After linearization of the DNA with Fok I, in vitro transcription with the MegShortScript kit yields 74-mer tRNA (i.e. lacking the 3' terminal CA nucleotides). EGFP mutants (pCS2gapEGFP and pEGFP-F Ser29TAG) were made following the Quickchange mutagenesis protocol (Stratagene).

### 3.4.3 Tissue culture

CHO cells were grown in Ham's F12 media and HEK cells were grown in DMEM, enriched with glutamine, fetal bovine serum (FBS, 10 %), penicillin, and streptomycin at 37°C and 5% CO<sub>2</sub>. 1 to 2 days prior to electroporation, the cells were passaged onto 35 mm tissue culture dishes such that confluency was typically 50% or less at the time of transfection.

Rat E18 hippocampal neurons were prepared as described previously [37]. Briefly, hippocampi were digested with 0.25% trypsin and then triturated. Cells plated in polylysine-coated 35 mm plastic dishes were maintained in Neurobasal medium supplemented with B27, 500  $\mu$ M glutamax, and 5% horse serum (Invitrogen). Transfections were done after 5 days in culture.

### 3.4.4 Electroporation

The DNA or tRNA to be electroporated into either CHO-K1, HEK cells or neurons was precipitated alone or as coprecipitates in ethanol and ammonium acetate, and left at -20°C for at least 1 hour. This was then microcentrifuged at 15,000 rpm, 4°C for 15 minutes, vacuum dried for 5 minutes, and resuspended in CO<sub>2</sub> independent medium to the desired final concentration. The cells were typically transfected with EGFP DNA at a concentration of 2.5  $\mu$ g/ $\mu$ l, with or without HSAS tRNA at a concentration of 4  $\mu$ g/ $\mu$ l. Immediately prior to electroporation, the cell tissue culture media was swapped to CO<sub>2</sub> independent media (with no glutamine, FBS or antibiotics). Approximately 5  $\mu$ l of the electroporation solution was applied to the cells, followed by application of electrical pulses. For CHO-K1 cells and HEK cells this was typically four

120 V pulses of 50 ms duration, and for neurons, four 160 V pulses of 25 ms duration. The CO<sub>2</sub> independent media was immediately replaced with fresh Ham's F12 for CHO-K1 cells, DMEM for HEK cells or the original neurobasal media for neurons, and the cells were placed back into the 37°C incubator. Imaging of EGFP was done as soon as 2 hours after transfection.

### 3.4.5 Microscopy

CHO-K1 cells, HEK cells and neurons were visualized with an inverted microscope (Olympus IMT2), a 250 W Hg/Xe lamp operating at 150 W, a GFP filter set (Chroma, model 41017) with an excitation band pass of 450 to 490 nm and an emission band pass of 500 to 550 nm, 10x/0.25NA or 40x/1.3NA lens, and a Photometrix Quantix CCD camera running Axon Imaging Workbench 4.0.

### 3.5 References

1. Cornish, V.W., et al., *Site-specific incorporation of biophysical probes into proteins*. Proc Natl Acad Sci USA, 1994. **91**: p. 2910-2914.
2. Cornish, V.W., D. Mendel, and P.G. Schultz, *Probing protein structure and function with an expanded genetic code*. Angew Chem Int Ed Engl, 1995. **34**: p. 621-633.
3. Dougherty, D.A., *Unnatural amino acids as probes of protein structure and function*. Curr Opin Chem Biol, 2000. **4**(6): p. 645-52.
4. Gillmore, M.A., L.E. Steward, and A.R. Chamberlin, *Incorporation of noncoded amino acids by in vitro protein biosynthesis*. Topics Curr Chem, 1999. **202**: p. 77-99.
5. Beene, D.L., D.A. Dougherty, and H.A. Lester, *Unnatural amino acid mutagenesis in mapping ion channel function*. Curr Opin Neurobiol, 2003. **13**(3): p. 264-70.
6. Nowak, M.W., et al., *In vivo incorporation of unnatural amino acids into ion channels in a Xenopus oocyte expression system*. Methods Enzymol., 1998. **293**: p. 504-529.
7. Nowak, M.W., et al., *Nicotinic receptor binding site probed with unnatural amino acid incorporation in intact cells*. Science, 1995. **268**(5209): p. 439-42.
8. Li, L.T., et al., *The tethered agonist approach to mapping ion channel proteins toward a structural model for the agonist binding site of the nicotinic acetylcholine receptor*. Chemistry & Biology, 2001. **8**(1): p. 47-58.
9. Petersson, E.J., et al., *A perturbed pK(a) at the binding site of the nicotinic acetylcholine receptor: Implications for nicotine binding*. J Am Chem Soc, 2002. **124**(43): p. 12662-12663.
10. Kearney, P.C., et al., *Determinants of nicotinic receptor gating in natural and unnatural side chain structures at the M2 9' position*. Neuron, 1996. **17**(6): p. 1221-9.
11. Miller, J.C., et al., *Flash decaging of tyrosine sidechains in an ion channel*. Neuron, 1998. **20**(4): p. 619-24.
12. Zhong, W., et al., *From ab initio quantum mechanics to molecular neurobiology: A cation- $\pi$  binding site in the nicotinic receptor*. Proc Natl Acad Sci USA, 1998. **95**: p. 12088-12093.

13. Beene, D., et al., *Cation- $\pi$  interactions in ligand recognition by serotonergic (5-HT<sub>3A</sub>) and nicotinic acetylcholine receptors: The anomalous binding properties of nicotine*. *Biochemistry*, 2002. **41**(32): p. 10262-10269.
14. England, P.M., et al., *Site-specific, photochemical proteolysis applied to ion channels in vivo*. *Proc Natl Acad Sci U S A*, 1997. **94**(20): p. 11025-30.
15. Tong, Y.H., et al., *Tyrosine decaging leads to substantial membrane trafficking during modulation of an inward rectifier potassium channel*. *J Gen Physiol*, 2001. **117**(2): p. 103-118.
16. Bobanovic, F., *Electroporation: A method for introduction of non-permeable molecular probes*, in *Biological Techniques: Fluorescent and luminescent probes for biological activity*, W.T. Mason, Editor. 1999, Academic Press: San Diego. p. 82-93.
17. Keown, W.A., C.R. Campbell, and R.S. Kucherlapati, *Methods for introducing DNA into mammalian cells*. *Methods Enzymol*, 1990. **185**: p. 527-37.
18. Negrutskii, B.S. and M.P. Deutscher, *Channeling of aminoacyl-tRNA for protein synthesis in vivo*. *Proc Natl Acad Sci U S A*, 1991. **88**(11): p. 4991-5.
19. Teruel, M.N., et al., *A versatile microporation technique for the transfection of cultured CNS neurons*. *J Neurosci Meth*, 1999. **93**: p. 37-48.
20. Teruel, M.N. and T. Meyer, *Electroporation-induced formation of individual calcium entry sites in the cell body and processes of adherent cells*. *Biophys J*, 1997. **73**: p. 1785-1796.
21. Saks, M.E., et al., *An engineered Tetrahymena tRNA<sup>Gln</sup> for in vivo incorporation of unnatural amino acids into proteins by nonsense suppression*. *J Biol Chem*, 1996. **271**(23169-23175): p. 23169-23175.
22. Capone, J.P., P.A. Sharp, and U.L. RajBhandary, *Amber, ochre and opal suppressor tRNA genes derived from a human serine tRNA gene*. *Embo J*, 1985. **4**(1): p. 213-21.
23. Nolkrantz, K., et al., *Electroporation of single cells and tissues with an electrolyte-filled capillary*. *Anal Chem*, 2001. **73**(18): p. 4469-77.
24. Olofsson, J., et al., *Single-cell electroporation*. *Curr Opin Biotechnol*, 2003. **14**(1): p. 29-34.
25. Ryttsen, F., et al., *Characterization of single-cell electroporation by using patch-clamp and fluorescence microscopy*. *Biophys J*, 2000. **79**(4): p. 1993-2001.
26. Rae, J.L. and R.A. Levis, *Single-cell electroporation*. *Pflugers Arch*, 2002. **443**(4): p. 664-70.

27. Rathenberg, J., T. Nevian, and V. Witzemann, *High-efficiency transfection of individual neurons using modified electrophysiology techniques*. J Neurosci Methods, 2003. **126**(1): p. 91-8.
28. Carnes, J., et al., *Stop codon suppression via inhibition of eRF1 expression*. Rna, 2003. **9**(6): p. 648-53.
29. Breitschopf, K., et al., *Identity elements of human tRNA(Leu): structural requirements for converting human tRNA(Ser) into a leucine acceptor in vitro*. Nucleic Acids Res, 1995. **23**(18): p. 3633-7.
30. Breitschopf, K. and H.J. Gross, *The exchange of the discriminator base A73 for G is alone sufficient to convert human tRNA(Leu) into a serine-acceptor in vitro*. Embo J, 1994. **13**(13): p. 3166-7.
31. Breitschopf, K. and H.J. Gross, *The discriminator bases G73 in human tRNA(Ser) and A73 in tRNA(Leu) have significantly different roles in the recognition of aminoacyl-tRNA synthetases*. Nucleic Acids Res, 1996. **24**(3): p. 405-10.
32. Himeno, H., et al., *Conversion of aminoacylation specificity from tRNA(Tyr) to tRNA(Ser) in vitro*. Nucleic Acids Res, 1990. **18**(23): p. 6815-9.
33. Lenhard, B., et al., *tRNA recognition and evolution of determinants in seryl-tRNA synthesis*. Nucleic Acids Res, 1999. **27**(3): p. 721-9.
34. Price, S., et al., *Crystallization of the seryl-tRNA synthetase:tRNAS(ser) complex of Escherichia coli*. FEBS Lett, 1993. **324**(2): p. 167-70.
35. Achsel, T. and H.J. Gross, *Identity determinants of human tRNA(Ser): sequence elements necessary for serylation and maturation of a tRNA with a long extra arm*. Embo J, 1993. **12**(8): p. 3333-8.
36. Wu, X.Q. and H.J. Gross, *The long extra arms of human tRNA((Ser)Sec) and tRNA(Ser) function as major identify elements for serylation in an orientation-dependent, but not sequence-specific manner*. Nucleic Acids Res, 1993. **21**(24): p. 5589-94.
37. Li, Y.X., et al., *Enhancement of neurotransmitter release induced by brain-derived neurotrophic factor in cultured hippocampal neurons*. J Neurosci, 1998. **18**(24): p. 10231-40.

## **Chapter 4**

Natural and Unnatural Amino Acid Incorporation into Ion Channels

Expressed in Mammalian Cells by Nonsense Suppression

## 4.1 Introduction

Unnatural amino acid incorporation into proteins by nonsense suppression has proven to be a valuable tool for structure-function studies [1-5]. Using the *in vivo* nonsense suppression methodology [6], information on ligand binding and ion channel gating mechanisms has been obtained on a variety of ion channels including the nicotinic ACh receptor (nAChR) [7-12], 5-HT<sub>3A</sub> receptor [13], and the Shaker [14] and Kir2.1 [15] potassium channels. To date, such studies have been limited to the *Xenopus* oocyte heterologous expression system. There would be clear benefits to expanding the technology to a mammalian cell expression system. This would provide a more relevant environment for many proteins of mammalian origin and would allow for studies of cell-specific signal transduction pathways.

With the electroporation protocol in hand (developed using the HSAS assay, Chapter 3), we were ready to apply the methodology toward the delivery of aminoacyl-tRNA to mammalian cells. Our initial assay involved the suppression of EGFP using THG73-aa. THG73 tRNA has proven to be effective for unnatural amino acid incorporation in the *Xenopus* oocyte expression system. We co-electroporated a variety of EGFP TAG mutants, with a variety of amino acids ligated to THG73, but never observed EGFP expression by nonsense suppression (details in Chapter 2). Although discouraging, we felt that this was most likely because the suppressed EGFP was below our detection limit. What we needed, therefore was a more sensitive assay.

Electrophysiology is one of the most sensitive assays available. Single ion channels can be detected within a cell because ion channels conduct electrical current, a

very sensitive measurement. Because it was ultimately of interest to incorporate unnatural amino acids into ion channels using the mammalian cells expression system, we decided to abandon the EGFP assay and to move on to ion channel expression instead. As described in the following sections, we first demonstrate natural and unnatural amino acid incorporation by nonsense suppression into the nicotinic acetylcholine receptor (nAChR), an ion channel that our lab is very familiar with. We then try to apply the methodology to less familiar systems, including the neuronal  $\alpha 4\beta 2$  AChR, and the neuronal NMDA (N-methyl D-aspartate) receptor.

## 4.2 Results and Discussion

### 4.2.1. nAChR expression by HSAS suppression

The nicotinic acetylcholine receptor (nAChR) is the most well-studied neuronal receptor [16]. The nAChR belongs to a superfamily of ion channels that includes the 5-HT<sub>3</sub>, GABA and glycine receptors, and functions both at the neuromuscular junction and within the CNS. The muscle-type nAChR is a pentameric channel composed of two  $\alpha$  subunits, and one of each  $\beta$ ,  $\delta$ , and  $\gamma$ . Our lab has studied the ligand-binding domain of the muscle-type nAChR extensively, using unnatural amino acid incorporation. These experiments thus far have been limited to the *Xenopus* oocyte expression system [6], so we were interested in extending the methodology to a mammalian cell system. This will allow us to perform studies of cell-specific signal transduction pathways, including those that involve the muscle-type nAChR.

In initial experiments, we wanted to establish that ion channels are efficiently expressed in mammalian cells by nonsense suppression. To do this, we turned to the HSAS assay. We relied on the mutation of a Leu residue in the M2 pore lining region, termed Leu9' [17], that is conserved in all known nAChR subunits. Earlier studies in *Xenopus* oocytes showed that the Leu9'Ser mutation of the  $\beta$  subunit leads to a  $\sim 40$ -fold decrease in the  $EC_{50}$  when compared to the wild-type channel [10, 18]. Therefore, suppression of the  $\beta 9'$ TAG by HSAS should lead to expression of channels that display a substantial shift in the dose-response relation, the characteristic  $\beta$ Leu9'Ser phenotype.

#### 4.2.1.1 Results

Transfection of CHO-K1 cells was achieved by electroporation of a 5  $\mu$ l solution containing HSAS, mutant  $\beta$  subunit mRNA (Leu9'TAG), and mRNA for the remaining wild-type subunits ( $\alpha$ ,  $\delta$ , and  $\gamma$ ). Also included was a reporter EGFP plasmid.

Expression of the nAChR was determined from whole-cell recordings of ACh-induced currents in EGFP-expressing CHO-K1 cells.

As shown in Figure 4.1, 24 hours after transfection the cells exhibit a strong ACh response that is not observed in non-transfected cells. All GFP-expressing cells exhibit an ACh response. Both the receptors generated from HSAS-suppressed  $\beta 9'$ TAG mutant mRNA and from the  $\beta$ Leu9'Ser conventional mutant showed substantial decreases in their  $EC_{50}$  values, relative to wild-type. Interestingly, the shift seen in CHO cells ( $\sim 10$  fold) is smaller than that seen in *Xenopus* oocytes, perhaps due to differential processing in the two different cell types. For the present purposes, however, the key is that the shift seen is the same whether the Leu9'Ser mutant is made by conventional mutagenesis or

nonsense suppression. This demonstrates that HSAS did indeed deliver serine during translation of the  $\beta$ Leu9'TAG subunit.

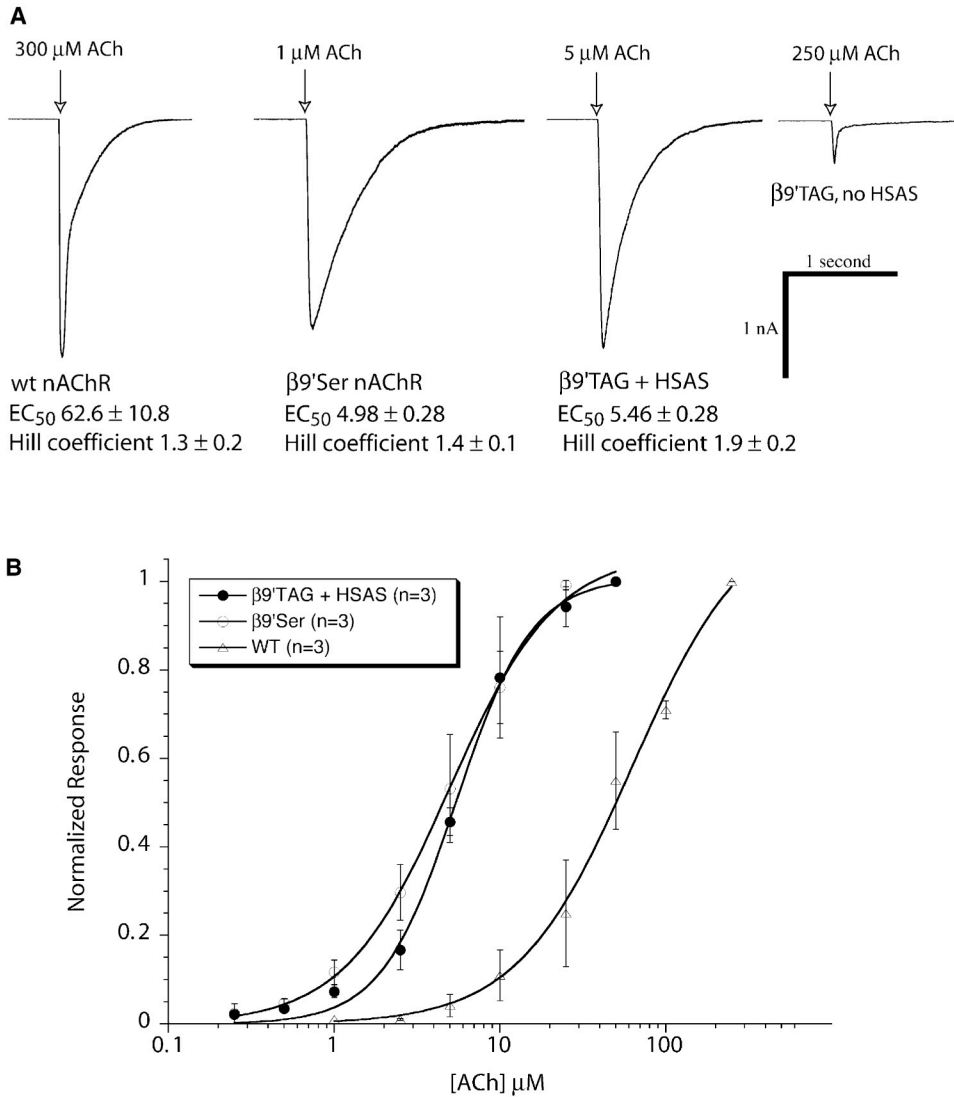


**Figure 4.1.** nAChR expression in CHO-K1 cells by nonsense suppression using HSAS tRNA. (A) CHO-K1 cells were electroporated with a 5  $\mu$ l solution containing  $\alpha$ ,  $\beta$ ,  $\delta$ , and  $\gamma$ , nAChR subunit mRNA, and reporter plasmid. Arrows indicate 25 ms pulses of ACh application. The first trace shows a typical response from cells transfected with the wild-type nAChR subunits (2  $\mu$ g/ $\mu$ l  $\alpha$ , 0.5  $\mu$ g/ $\mu$ l each  $\beta$ ,  $\delta$ , and  $\gamma$ ). The second trace is a response of cells transfected with the  $\beta$ Leu9'Ser mutant (0.15  $\mu$ g/ $\mu$ l) and the remaining wild-type subunits (2  $\mu$ g/ $\mu$ l  $\alpha$ , 0.5  $\mu$ g/ $\mu$ l each  $\delta$ , and  $\gamma$ ). The third trace is a response from cells transfected with mutant  $\beta$ Leu9'TAG mRNA (0.15  $\mu$ g/ $\mu$ l), the remaining wild-type subunits (1  $\mu$ g/ $\mu$ l  $\alpha$ , 0.5  $\mu$ g/ $\mu$ l each  $\delta$ , and  $\gamma$ ), and HSAS tRNA (2  $\mu$ g/ $\mu$ l). The fourth trace shows a response from cells transfected with mutant  $\beta$ Leu9'TAG mRNA and other subunits, in the absence of HSAS tRNA (read-through). The reporter plasmid EGFP-N1 (0.5  $\mu$ g/ $\mu$ l) was included in all cases, and recordings were done from EGFP-expressing cells. The corresponding  $EC_{50}$  values are also shown. (B) ACh dose-response curves for wt nAChR (triangle),  $\beta$ Leu9'Ser nAChR (open circle), and HSAS-suppressed nAChR (closed circle).

#### 4.2.1.2 Discussion

We demonstrate here that CHO-K1 cells readily aminoacylate exogenous HSAS tRNA with serine, and use it for expression of the nAChR by nonsense suppression. This is clearly demonstrated by HSAS nonsense suppression of  $\beta$  Leu9'TAG of the muscle type nAChR, which shows the same characteristic ACh  $EC_{50}$  shift as the conventional  $\beta$  Leu9'Ser mutant. Importantly, the magnitude of the ACh response for the HSAS-suppressed channels is comparable to those for the wild-type and  $\beta$ Leu9'Ser nAChR systems. This establishes that ion channel expression is not tRNA limited, validating that electroporation leads to highly efficient delivery of tRNA to the cells.

#### 4.2.2 nAChR expression by unnatural amino acid incorporation

With the basic protocol being established using the HSAS suppressor, we turned our attention to unnatural amino acid incorporation. Because we are familiar with incorporating unnatural amino acids into the muscle-type nAChR in the *Xenopus* oocyte expression system, we turned to this receptor to optimize aminoacyl-tRNA delivery to mammalian cells. Using our previous experience, we designed an experiment that would produce a distinct phenotype upon unnatural amino acid incorporation. Our studies of the agonist-binding site of the nAChR established a critical role for Trp  $\alpha$ 149 in agonist binding [12]. Specifically, incorporation of a fluorinated Trp series at  $\alpha$  Trp149 - and only  $\alpha$  Trp149 - leads to a right shift of the ACh  $EC_{50}$  with increasing Trp fluorination. In fact, when the  $EC_{50}$  ( $\log[EC_{50}/EC_{50}wt]$ ) is plotted against the calculated gas-phase cation- $\pi$  binding energy for each fluorinated Trp at  $\alpha$ 149, there is a linear relationship (Figure 4.2). We attribute this to a decrease in the cation- $\pi$  binding ability of the fluoro-

Trp derivatives. We therefore set out to reproduce these results in a mammalian cell expression system.

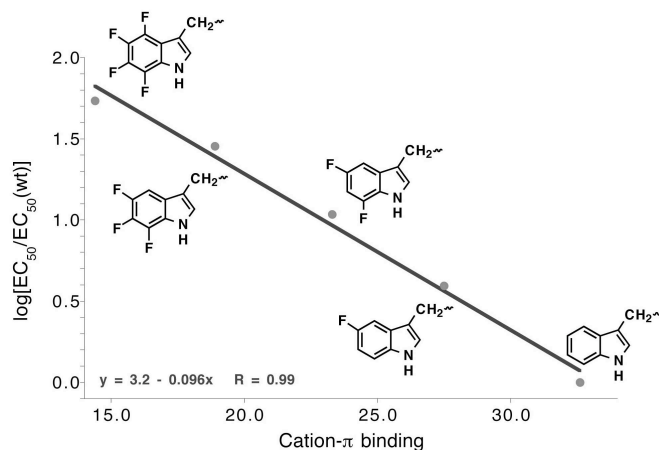


**Figure 4.2.** The  $\alpha$ Trp149 of the muscle-type nAChR interacts with acetylcholine via a cation- $\pi$  type interaction. This plot demonstrates a linear correlation between *ab initio* calculations of the cation- $\pi$  binding energy of the fluorinated Trp residues shown, and the in vivo measurements of the  $EC_{50}$ , measured for acetylcholine.

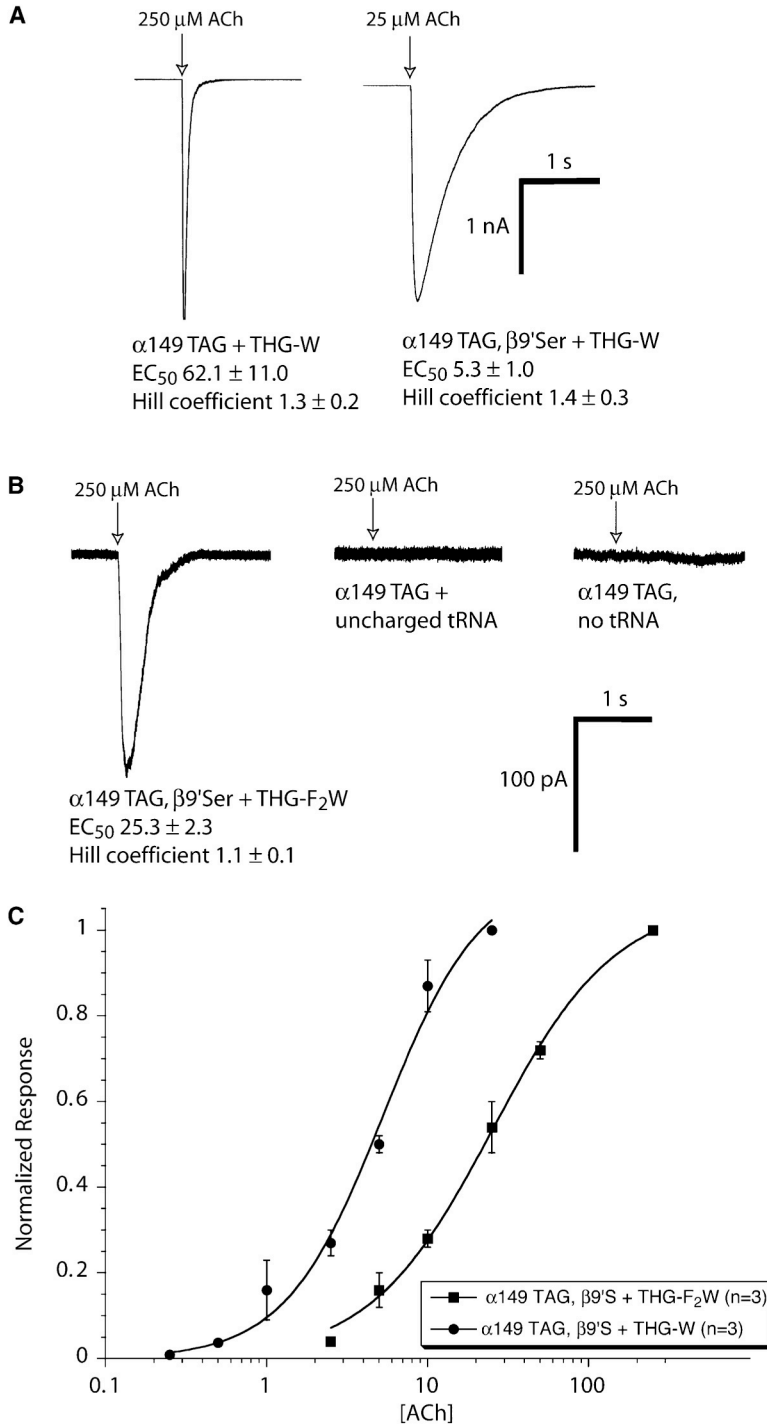
#### 4.2.2.1 Results

Using the electroporation protocol, we delivered mutant  $\alpha$  subunit mRNA (149TAG), mRNA for the remaining subunits ( $\beta$ Leu9'Ser mutant,  $\delta$ , and  $\gamma$ ), and a reporter EGFP plasmid. Also included was the tRNA THG73 that has proven to be effective for studies in *Xenopus* oocytes, chemically aminoacylated with either Trp (wild-type) or 5,7-difluorotryptophan (THG-F<sub>2</sub>Trp).

In measurements 24 hours after transfection, currents from 100 pA to 2 nA are seen in response to saturating ACh concentrations. As shown in Figure 4.3, when THG73 is used to deliver Trp, a wild-type channel is produced. Most importantly, THG73 aminoacylated with F<sub>2</sub>Trp leads to a characteristic shift in the dose-response curve to higher  $EC_{50}$ . The results agree well with analogous experiments performed in

*Xenopus* oocytes, and they convincingly demonstrate successful incorporation of an unnatural amino acid. Control experiments using THG73 that has not been aminoacylated gave no response.

**Figure 4.3 (next page).** Incorporation of natural and unnatural amino acids into the nAChR expressed in CHO-K1 cells by nonsense suppression using chemically aminoacylated THG73 tRNA. CHO-K1 cells were electroporated with a 5  $\mu$ l solution containing  $\alpha$ 149TAG,  $\beta$  or  $\beta$ Leu9'Ser,  $\delta$ , and  $\gamma$  nAChR subunit mRNA, THG-aa tRNA, and reporter plasmid. Arrows indicate 25 ms pulses of ACh application. (A) The first trace shows wild-type recovery of the nAChR by suppression of  $\alpha$ 149TAG mRNA with THG73 tRNA aminoacylated with Trp (THG-W) (2  $\mu$ g/ $\mu$ l  $\alpha$ 149TAG, 0.5  $\mu$ l each  $\beta$ ,  $\delta$ , and  $\gamma$ , 4  $\mu$ g/ $\mu$ l THG-W). The second trace shows wild-type recovery of the  $\beta$ Leu9'Ser mutant nAChR channel by suppression of  $\alpha$ 149TAG mRNA with THG-W (2  $\mu$ g/ $\mu$ l  $\alpha$ 149TAG, 0.5  $\mu$ l each  $\beta$ Leu9'Ser,  $\delta$ , and  $\gamma$ , 4  $\mu$ g/ $\mu$ l THG-W). (B) The first trace shows ACh response from a cell expressing the unnatural amino acid 5,7-difluorotryptophan (THG-F<sub>2</sub>W) at  $\alpha$ 149 of the nAChR (2  $\mu$ g/ $\mu$ l  $\alpha$ 149TAG, 0.5  $\mu$ l each  $\beta$ Leu9'Ser,  $\delta$ , and  $\gamma$ , 3  $\mu$ g/ $\mu$ l THG-F<sub>2</sub>W). The second and third traces show that there is no ACh response from cells transfected with mRNA only, with or without uncharged tRNA. (C) ACh dose response curves for THG-W suppressed  $\alpha$ 149TAG/ $\beta$ Leu9'Ser nAChR (closed circle) and THG-F<sub>2</sub>W suppressed  $\alpha$ 149TAG/ $\beta$ Leu9'Ser nAChR (closed square).



#### 4.2.2.2 Discussion

We show that microelectroporation can deliver chemically aminoacylated tRNA to mammalian cells. This is the first example of site-specific incorporation of an unnatural amino acid into a protein expressed in a mammalian cell using chemically aminoacylated-tRNA. This extension of the nonsense suppression methodology for unnatural amino acid incorporation should greatly expand the utility of the method for studying mammalian proteins in a more physiologically relevant system.

Recently, RajBhandary and coworkers have shown the delivery of aminoacyl-tRNA obtained intact from *E. coli* to COS-1 cells using the transfection reagent Effectene (Qiagen) [19]. We saw no success with this method, as described in Chapter 2. Most likely, the difference between the two studies is the nature of the assays employed. In their studies, Kohrer et al. harvested transfected COS-1 cells and then employed the highly sensitive biochemical CAT assay because protein expression was too low to be observed on a single-cell level. In the present work, we observe much higher levels of protein expression, and single cells can be assayed. While there are other important differences between the two studies, our work thus far indicates that for studies at the single-cell level, electroporation is a more promising transfection method.

A recent report from Yokoyama and coworkers showed site-specific incorporation of unnatural amino acids in proteins in mammalian cells [20]. They expressed in CHO-Y cells a mutant *E. coli* tyrosine synthetase that aminoacylates *B. Stearothermophilus* amber suppressor tRNA with 3-iodo-L-tyrosine. This is significant work toward engineering cells with novel amino acids, but is complicated by the requirement that each new amino acid has a specific engineered synthetase and tRNA.

For our purposes, chemical aminoacylation of tRNA has the distinct advantage of not being amino acid specific and no protein engineering is required, and therefore it is a more general technique.

Finally, Vogel and coworkers independently demonstrated nonsense suppression of EGFP with aminoacyl-tRNA [21]. They microinjected CHO cells with in vitro transcribed *E. coli* amber suppressor tRNA that was chemically aminoacylated with wild-type leucine, along with the Leu64TAG mutant EGFP mRNA reporter gene, leading to the recovery of wild-type EGFP expression. This is promising work because like THG73, this tRNA was shown to be orthogonal, such that delivery of nonaminoacyl tRNA did not lead to EGFP expression. For many systems, microinjection may represent a viable approach. However, in our hands electroporation is far less tedious, since hundreds of cells can be transfected in a matter of seconds. The present method also appears to be more general because we were able to transfect different types of adherent cells with equal efficiency and with less cell mortality than single-cell gene transfer methods such as microinjection.

#### 4.2.3 Attempts at neuronal $\alpha 4\beta 2$ expression by nonsense suppression

We are particularly interested in studying the biophysical properties of nicotine binding to neuronal receptors. It is of particular interest that, from our studies, the step-wise increase in the  $EC_{50}$  observed for ACh binding with increasing fluorination at  $\alpha$ Trp149 of the muscle-type nAChR is not observed for nicotine [13] (Figure 4.4). In fact, no aromatic residue located within the binding cleft of the muscle type nAChR has

been shown to interact with nicotine via a cation- $\pi$  type interaction [22]. However, this may not be surprising since nicotine is a poor agonist for this receptor. The majority of high affinity nACh receptors in the brain are the  $\alpha 4\beta 2$  receptor. Nicotine binding has been accounted for by the neuronal nAChR receptors  $\alpha 4\beta 2$  and  $\alpha 7$ , and these receptors show a higher affinity to nicotine than they do to ACh [16]. Furthermore, studies suggest that the behavioral effects of nicotine in animals is predominantly mediated by the  $\alpha 4\beta 2$  receptor (reviewed in [23]).

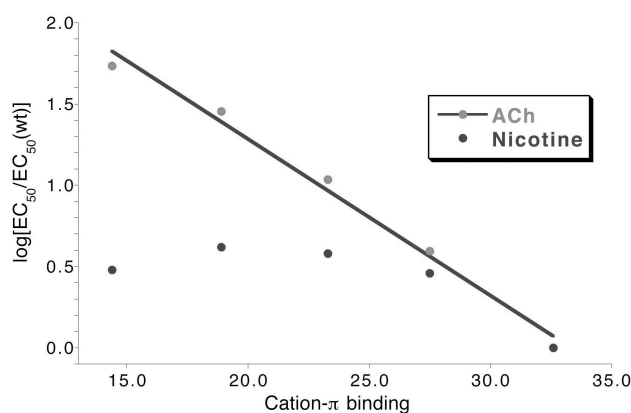


**Figure 4.4.** The anomalous behavior of nicotine binding at the muscle-type nAChR. This plot demonstrates that nicotine does not follow the same trend as acetylcholine when the fluorinated Trp residues are incorporated at  $\alpha$ Trp149, and thus does not interact at this site by a cation- $\pi$  type interaction.

We are interested in incorporating the fluoro-tryptophan series at key aromatic residues within the neuronal nAChRs to test if nicotine is binding via a cation- $\pi$  interaction. The homologous tryptophan to  $\alpha 149$  of the muscle type receptor is Trp182 in  $\alpha 4$ , so we are particularly interested in incorporating the fluorinated Trp series at this position of the  $\alpha 4\beta 2$  receptor. Unfortunately, attempts thus far have proved to be disappointing, as these receptors were resistant to unnatural amino acid incorporation in

the *Xenopus* oocyte expression system. Dr. Gabriel Brandt went to heroic efforts to increase the surface expression of both  $\alpha 4\beta 2$  and  $\alpha 7$  in *Xenopus* oocytes [22]. These included optimizing the expression vector, overexpressing elongation factors, trying to reduce clatherin-mediated endocytosis by co-expression of a dominant-negative dynamin, overexpression of ER-chaperones (BiP), insertion of forward-trafficking signals for greater surface expression, and multiple injections into oocytes. Of all of these, only multiple injections had any measurable effect, but the whole-cell currents were still too small to generate reliable dose-response relations. Given that the neuronal nAChRs we are studying are mammalian in origin, we speculated that the *Xenopus* oocyte expression system may not be appropriate for these receptors. This in turn may have led to the poor expression observed. With a mammalian expression system now in hand, we set out to express  $\alpha 4\beta 2$  receptors in mammalian cells by nonsense suppression.

#### 4.2.3.1 Results

The mRNA for the human  $\alpha 4$  and  $\beta 2$  subunits was made by in vitro transcription, from the Not I linearized pAMV constructs (optimized for *Xenopus* oocyte expression). In initial experiments, CHO-K1 cells were transfected with mRNA, along with the reporter plasmid EGFP-N1, by electroporation. ACh and nicotine responses were measured from EGFP expressing cells by whole-cell patch clamping. The responses from transfected CHO-K1 cells were small, at best, on the order of 10s of pA. There was also a great deal of inconsistency in expression levels from day to day, using the same mRNA stocks and same transfection protocol. On many days the cells would fail to express  $\alpha 4\beta 2$  all together.

Given the inconsistency of mRNA expression, the  $\alpha 4$  and  $\beta 2$  subunits were subcloned into the mammalian expression vector pCI-neo at the Mlu I and Sal I sites. Using electroporation, CHO-K1 cells were transfected with these constructs. Whole-cell currents measured in response to ACh and nicotine were significantly larger in comparison to the mRNA transfections, on the order of  $\sim 100$  pA to 1 nA (Figure 4.5).

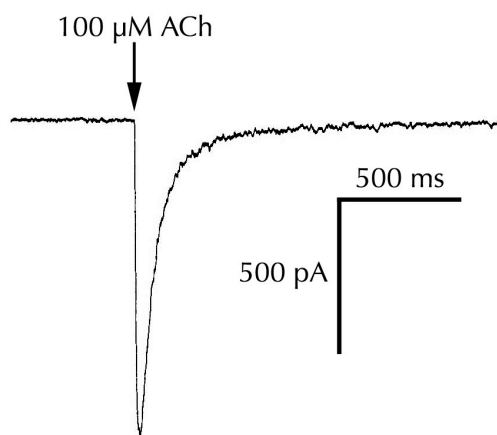


**Figure 4.5.** A typical whole-cell patch clamp response from a CHO-K1 cell transfected with a  $5 \mu\text{l}$  solution containing the  $\alpha 4$  and  $\beta 2$  subunits in pCI-neo, ( $2 \mu\text{g}/\mu\text{l}$  each), along with an EGFP-N1 reporter plasmid ( $0.15 \mu\text{g}/\mu\text{l}$ ). The arrow indicates a 25 ms pulse of a  $100 \mu\text{M}$  solution of ACh.

We next set out to express the  $\alpha 4\beta 2$  receptor by nonsense suppression in CHO-K1 cells using THG73 tRNA. The homologous tryptophan to  $\alpha 149$  of the muscle type receptor is Trp182 in  $\alpha 4$ , so we were interested in incorporating the fluorinated Trp series at this site. Unfortunately, when cells were transfected with the  $\alpha\text{Trp182TAG}$  mutant DNA (or mRNA) along with  $\beta 2$  and THG-W or THG-F<sub>2</sub>W tRNA, no expression was observed. Transfection was done using a transfection solution at a variety of concentrations, up to concentrations as high as  $7 \mu\text{g}/\mu\text{l}$   $\alpha\text{Trp182TAG}$  DNA (or mRNA)

and 7  $\mu\text{g}/\mu\text{l}$  of THG-aa (along with 1  $\mu\text{g}/\mu\text{l}$  of the  $\beta 4$  subunit and 0.5  $\mu\text{g}/\mu\text{l}$  of the EGFP reporter plasmid). Under no circumstances was any sign of suppression observed.

#### 4.2.3.2 Discussion

It is not readily apparent why expression of the  $\alpha 4\beta 2$  receptor by nonsense suppression failed in both the *Xenopus* oocyte and mammalian cell expression systems. The HSAS suppression experiments described in Chapter 3 and in section 4.2.1 demonstrate that the electroporation protocol delivers sufficient tRNA to cells such that suppression is not tRNA limited. Furthermore, the successful incorporation of natural and unnatural amino acids into the muscle-type nAChR using THG73-aa demonstrates that this tRNA is fully functional in mammalian cells as a suppressor tRNA. It is therefore curious that the wild-type  $\alpha 4\beta 2$  receptor expresses so well in mammalian cells (when DNA is used in transfection), while expression by nonsense suppression cannot be achieved. It may be that upon translation, the  $\alpha 4\beta 2$  receptor is processed differently than the muscle-type receptor, and that this processing is not compatible with nonsense suppression. Or perhaps the mutant  $\alpha 4$  Trp182TAG mRNA is more susceptible to nonsense-mediated decay (NMD), a process by which transcripts containing premature termination codons are degraded within a cell [24, 25]. NMD seems unlikely, however, since we don't believe it has been a problem for any other systems we have studied. Also, NMD has more to do with the relative position of premature termination codons relative to introns, and our mRNA lacks introns.

It seems that any future studies of the  $\alpha 4\beta 2$  receptor using unnatural amino acids will have to look beyond what we now know as the nonsense suppression methodology.

I suspect that differential processing of the neuronal  $\alpha 4\beta 2$  receptor, compared to other proteins that we have studied, is possibly incompatible with our current methodology. Perhaps if expressed in neurons, this ion channel would be processed and delivered to the surface more efficiently, and this could be one way to address this problem. Having a better understanding of how these ion channels are processed during translation will help us to optimize the method.

#### 4.2.4 NMDA receptor expression by nonsense suppression

The NMDA receptor belongs to the family of glutamate ion channels, found primarily in the central nervous system, which constitutes the vast majority of excitatory neurotransmission in the brain. This receptor is a coincidence detector, important for long-term potentiation (LTP) in the hippocampus. Channel opening requires both agonist-binding as well as depolarization to relieve  $Mg^{2+}$  block of the pore. This receptor has nonspecific cation conductance, with high calcium permeability ( $P_{Ca}/P_{K,Na,Cs} = 3.1 - 11$ ).  $Ca^{2+}$  entry into the cell combined with simultaneous firing of the pre and post synapse strengthens synaptic connections and induces LTP. Therefore, its role in neuronal development and synaptic plasticity is central to the mechanisms of learning and memory (reviewed in [26, 27]).

The NMDA receptor subunit stoichiometry is believed to be tetrameric, consisting of two NR1 subunits and two NR2 subunits. The subunits resemble those of potassium channels with inverted topology, with three transmembrane domains and a re-entrant loop

(M2) that lines the pore. Activation of the NMDA receptor is achieved by the binding of glutamate to NR2 and the essential co-agonist glycine to NR1 [26, 27].

There is now enough known about the NMDA receptor at a molecular level to design experiments using unnatural amino acids. For example, the crystal structure of the extracellular glycine-binding domain has recently been solved [28], and it provides a good framework to develop biophysical experiments aimed at understanding glycine modulation and channel gating. Also, residues implicated in channel modulation by phosphorylation, nitrosylation, glycosylation, reduction and oxidation, as well as modulation by pH and zinc, have been identified [26, 27]. We are therefore very interested in using unnatural amino acid incorporation to better understand the functioning of the NMDA receptor.

Because the NMDA receptor has never been studied using unnatural amino acids, we wanted to first design a relatively straightforward "proof of principle" experiment, with interpretable results. As discussed above,  $Mg^{2+}$  blocks the channel of the NMDA receptor by binding to residues in the M2 pore-lining region of the receptor. It has been shown that for receptors composed of NR1-1a and NR2b, that when Trp607 of the NR2b subunit was mutated to the nonaromatic residues Leu, Asn or Ala, the  $Mg^{2+}$   $IC_{50}$  increased by an order of magnitude from 20  $\mu M$  to 200 - 300  $\mu M$  [29]. Mutation of Trp607 to the aromatic residues Phe and Tyr had minimal effect on the  $Mg^{2+}$   $IC_{50}$ . From these data it was suggested that  $Mg^{2+}$  binds at Trp607 via a cation- $\pi$  type interaction. This effect was not seen at any other Trp residue in the NR2b subunit (Trp610), in the homologous NR2a Trp residues (Trp606 and Trp609), or in the homologous NR1-1a Trp residues (Trp608, Trp611). We are therefore interested in incorporating the fluorinated

Trp series (that was used to identify a cation- $\pi$  interaction between ACh and the nAChR) to identify a cation- $\pi$  interaction between  $Mg^{2+}$  and Trp607 of NR2b. Since we already have all the unnatural amino acids necessary, no synthesis is required. Furthermore, these residues have already been shown to be functional in a variety of expression systems. Finally, if  $Mg^{2+}$  binding does occur via a cation- $\pi$  type interaction, then the receptor has a measurable phenotype - the  $Mg^{2+}$   $IC_{50}$ .

#### 4.2.4.1 Results

The NMDA constructs (rat) NR1-1a (pCI-neo), NR2a (pCI-neo) and NR2b (pcDNA1) were obtained from the labs of Stephen Traynelis. NR1-1a and NR2a or NR2b were co-electroporated into CHO-K1 cells, along with an EGFP-N1 reporter plasmid. It can be seen in Figure 4.6 that the NR1-1a and NR2a constructs express well in CHO-K1 cells. Responses on the order of  $\sim 1$  nA or greater were typical. Expression of the NR2b construct was less efficient, however, and responses usually were on the order of 10s to 100s of pA.

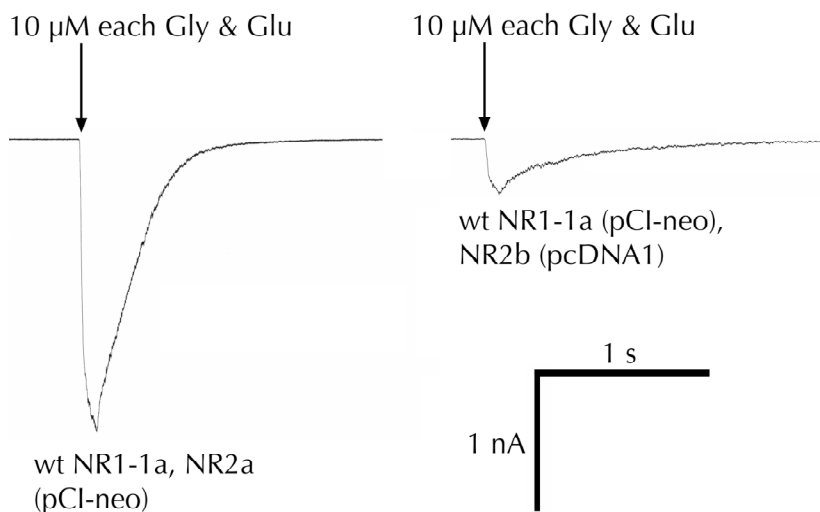


**Figure 4.6.** Expression of wt NMDA receptors in CHO-K1 cells. CHO-K1 cells were transfected with a 5  $\mu$ l solution containing the NR1-1a and NR2a (in pCI-neo) or NR2b (in pcDNA1) subunits (2  $\mu$ g/ $\mu$ l each). The first trace shows a whole-cell response from a cell expressing the NR1-1a and NR2a subunits. The second trace is a response of a cell expressing the NR1-1a and NR2b subunits. The arrows indicate a 50 ms pulse of 10  $\mu$ M each glutamate and glycine.

Initial experiments in studying  $Mg^{2+}$  block of the NMDA receptor were done using the same fast perfusion system as done for all the electrophysiology experiments, with quick pulses of drug application (25 - 50 ms). Since the  $IC_{50}$  for  $Mg^{2+}$  is known to be  $\sim 20$   $\mu$ M, a 300  $\mu$ M  $Mg^{2+}$  solution along with 10  $\mu$ M of each glutamate and glycine was applied to CHO-K1 cells expressing the NMDA receptor. It was expected that there would be no response due to total channel block. Surprisingly, there was minimal difference between the responses with or without  $Mg^{2+}$  (Figure 4.7).

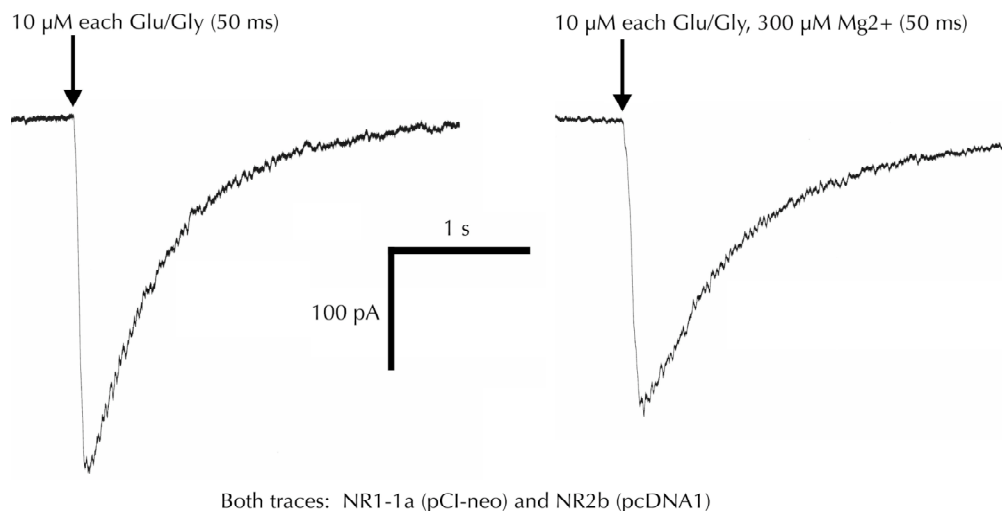


**Figure 4.7.** Expression and Mg<sup>2+</sup> block (50 ms application) of wt NMDA receptors. CHO-K1 cells were transfected with a 5 μl solution containing the NR1-1a (in pCI-neo) and NR2b (in pcDNA1) subunits (2 μg/μl each). The first trace shows a whole-cell response upon a 50 ms pulse of 10 μM each glutamate and glycine. The second trace is a response upon a 50 ms pulse of 10 μM each glutamate and glycine and 300 μM Mg<sup>2+</sup>.

It was speculated that the Mg<sup>2+</sup> was having no effect because the duration of drug application was too short. That is, the rate of agonist binding and channel opening may be faster than the kinetics of Mg<sup>2+</sup> block. To assess this, the drugs were applied for longer durations. As expected, with a 1 second drug application, channel block was observed with a 10 μM Mg<sup>2+</sup> application, and almost total channel block was observed with 300 μM Mg<sup>2+</sup> (Figure 4.8). This demonstrates that longer applications of Mg<sup>2+</sup> are required to observe channel block.

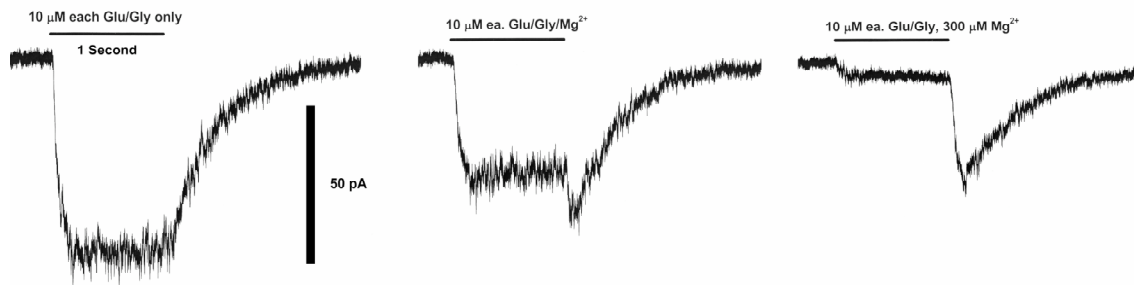


**Figure 4.8.** Expression and  $Mg^{2+}$  block (1 s application) of wt NMDA receptors. CHO-K1 cells were transfected with a 5  $\mu$ l solution containing the NR1-1a (in pCI-neo) and NR2b (in pcDNA1) subunits (2  $\mu$ g/ $\mu$ l each). The first trace shows a whole-cell response upon a 1 s pulse of 10  $\mu$ M each glutamate and glycine. The second trace is a response upon a 1 s pulse of 10  $\mu$ M each glutamate, glycine and  $Mg^{2+}$ . The third trace is a response upon a 1 s pulse of 10  $\mu$ M each glutamate, glycine and 300  $\mu$ M  $Mg^{2+}$ .

An attempt to make a variety of NMDAR mutants was pursued in order to study the role of pore-lining tryptophan residues in  $Mg^{2+}$  channel block (both by Quickchange and PCR mutagenesis). These included the NR2b Trp607TAG and Trp610TAG mutants, the NR2a Trp606TAG and Trp609TAG mutants and the NR1-1a Trp608TAG and Trp611TAG mutants. Of these, the only two that were successfully obtained (by PCR mutagenesis) were the NR2b Trp607TAG and NR2a Trp609TAG. With these in hand, CHO-K1 cells were transfected with NR1-1a, one of the mutant NR2 constructs, along with THG-W tRNA (to look for wild-type recovery of both NMDA receptors). Unfortunately, no expression by nonsense suppression was observed with the NR2b Trp607TAG mutant. However, it can be seen in Figure 4.9 that wild-type recovery by nonsense suppression of the NR2a subunit was successful. Responses on the order of 50 pA were observed with a 50 ms pulse of 10  $\mu$ M each glutamate and glycine. There was minimal read-through of the mutant NR2a Trp606TAG in the absence of aminoacyl-tRNA. This demonstrates that the NMDA receptor can be expressed by nonsense suppression.

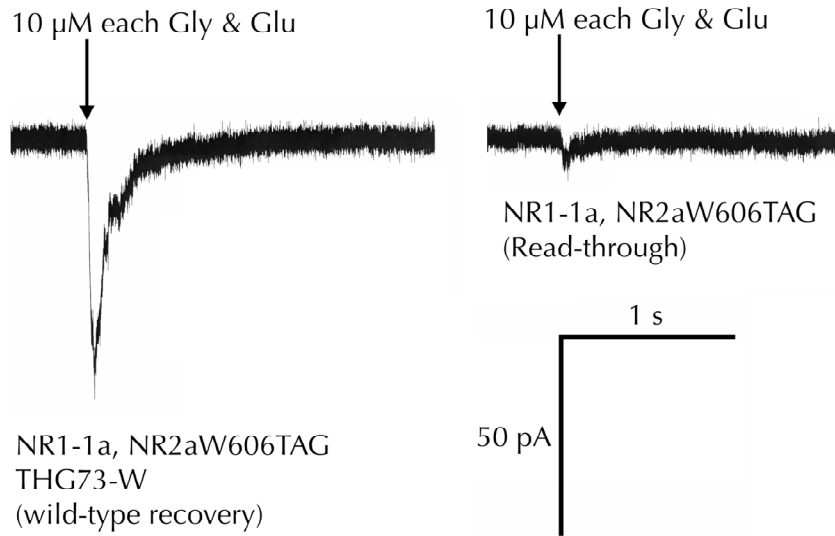


**Figure 4.9.** Expression of wt NMDA receptors in CHO-K1 cells by nonsense suppression. The first trace shows whole-cell response from CHO-K1 cells that were transfected with a 5  $\mu$ l solution containing the NR1-1a (1  $\mu$ g/ $\mu$ l) and NR2a Trp606TAG (4  $\mu$ g/ $\mu$ l each) (both in pCI-neo), and THG-W (5  $\mu$ g/ $\mu$ l). The second trace is a response of a cell expressing the NR1-1a and mutant NR2b Trp606TAG subunits, with 74mer THG73 tRNA (5  $\mu$ g/ $\mu$ l). The arrows indicate a 50 ms pulse of 10  $\mu$ M each glutamate and glycine.

#### 4.2.4.2 Discussion

The above results demonstrate that the NMDA receptor expresses well in mammalian cells, using the electroporation transfection protocol. The wild-type receptor containing the NR2a subunit consistently had maximal responses on the order of nAs. However, NR2b expressing receptors had much smaller signals. This difference is most likely due to the fact that the NR2a was in pCI-neo, a high expression vector, and NR2b construct was in the poorly expressing vector pcDNA1.

Attempts were made to subclone the gene encoding for the NR2b subunit into pCI-neo in order to increase its expression levels in CHO-K1 cells. However, the

pcDNA1 construct was extremely resistant to sequencing, as well as to mutagenesis by Quickchange or PCR. I was unfortunately unable to determine the sequence flanking the NR2b coding region, making it impossible to do the necessary molecular biology. The best course of action to take for future studies would be to obtain an NR2b construct that is already in a mammalian expression vector from another lab.

An important result from these experiments is that the NMDA receptor can be expressed by nonsense suppression. This was shown by wild-type recovery of receptors containing the NR1-1a and NR2a subunits, using THG-W. Nonsense suppression of the NR2a Trp606TAG mutant DNA gave maximal responses on the order of 50 pA, while cells transfected with this mutant in the absence of aminoacyl-tRNA had minimal read-through.

Unfortunately, no wild-type recovery was observed for the NR2b Trp607TAG subunit, which is the residue implicated in making a cation- $\pi$  interaction with  $Mg^{2+}$ , and therefore was the site at which we had hoped to incorporate the fluoro-tryptophan series. We suspect that nonsense suppression did not work for this construct was because it is in a poorly expressing vector (pcDNA1). Judging from the nAChR nonsense suppression experiments (4.2.2), and the NR2a suppression shown above, it seems that the wild-type receptor needs to generate whole-cell responses on the order of  $\sim 1$  nA or greater in order to observe expression by nonsense suppression.

Another important result from these experiments is that nonsense suppression was achieved by electroporation of DNA that encodes for the NMDA subunits, rather than mRNA as has been traditionally done. This further simplifies the mammalian cell

nonsense suppression method, since mRNA synthesis can be of inconsistent quality, and since mRNA itself is inherently less stable and more difficult to work with than DNA.

Finally, these results demonstrate that NMDA expression is compatible with nonsense suppression. This is very exciting, because one can imagine many experiments using unnatural amino acids for this receptor. For example, zinc and redox modulation can be studied using caged-cysteine; phosphorylation can be studied using the phospho-amino acid analogues that are currently in progress (Dr. Gabriel Brandt and E. James Petersson); glycine modulation can be studied using the crystal structure as a model; and channel gating can be studied using hydroxy acids and the backbone cleaving residues 5-(*o*-nitrobenzyl)selenyl-2-hydroxypentanoic acid (NbSeOH) [30] and nitrophenylglycine [14]. This will be an exciting area for future studies.

### **4.3 Conclusions**

Presented is a general method to deliver aminoacyl-tRNA, mRNA and DNA simultaneously to mammalian cells by electroporation. Both natural and unnatural amino acids chemically appended to a suppressor tRNA are site-specifically incorporated into the nicotinic acetylcholine receptor. These are very exciting results, as they demonstrate that the nonsense suppression method of unnatural amino acid incorporation can be done in a mammalian cell expression system. Furthermore, we show the first demonstration of NMDA expression by nonsense suppression. This demonstrates that the methodology can be applied to the family of glutamate receptors, an entirely new class of neuronal ion channels in our hands.

In conclusion, we describe the first general method for unnatural amino acid incorporation in mammalian cells. By not being limited to the *Xenopus* oocyte or in vitro expression systems, this will greatly expand the use of unnatural amino acids to studying protein structure-function relationships in cell-specific signaling cascades. We therefore feel that this method will advance our own studies on neuronal ion channels, as well as making the use of unnatural amino acids more attainable to a broader cross-section of researchers.

## 4.4 Experimental Methods and Materials

### 4.4.1 Materials

Restriction enzymes and T4 RNA ligase were purchased from New England Biolabs (Beverly, MA). The mMessage mMachine and MegaShortScript in vitro transcription kits were purchased from Ambion (Austin, TX). Maxiprep kits used for plasmid isolation were purchased from Qiagen (Valencia, CA). pEGFP-N1, a soluble EGFP construct was purchased from BD Biosciences Clontech (Palo Alto, CA). The NR1-1a (pCI-neo), NR2a (pCI-neo) and NR2b (pcDNA1) were obtained from Prof. Stephen Traynelis (Emory, GA). Ham's F12 tissue culture media was purchased from Irvine Scientific (Santa Ana, CA), and CO<sub>2</sub> independent was purchased from GIBCO Introgen Corporation (Carlsbad, CA). The microelectroporator was built on site.

### 4.4.2 Mutagenesis, mRNA and tRNA synthesis

THG73 tRNA, THG-W and THG-F2W have been described elsewhere. Briefly, linearization of pUC19 containing the THG73 gene with Fok I yeilds 74-mer tRNA upon in vitro transcription with the MegaShortScript kit. THG73 74-mer was then ligated to dCA-W or dCA-F2W with T4 RNA ligase to generate THG73-aa.

Mutagenesis of the NMDA subunits was done using the Quickchange mutagenesis protocol (Stratagene), or using standard PCR mutagenesis. The wild-type neuronal nAChR subunits  $\alpha 4$ ,  $\alpha 4$  182TAG and wild-type  $\beta 2$  were removed from the pAMV expression vector by PCR, while introducing an Mlu I mutation at the 5'terminus

at the same time. This was trimmed with Mlu I and Sal I, and subcloned into pCI-neo at the corresponding sites.

The mRNA that codes for the muscle-type nAChR ( $\alpha$ ,  $\beta$ ,  $\delta$  and  $\gamma$ ) or the neuronal  $\alpha 4$  and  $\beta 2$  AChR subunits was obtained by linearization of the expression vector (pAMV) with Not I, followed by in vitro transcription using the mMessage mMachine kit.

#### 4.4.3 Tissue culture

CHO cells were grown in Ham's F12 media and HEK cells were grown in DMEM, at 37°C and 5% CO<sub>2</sub>, enriched with glutamine, fetal bovine serum (FBS, 10 %), penicillin, and streptomycin. 1 to 2 days prior to electroporation, the cells were passaged onto 35 mm tissue culture dishes such that confluency was typically 50% or less at the time of transfection.

#### 4.4.4 Electroporation

The DNA, mRNA or tRNA to be electroporated into CHO-K1 was precipitated alone or as co-precipitates in ethanol and ammonium acetate, and left at -20°C for at least 1 hour. For THG73-aa, the amino acids have an o-nitroveratryloxycarbonyl (NVOC) protecting group at the N-terminus and were photo-deprotected immediately prior to electroporation. This consisted of irradiating a 15  $\mu$ l solution of THG73-aa (1  $\mu$ g/ $\mu$ l) in 1 mM NaOAc (pH 4.5) for 6 minutes, using a 1000 W Hg/Xe arc lamp (Oriel, Stratford, CT) operating at 400 W, equipped with WG355 and UG11 filters (Schott, Duryea, PA). Reporter EGFP DNA and the AChR subunit mRNA or NMDA subunit DNA was then

combined with this and precipitated with ammonium acetate and ethanol. This was then microcentrifuged at 15,000 rpm, 4°C for 15 minutes, vacuum dried for 5 minutes, and resuspended in CO<sub>2</sub> independent medium to the desired final concentration. Immediately prior to electroporation, the cell tissue culture media was swapped to CO<sub>2</sub> independent media (with no glutamine, FBS or antibiotics). Approximately 5  $\mu$ l of the electroporation solution was applied to the cells, followed by application of electrical pulses. For CHO-K1 cells this was typically four 120 V pulses of 50 ms duration. The CO<sub>2</sub> independent media was immediately replaced with fresh Ham's F12, and the cells were placed back into the 37°C incubator. Electrophysiological recordings were done 24 hours after transfection.

#### 4.4.5 Microscopy

CHO-K1 cells were visualized with an inverted microscope (Olympus IMT2), a 250 W Hg/Xe lamp operating at 150 W, a GFP filter set (Chroma, model 41017) with an excitation band pass of 450 to 490 nm and an emission band pass of 500 to 550 nm, 10x/0.25NA or 40x/1.3NA lens, and a Photometrix Quantix CCD camera running Axon Imaging Workbench 4.0.

#### 4.4.6 Electrophysiology

Whole-cell recordings were performed on EGFP-expressing (reporter gene) cells. The cells were visualized using an inverted microscope as described above. Patch electrodes (borosilicate, 4-6 M $\Omega$ ) were filled with a pipette solution containing 88 mM KH<sub>2</sub>PO<sub>4</sub>, 4.5 mM MgCl<sub>2</sub>, 0.9 mM EGTA, 9 mM HEPES, 0.4 mM CaCl<sub>2</sub>, 14 mM creatine

phosphate, 4 mM Mg-ATP, 0.3 mM GTP (Tris salt), adjusted to pH 7.4 with KOH. The recording solution contained 150 mM NaCl, 4 mM KCl, 2mM CaCl<sub>2</sub>, 2mM MgCl<sub>2</sub>, 2 mM glucose, 10 mM HEPES, adjusted to pH 7.4 with NaOH. When recording from ACh receptors, 1  $\mu$ M atropine was added (metabotropic AChR blocker). When recording from NMDA receptors, the Mg<sup>2+</sup> was left out, and added back at the desired concentration. Standard whole-cell recordings were done using an Axopatch 1-D amplifier, low-pass filter at 2-5 kHz and digitized online at 20 kHz (pClamp 8, Foster City, CA). The membrane potential was held at -60 mV.

Acetylcholine (ACh), glutamate (Glu), glycine (Gly) or Mg<sup>2+</sup> was delivered using a two-barrel glass theta tube (outer diameter  $\sim$  200  $\mu$ m, pulled from 1.5 mm diameter theta borosilicate tubing) connected to a peizo-electric translator (Burleigh LSS-3100, Fisher, NY). Each barrel of the theta tube was fed from a 12-way manifold. This allowed up to 12 different solutions to be fed in either the control or agonist barrel. Agonists were applied for 25 ms for AChR, and 50 ms or 1 s for the NMDAR, which was triggered by pClamp 8 software. The voltage input to the high-voltage amplifier (Burleigh PZ-150M, Fishers, NY) used to drive the piezo translator was filtered at 150 Hz by an 8-pole Besel filter (Frequency Devices, Haverhill, MA), to reduce oscillations from rapid pipette movement. Solution exchange rates measured from open tip junction potential changes upon application with 10% recording solution were typically  $\sim$  300  $\mu$ s (10% - 90% peak time).

## 4.5 References

1. Cornish, V.W., et al., *Site-specific incorporation of biophysical probes into proteins*. Proc Natl Acad Sci USA, 1994. **91**: p. 2910-2914.
2. Cornish, V.W., D. Mendel, and P.G. Schultz, *Probing protein structure and function with an expanded genetic code*. Angew Chem Int Ed Engl, 1995. **34**: p. 621-633.
3. Dougherty, D.A., *Unnatural amino acids as probes of protein structure and function*. Curr Opin Chem Biol, 2000. **4**(6): p. 645-52.
4. Gillmore, M.A., L.E. Steward, and A.R. Chamberlin, *Incorporation of noncoded amino acids by in vitro protein biosynthesis*. Topics Curr Chem, 1999. **202**: p. 77-99.
5. Beene, D.L., D.A. Dougherty, and H.A. Lester, *Unnatural amino acid mutagenesis in mapping ion channel function*. Curr Opin Neurobiol, 2003. **13**(3): p. 264-70.
6. Nowak, M.W., et al., *In vivo incorporation of unnatural amino acids into ion channels in a Xenopus oocyte expression system*. Methods Enzymol., 1998. **293**: p. 504-529.
7. Nowak, M.W., et al., *Nicotinic receptor binding site probed with unnatural amino acid incorporation in intact cells*. Science, 1995. **268**(5209): p. 439-42.
8. Li, L.T., et al., *The tethered agonist approach to mapping ion channel proteins toward a structural model for the agonist binding site of the nicotinic acetylcholine receptor*. Chemistry & Biology, 2001. **8**(1): p. 47-58.
9. Petersson, E.J., et al., *A perturbed pK(a) at the binding site of the nicotinic acetylcholine receptor: Implications for nicotine binding*. J Am Chem Soc, 2002. **124**(43): p. 12662-12663.
10. Kearney, P.C., et al., *Determinants of nicotinic receptor gating in natural and unnatural side chain structures at the M2 9' position*. Neuron, 1996. **17**(6): p. 1221-9.
11. Miller, J.C., et al., *Flash decaging of tyrosine sidechains in an ion channel*. Neuron, 1998. **20**(4): p. 619-24.
12. Zhong, W., et al., *From ab initio quantum mechanics to molecular neurobiology: A cation- $\pi$  binding site in the nicotinic receptor*. Proc Natl Acad Sci USA, 1998. **95**: p. 12088-12093.

13. Beene, D., et al., *Cation- $\pi$  interactions in ligand recognition by serotonergic (5-HT<sub>3A</sub>) and nicotinic acetylcholine receptors: The anomalous binding properties of nicotine*. *Biochemistry*, 2002. **41**(32): p. 10262-10269.
14. England, P.M., et al., *Site-specific, photochemical proteolysis applied to ion channels in vivo*. *Proc Natl Acad Sci U S A*, 1997. **94**(20): p. 11025-30.
15. Tong, Y.H., et al., *Tyrosine decaging leads to substantial membrane trafficking during modulation of an inward rectifier potassium channel*. *J Gen Physiol*, 2001. **117**(2): p. 103-118.
16. Corringer, P.J., N. Le Novère, and J.P. Changeux, *Nicotinic receptors at the amino acid level*. *Annual Review of Pharmacology and Toxicology*, 2000. **40**: p. 431-458.
17. Charnet, P., et al., *An open-channel blocker interacts with adjacent turns of  $\alpha$ -helices in the nicotinic acetylcholine receptor*. *Neuron*, 1990. **4**(1): p. 87-95.
18. Labarca, C., et al., *Channel gating governed symmetrically by conserved leucine residues in the M2 domain of nicotinic receptors*. *Nature*, 1995. **376**(6540): p. 514-516.
19. Kohrer, C., et al., *Import of amber and ochre suppressor tRNAs into mammalian cells: a general approach to site-specific insertion of amino acid analogues into proteins*. *Proc Natl Acad Sci U S A*, 2001. **98**(25): p. 14310-5.
20. Sakamoto, K., et al., *Site-specific incorporation of an unnatural amino acid into proteins in mammalian cells*. *Nucleic Acids Res*, 2002. **30**(21): p. 4692-9.
21. Ilegems, E., H.M. Pick, and H. Vogel, *Monitoring mis-acylated tRNA suppression efficiency in mammalian cells via EGFP fluorescence recovery*. *Nucleic Acids Res*, 2002. **30**(23): p. e128.
22. Brandt, G.S., *Site-specific incorporation of synthetic amino acids into functioning ion channels*, in *Chemistry*. 2003, California Institute of Technology: Pasadena. p. 206.
23. Paterson, D. and A. Nordberg, *Neuronal nicotinic receptors in the human brain*. *Prog Neurobiol*, 2000. **61**(1): p. 75-111.
24. Parker, R. and H. Song, *The enzymes and control of eukaryotic mRNA turnover*. *Nat Struct Mol Biol*, 2004. **11**(2): p. 121-7.
25. Le Hir, H., A. Nott, and M.J. Moore, *How introns influence and enhance eukaryotic gene expression*. *Trends Biochem Sci*, 2003. **28**(4): p. 215-20.
26. Dingledine, R., et al., *The glutamate receptor ion channels*. *Pharmacol Rev*, 1999. **51**(1): p. 7-61.

27. Carroll, R.C. and R.S. Zukin, *NMDA-receptor trafficking and targeting: implications for synaptic transmission and plasticity*. Trends Neurosci, 2002. **25**(11): p. 571-7.
28. Furukawa, H. and E. Gouaux, *Mechanisms of activation, inhibition and specificity: crystal structures of the NMDA receptor NR1 ligand-binding core*. Embo J, 2003. **22**(12): p. 2873-85.
29. Williams, K., et al., *The selectivity filter of the N-methyl-D-aspartate receptor: a tryptophan residue controls block and permeation of Mg<sup>2+</sup>*. Mol Pharmacol, 1998. **53**(5): p. 933-41.
30. Zacharias, N.M., *Chemical-scale manipulation of ion channels: in vivo nonsense suppression and targeted disulfide crosslinking*, in *Chemistry*. 2004, California Institute of Technology: Pasadena. p. 139.